

**THE OPTICAL RESOLUTION
OF
ALBUTEROL**

by

Anne Therese Stevens

B.Sc (Honours) University of Cape Town

Thesis presented for the degree of
MASTER OF SCIENCE
in the
Department of Chemistry
UNIVERSITY OF CAPE TOWN

Supervisors: Prof. M.R. Caira
Prof. R. Hunter
Prof. L.R. Nassimbeni

February 1998

The University of Cape Town has been given
the right to reproduce this thesis in whole
or in part. Copyright is held by the author.

The copyright of this thesis vests in the author. No quotation from it or information derived from it is to be published without full acknowledgement of the source. The thesis is to be used for private study or non-commercial research purposes only.

Published by the University of Cape Town (UCT) in terms of the non-exclusive license granted to UCT by the author.

ABSTRACT

The acetonide derivative of (rac)-albuterol has been prepared and used as a substrate in co-crystallisation experiments with several acidic resolving agents. Successful resolution of the acetonide was achieved with both di-*O*-benzoyl- and di-*O*-toluoyltartaric acid, with the (2*S*,3*S*)-enantiomer of the acid selectively co-crystallising with the desired (*R*)-albuterol acetonide. High performance liquid chromatography on a chiral stationary phase, and ¹H NMR experiments using a chiral shift reagent were used to assess the optical purity of the resolved material. Acid hydrolysis of the resolved acetonide gave rise to the target, (*R*)-albuterol, which was isolated as an acetate salt. The inferred absolute configuration of the resolved acetonide was assessed by ¹H NMR analysis of its (*R*)-Mosher ester, and confirmed by an X-ray structural determination of its (*R*)-phenylethylurea derivative.

For Jonathan

ACKNOWLEDGEMENTS

I would like to extend a special word of thanks to:

My supervisors: Professor Mino Caira, Professor Luigi Nassimbeni, and Professor Roger Hunter for their guidance, enthusiasm and faith in me.

Colleagues in both the organic synthesis and crystallography research groups for their friendship and support.

Professor James Bull and Dr Kelly Chibale for many helpful discussions.

Dr Susan Bourne and Dr Anita Coetzee for the X-ray data collections and assistance with some of the crystallographic aspects of this thesis.

Piero Benincasa, Dr Krassi Dimitrova, Noel Hendricks and Ricardo Donn for their analytical services.

Dr Janet Scott, Rainer Clauss and other members of the research department at FCC for their assistance with the HPLC analyses.

South African Druggists, Fine Chemicals Corporation and the FRD for financial support.

My family, friends and especially my husband for their support.

ABBREVIATIONS

2D	two-dimensional
DCC	dicyclohexylcarbodiimide
de	diastereomeric excess
dec.	decomposed
DMAP	4-(dimethylamino)-pyridine
DMSO	dimethylsulfoxide
DOBT	di- <i>O</i> -benzoyltartaric acid
DOTT	di- <i>O</i> -toluoyltartaric acid
ee	enantiomeric excess
F	structure factor
FDA	US Food and Drug Administration
gc	gas chromatography
HETCOR	heteronuclear chemical shift correlation
HMQC	heteronuclear multiple quantum correlation
HOBt	1-hydroxybenzotriazole
hplc	high performance liquid chromatography
lit.	literature
mp	melting point
MTPA	methoxytrifluoromethylphenylacetic acid
MTPACl	methoxytrifluoromethylphenylacetic acid chloride
NMR	nuclear magnetic resonance
OAM	<i>O</i> -acetylmandelic acid
PCC	pyridinium chlorochromate
ppm	parts per million
RT	room temperature
tlc	thin layer chromatography
Z	number of asymmetric units in the unit cell

CONTENTS

Abstract

Acknowledgements

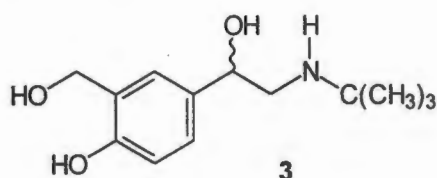
Abbreviations

Table of Contents

CHAPTER 1	INTRODUCTION	1
1.1	Chiral Drugs	1
1.1.1	Background	1
1.1.2	Producing Single Enantiomers	2
1.2	Racemate Resolution <i>via</i> Crystallisation	5
1.2.1	Direct Crystallisation	5
1.2.2	Resolution by Diastereomer Formation	6
1.3	Racemisation	10
1.4	Determination of Enantiomer and Diastereomer Composition	11
1.5	Albuterol	12
1.5.1	Synthesis of (rac)-Albuterol	12
1.5.2	Synthesis of (<i>R</i>)-Albuterol	13
1.5.3	Determination of Enantiomer Composition of Albuterol	14
1.6	The Approach taken in this work	15
CHAPTER 2	DERIVATISATION AND RESOLUTION STUDIES	16
2.1	Derivatisation of Albuterol	16
2.2	Space Group Determination of Albuterol Acetonide	19
2.3	Diastereomeric Salt Formation	21
2.4	Determination of Enantiomeric Purity	26
2.4.1	¹ H Nuclear Magnetic Resonance	26
2.4.2	High Performance Liquid Chromatography	29
2.5	Resolution Studies	32
2.6	Hydrolysis of Albuterol Acetonide	34
2.7	Racemisation Studies	37

CHAPTER 3	DETERMINATION OF ABSOLUTE CONFIGURATION	41
3.1	Introduction	41
3.2	The DOBT and DOTT Salts of Albuterol Acetonide	41
3.3	Structure Determination of (+)-Albuterol Acetonide	42
3.4	Covalent Diastereomer Formation	46
3.4.1	Mandelate derivatives of (-)-Albuterol Acetonide	46
3.4.2	Camphor Sulfonyl derivatives of (-)-Albuterol Acetonide	47
3.4.3	Mosher's Ester of (-)-Albuterol Acetonide	48
3.4.4	Phenylethylurea derivatives of (+)-and (-)-Albuterol Acetonide	52
3.4.5	Crystal structure of (<i>R</i>)-Phenylethylurea of (+)-Albuterol Acetonide	54
CHAPTER 4	CONCLUSION	57
CHAPTER 5	EXPERIMENTAL	58
5.1	General	58
5.2	Syntheses	59
5.3	Analyses	72
5.3.1	X-ray Powder Diffraction Patterns	72
5.3.2	NMR Determination of optical purity of (<i>R</i>)-Albuterol Acetonide	72
5.3.3	Chiral High Performance Liquid Chromatography	73
5.4	Crystal Structure Determinations	75
5.4.1	(<i>rac</i>)-Albuterol Acetonide	75
5.4.2	(<i>R</i>)-Albuterol Acetonide	75
5.4.3	(<i>R</i>)-Phenylethylurea of (<i>S</i>)-Albuterol Acetonide	77
References		78
APPENDIX 1		83
APPENDIX 2		88
APPENDIX 3		94

In addition to the development of new molecules, there has also been much interest in the redevelopment of drugs whose active ingredient is the single enantiomer of a previously approved racemate. Although there is pessimism about the initial promise held in these racemic switches,⁵ an incentive announced by the FDA recently⁹ extends the marketing exclusivity of these drugs to five years. It is into this category that the drug under investigation in this work, albuterol (or salbutamol) **3**, falls.



1.1.2 Producing Single Enantiomers

Driven by these trends in the pharmaceutical industry, enantioselective production and analytical technology have become extremely active areas of research. There are 3 broad approaches to producing single enantiomers (Fig. 1.1) which have been extensively reviewed.¹⁰⁻¹³

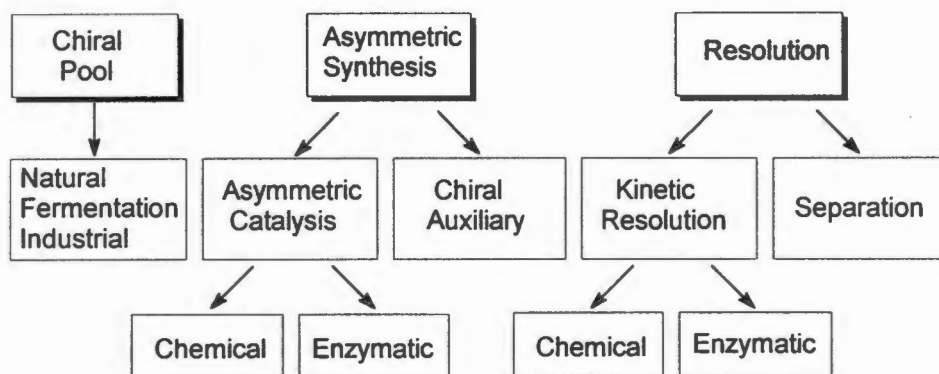
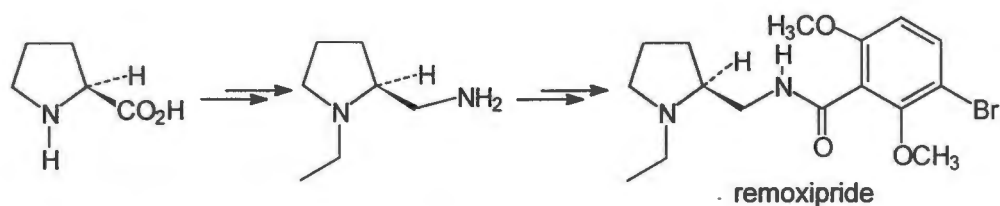


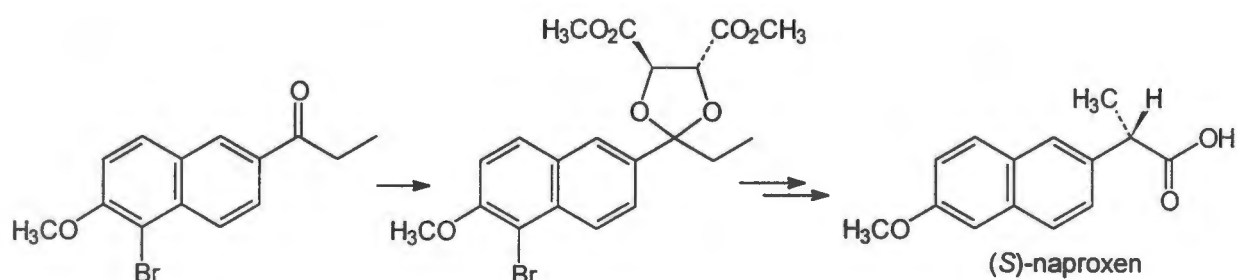
Fig 1.1: Approaches to the manufacture of single isomers

The chiral pool methods utilise abundantly available chiral starting materials of high optical purity which are transformed into the drug while maintaining the integrity of the desired chiral centres. The starting material may have its source in nature, *e.g.* (*S*)-proline used in the synthesis of the neuroleptic remoxipride (Scheme 1.1),¹⁴ or in *de novo* fermentation processes whereby carbohydrate feedstocks are converted to both simple molecules, *e.g.* *L*-amino acids, and more complex antibiotics, vitamins and hormones. Enantiopure products that are now routinely synthesised on a large scale can also be regarded as part of the chiral pool. This is exemplified by (*R*)-phenylglycine which is contained as a side chain in several β -lactam antibiotics.

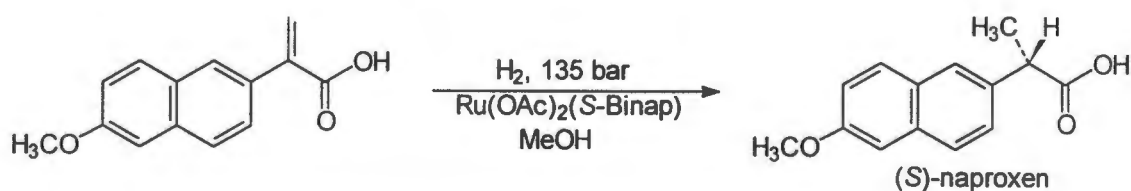


Scheme 1.1: The synthesis of remoxipride from (*S*)-proline

In asymmetric synthesis, a prochiral starting material is stereoselectively converted into a chiral product. An enantiomerically pure reagent may be used in stoichiometric or catalytic amounts to induce the required chirality. This can be illustrated by two routes developed for the synthesis of the analgesic, (*S*)-naproxen. In the former case, (*2R,3R*)-tartaric acid is used as a chiral auxiliary in a synthesis called the Zambon process¹⁵ (Scheme 1.2). Alternatively, hydrogenation using a chiral ruthenium catalyst¹⁶ results in a product of high optical purity (Scheme 1.3).

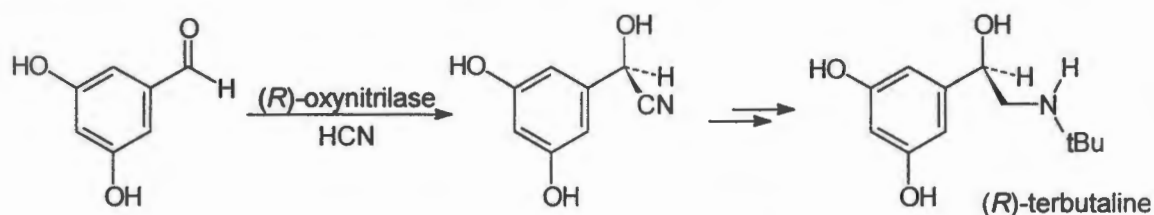


Scheme 1.2: The Zambon process for (*S*)-naproxen



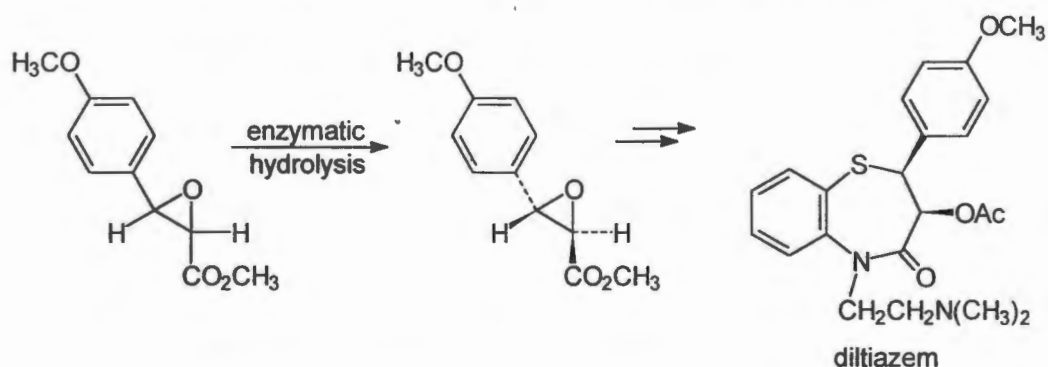
Scheme 1.3: Synthesis of (*S*)-naproxen using asymmetric hydrogenation

Although the majority of enzymatic transformations currently in use are kinetic resolutions, a number of truly asymmetric transformations are available and this pool of reactions is constantly increasing. An attractive route to enantiopure β -amino alcohols, of which albuterol is one, is *via* optically active cyanohydrins and this has recently been achieved for the bronchodilator (*R*)-terbutaline¹⁷ (Scheme 1.4).



Scheme 1.4: Biocatalytic route to *(R)*-terbutaline

The catalysis of kinetic resolutions may once again be chemical or biological. Diltiazem, a drug included in the chiral top 10,¹⁸ is currently manufactured using an enzymatic resolution of the earliest chiral intermediate in the synthesis.¹⁹ As depicted in Scheme 1.5, the unwanted isomer is hydrolysed leaving the desired enantiomer as the substrate for further transformation.



Scheme 1.5: Enzymatic route to diltiazem

As illustrated by diltiazem, epoxides form intermediates in a vast number of syntheses and the kinetic resolution thereof using chiral metal complexes as catalysts is becoming a highly commercialised area of research. One of the newest such catalysts developed by Jacobsen at Harvard university²⁰ has been licensed to ChiRex by the University.

The most frequently used approaches for the separation of enantiomers on a commercial scale involve crystallisation processes. These were used in this work and are discussed in Section 1.2. Large scale preparative separation *via* chromatographic methods has not been used to any great extent to date but this option is becoming more viable with advances in the development of chiral stationary phases and moving bed technology. Another area of separation which holds great promise but is still in its infancy is that of enantioselective transport through membranes. The latter two separation methods are the topics of chapters in a recent review on chiral separations.²¹

1.2 Racemate Resolution *via* Crystallisation

1.2.1 Direct Crystallisation

Racemate resolution *via* direct crystallisation is dependent on the occurrence of the crystalline substance as a conglomerate as opposed to a racemic compound. Although a bulk conglomerate is optically neutral, individual crystals contain only one enantiomer whereas crystals of a racemic compound are themselves racemic. Several methods are used for the identification of a conglomerate.²² These include comparison of the solid state infra-red spectra and the X-ray powder diffraction patterns of the racemate with those of an individual enantiomer. They will be identical in the case of a conglomerate. It is estimated that only 5-10% of all organic compounds crystallise as conglomerates.²³ Where salt formation of a molecule with an achiral acid or base is possible, the likelihood of a conglomerate increases 2-3 times.²⁴ The first substance ever resolved, sodium ammonium tartrate, by Pasteur in 1848,²⁵ crystallises as a conglomerate whilst tartaric acid is a racemic compound. The properties, behaviour and resolution of conglomerates is well understood and has been fully documented by Jaques, Collet and Wilen.²⁴

There are two main approaches to conglomerate resolution. In the first, the separation is based on the spontaneous resolution that occurs upon crystallisation. The individual crystals may be manually sorted in a process called triage, as by Pasteur, but this is obviously only suitable on a very small scale and is dependent on the crystals having hemihedral faces so that enantiomeric crystals can be recognised optically. A more practical alternative consists of the localisation of individual enantiomers on suitably positioned seed crystals within a supersaturated solution of the racemate. This method is used by Merck for the resolution of an intermediate in the synthesis of α -methyl-*L*-dopa.²⁶

The second approach is referred to as “preferential crystallisation” or “resolution by entrainment”. It consists of collecting alternate crops of each enantiomer in a single vessel. Seeds of one enantiomer (say the (+)-enantiomer) are added to a solution artificially enriched with that isomer. A crop of material equal to twice the weight of the original enrichment is collected and replaced with an equal amount of racemate. The solution is then seeded with the (-)-enantiomer and the process repeated. These steps can theoretically be repeated *ad infinitum*,

but build-up of impurities in the solution prevents this. This method has been used for more than 30 years by Roussel-Uclaf for the production of chloramphenicol.²⁷

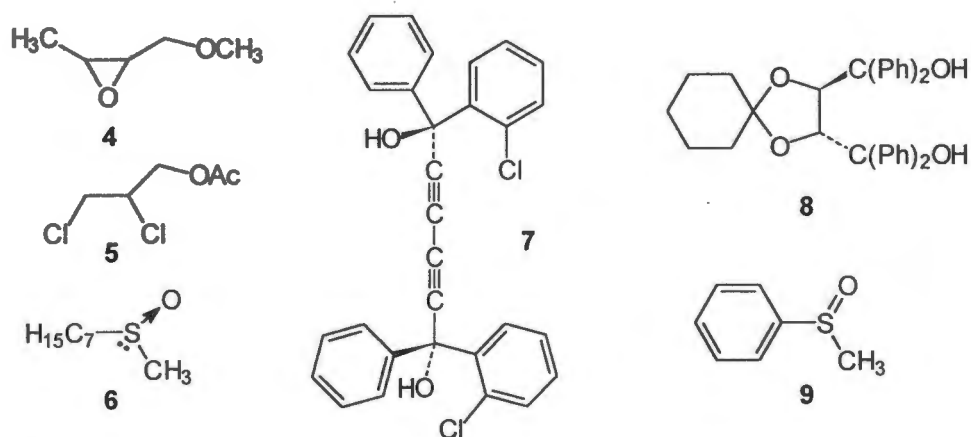
1.2.2 Resolution by Diastereomer Formation

Unlike enantiomers, diastereomeric pairs may have significantly differing physical properties that can form the basis for their separation. When using crystallisation techniques, the separation depends entirely on differences in solubility. Diastereomeric pairs are usually considered in two broad categories, *viz.* covalent diastereomers and dissociable diastereomers.

Resolution *via* covalent diastereomers is frequently used on a laboratory scale (often with chromatographic separations) but is not favoured in industry since the formation and cleavage of these compounds, and recovery of resolving agent, is usually more complex and prone to racemisation than that of dissociable diastereomers.

Dissociable diastereomers include diastereomeric salts and complexes. The formation of crystalline diastereomeric salts between racemic substrates and optically active resolving agents is widely used industrially and provides a large proportion of those optically active drugs that are not derived from natural products.¹⁰ This was the resolution process applied in this work and is described in more detail in Section 1.2.2.1.

There are, however, molecules of commercial interest such as **4-6** below²⁸ which are devoid of suitable functionality for salt formation. These could be resolved by the formation of diastereomeric complexes which can be Lewis acid-base pairs, diastereomeric metal complexes, inclusion compounds and quasi-racemates. Compound **7** has been shown to form 1:1 inclusion compounds with **4-6** providing products of high optical purity.²⁹ The cost of producing such chiral host molecules is often prohibitive and chiral pool materials are being explored as a departure point for the synthesis of hosts such as **8** (derived from (2*S*,3*S*)-tartaric acid) which has resolved **9**, a useful chiral synthon.³⁰



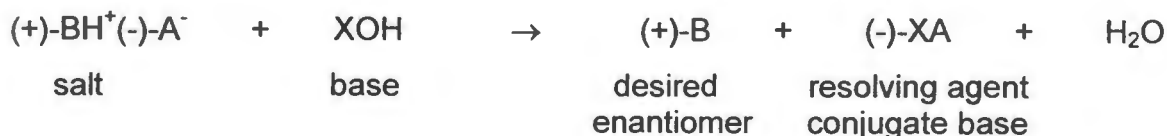
1.2.2.1 Diastereomeric Salt Formation

The process is referred to as “classical resolution” and was discovered by Pasteur in 1853 when he obtained the optically pure antipodes of tartaric acid by resolving with (+)-quinocine and (+)-cinchonidine³¹ respectively. The process of diastereomeric salt formation between a racemic base (B) and an acidic resolving agent (A) can be summarised as follows:

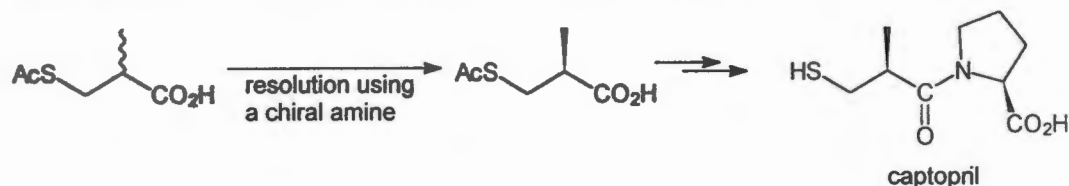


The nomenclature used to describe the two salts stems from a proposal made by Ugi³² in which the diastereomer resulting from enantiomers of like sign of rotation is referred to as the positive, or p-salt and that comprising enantiomers of unlike sign is thus the n-salt. This convention does not take the absolute configuration at any of the centres into account.

If the difference in solubility of the two salts is large enough, the less soluble salt can be crystallised. The desired, optically pure enantiomer is then removed from the diastereomer and the resolving agent recycled:



Despite this resolution technique having been investigated and used for over a century, it is still impossible to predict the course of a resolution²⁴ and as a result, it is often viewed as being too “low tech” and empirical to warrant serious effort. A strategy toward such resolutions has been compiled by Wilen *et al*³³ and success is frequently achieved on substrates bearing suitable functionality. The Andeno route to captopril, an ACE inhibitor which grossed \$1670 million in sales during 1995,³⁴ is *via* the optical resolution of an early intermediate³⁵ which is later coupled to (*S*)-proline in order to introduce the second stereogenic centre (Scheme 1.6).



Scheme 1.6: Andeno approach to captopril

Several approaches have been used in attempts to rationalise resolution results. Ács, Fogassy and co-workers have been able to evaluate and interpret the results of some optical resolutions by determining thermodynamic constants and X-ray structures.^{36,37} Ács has also analysed the chiral discrimination ability of tartaric acid in terms of a three-point interaction model.³⁸ Separate studies on crystal structures of diastereomeric salt pairs by Gould³⁹ and Arnett⁴⁰ both conclude that weak van der Waals interactions probably determine the course of a classical resolution. Viewing the problem from an entirely different angle, Ariaans *et al*⁴¹ have attempted to compute correlations between physical properties of resolving agents and resolution efficiencies using Principal Component Analysis, from which they concluded that parameters which relate to the chirality of the compound, *e.g.* measurable diastereomeric interactions, are required to obtain correlation. A quantitative approach has been taken in a study by Leusen⁴² in which experimentally determined lattice energies were compared to those determined using Molecular Mechanics calculations on X-ray data. Limitations in the computational methods presently available hampered accurate calculation of these energies. It is further pointed out by Leusen that most of the rationalisations put forward rely on known X-ray structures. In order to develop a truly predictive model, a method to predict crystal packing of the salts must be developed. This has thus far only been achieved for simple hydrocarbons.^{43,44}

In contrast to the initial resolution, the optimisation thereof is a well understood area.²⁴ The solubilities of a three component system (two diastereomers and one solvent) are represented in simple cases by means of a ternary phase diagram as in Fig. 1.2.

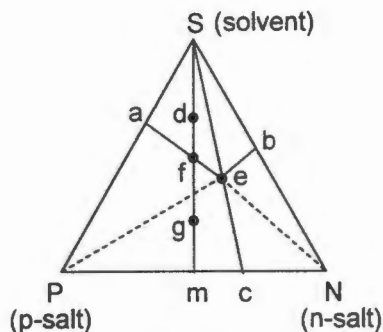


Figure 1.2: Ternary phase diagram for unsolvated salts

The diagram gives the solubility of each salt (points a and b) and of mixtures of the salts (ae and be) in the solvent at a particular temperature. For many organic mixtures, the eutectic composition, c, is not very temperature dependent, thus simplifying the optimisation.⁴⁵

The following regions define four specific conditions the resolution mixture may be in:

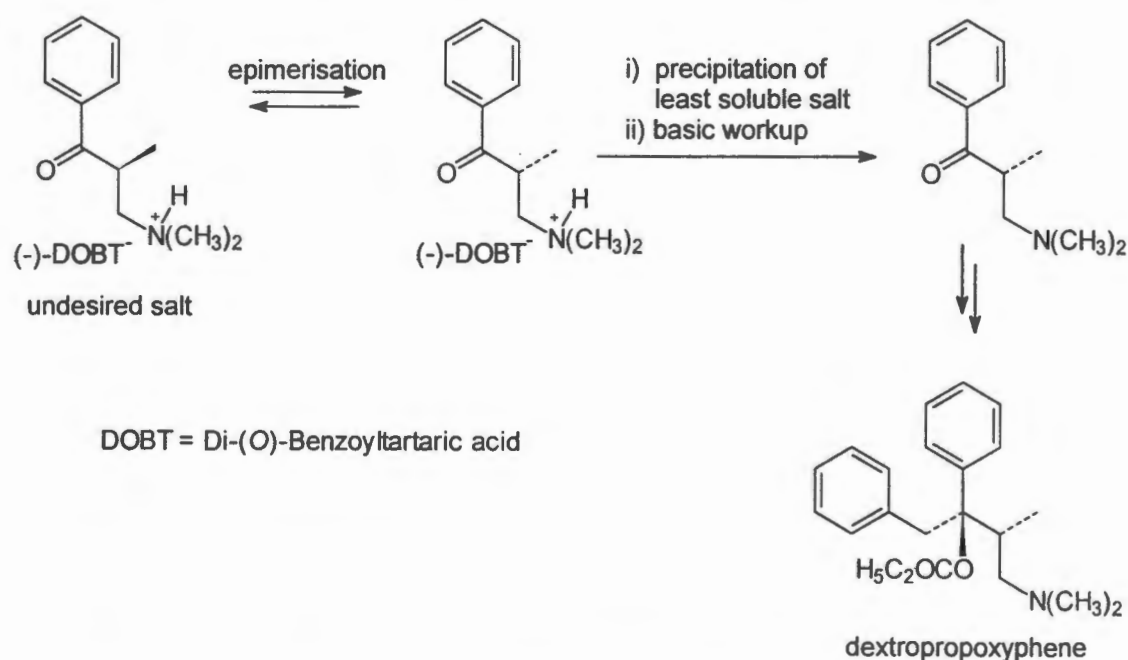
- i) Saeb: both salts are unsaturated
- ii) aeP: solid p-salt is in equilibrium with a solution of both salts as defined by ae
- iii) beN: solid n-salt is in equilibrium with a solution of both salts as defined by be
- iv) PeN: Saturated solution of composition c in equilibrium with solid p- and n-salts

In a typical resolution experiment, an unsaturated 1:1 solution of the salts as represented by d will be prepared. As the solvent volume decreases d will descend down tie line Sm to point f where the less soluble p-salt becomes saturated and begins to crystallise. Further removal of much solvent can result in the saturation of the solution with respect to the undesired n-salt as well (point g) and the salts will crystallise together.

Construction of such a diagram is a tedious process and requires the availability of both salts, but it should be undertaken during the development phase of industrial resolutions where the gains in both chemical and optical yield would be economically significant.

1.3 Racemisation

Where a resolution step is used to produce a single enantiomer, the ability to racemise and recycle the unwanted enantiomer frequently determines the economic viability of the process. The ideal situation in a resolution occurs when it can be carried out under conditions in which the enantiomer or diastereomer remaining in solution undergoes spontaneous epimerisation. The once-through theoretical yield thus increases from 50% to 100%. When crystallisation is the mode of resolution, the overall process constitutes a crystallisation-induced asymmetric transformation. This is illustrated by the industrial synthesis of the Eli Lilly analgesic, dextropropoxyphene (Scheme 1.7).⁴⁶



Scheme 1.7: Industrial synthesis of dextropropoxyphene using a crystallisation-induced asymmetric transformation

Chiral amines and amino acids are susceptible to racemisation *via* transient, reversible Schiff base formation in the presence of catalytic amounts of carbonyl compounds. This has been applied in one-pot resolution procedures for multikilo syntheses of amine intermediates.^{47,48}

Where there is no possibility for such one-pot procedures, standard racemisation techniques, such as base-mediated enolisation, are applied to the isolated unwanted diastereomer or enantiomer. These have been reviewed by Eliel *et al.*²²

1.4 Determination of Enantiomer and Diastereomer Composition

The most common way to describe stereoisomer mixtures is as the excess of one stereoisomer over the other (as a percentage). The enantiomeric excess is thus given by:

$$ee = 100 \frac{(X_R - X_S)}{(X_R + X_S)} \quad \text{where} \quad \begin{array}{l} X_R = \text{no of moles (R)-enantiomer} \\ X_S = \text{no of moles (S)-enantiomer} \end{array}$$

The scope of analyses employed is large and these have been reviewed and summarised as presented in Table 1.1 below.²²

Table 1.1: Methods for the determination of Enantiomer and Diastereomer composition

Basis of Measurement	Nature of Measurement	Species
Chiroptical	Optical rotation, α	E or D
	Circular polarisation of emission	E
Diastereotopicity (external measurement)	NMR-diastereomers in achiral solvents	D
	NMR-enantiomers in chiral solvents	E
	NMR-with chiral shift reagents	E
Diastereomeric Interactions (separations)	Chromatography on diastereoselective stationary phases: gc, hplc, tlc	D
	hplc with chiral solvent	E
	Chromatography on enantioselective stationary phases: gc, hplc, tlc	E
	Electrophoresis with enantioselective supporting electrolyte	E
Kinetics	Product composition	D or E
Enzyme Specificity	Quantitative enzyme-catalysed reaction	E
Fusion Properties	Differential scanning calorimetry	D or E
Isotope dilution	Isotope analysis	E
Potentiometry	Potential of an electrochemical cell	E

E = enantiomer

D = diastereomer

1.5 Albuterol

It is estimated that 5% of Western society will suffer from bronchial asthma at some time in their lives.⁴⁹ The disease is characterised in its early stages by breathlessness and wheezing due to constriction of respiratory smooth muscle, which is easily reversed by the administration of a bronchodilator. Of the bronchodilators, the β_2 -adrenergic receptor agonists produce the greatest effects and albuterol **3** is preferred as a first choice treatment for relief of these acute symptoms.⁵⁰ The drug was developed in the late 1960's, in a process that has been reviewed by Lunts,⁵¹ and marketed as a racemate. The assignment of absolute configuration of the enantiomers of albuterol was achieved in 1971⁵² and these are illustrated in Fig. 1.3. The bronchodilatory activity was shown to reside largely in the (*R*)-enantiomer. More recently, the realisation that the "inactive" enantiomers of the β_2 -adrenergic receptor agonists may be associated with toxic effects, as well as the need to investigate the relationship between enantiomers and side effects, which include tremor and reduction of renal function,⁵³ have led to a number of publications⁵⁴⁻⁵⁶ and culminated in the submission of an NDA (New Drug Application) for (*R*)-albuterol with the FDA in August 1997.

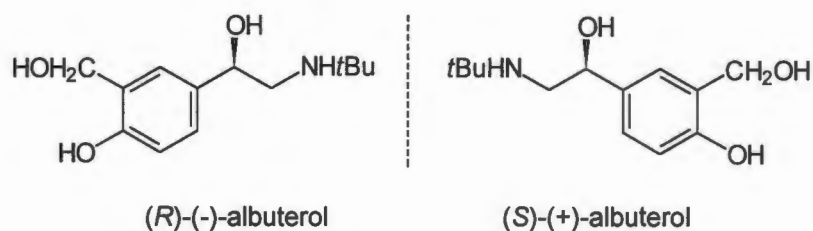
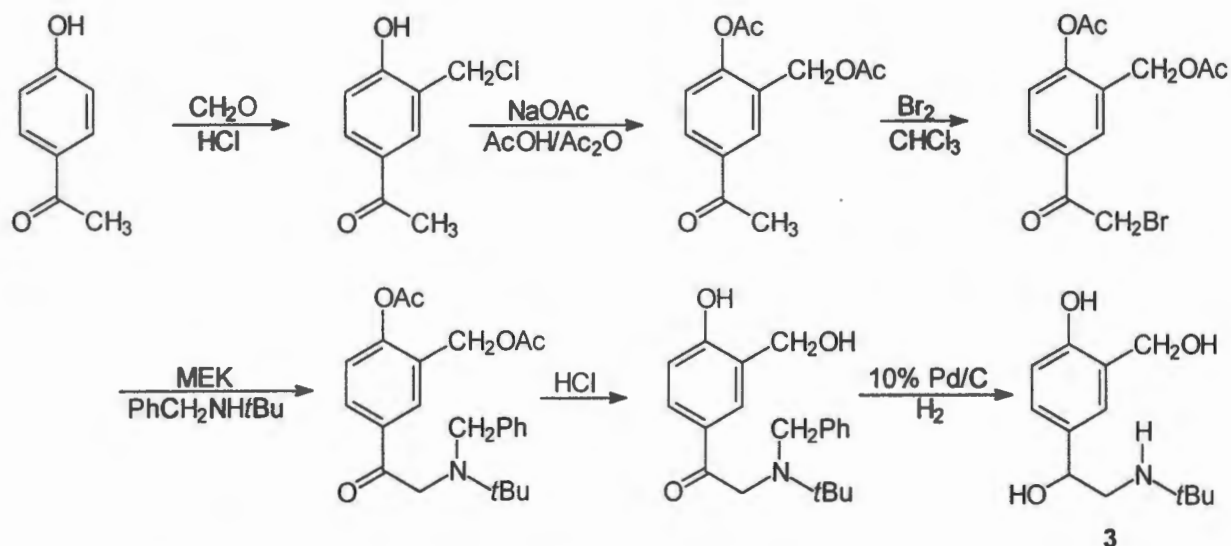


Figure 1.3: The enantiomers of albuterol

1.5.1 Synthesis of (rac)-Albuterol

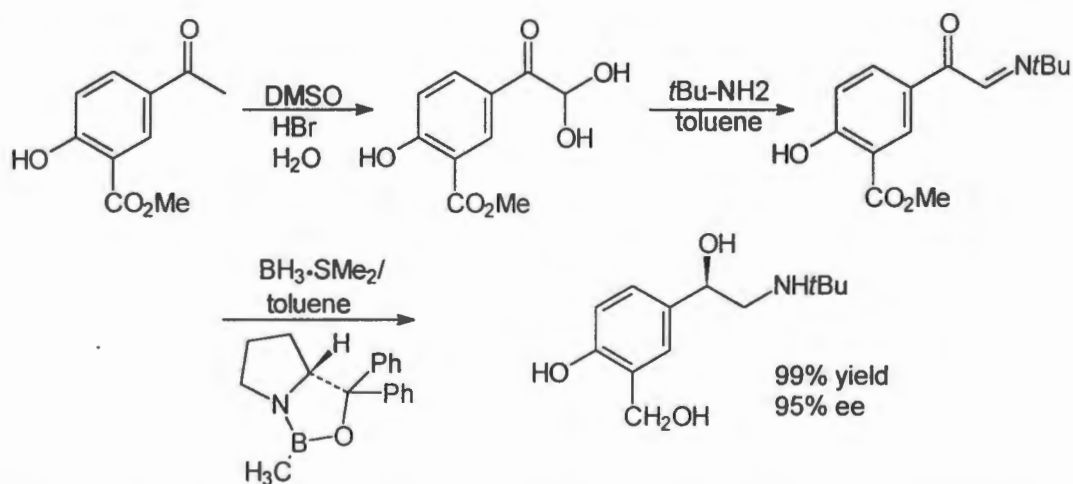
Albuterol has been the target of a number of synthetic approaches which have recently been reviewed.⁵³ Along with standard functional group manipulations, three types of reaction utilised in the syntheses stand out: electrophilic aromatic substitutions, nucleophilic addition or condensation with a *t*-butylamine, and reduction of carbonyl groups to the corresponding hydroxymethylene groups. These concepts are illustrated in a typical industrial route to albuterol⁵⁷ (Scheme 1.8).



Scheme 1.8: Synthesis of (rac)-albuterol from 4-hydroxyacetophenone.

1.5.2 Synthesis of (*R*)-Albuterol

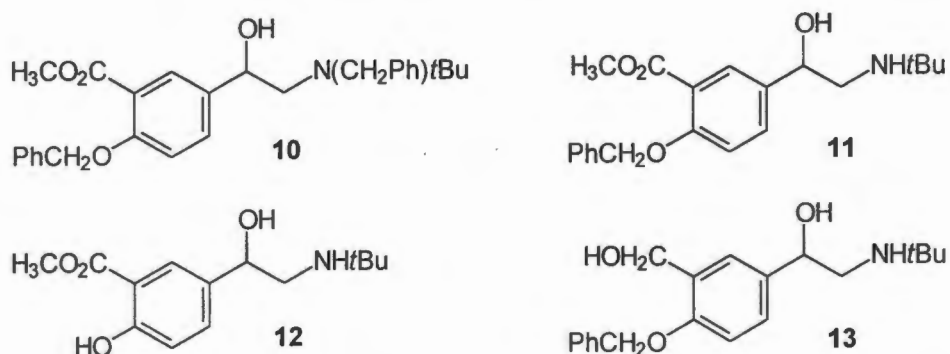
The most successful asymmetric synthesis of albuterol in homochiral form is based on enantioselective reduction using chiral oxazaborolidine catalysts.^{58,59} Optimum results were obtained on reduction of the benzyl-protected α -ketoimine as outlined in Scheme 1.9.



Scheme 1.9: Asymmetric synthesis of (*R*)-albuterol from methyl-5-acetylsalicylate

Difficulties in the classical resolution of (rac)-albuterol have been reported.⁵² The best result obtained in recent studies has been resolution with (*S*)-naproxen to produce (*R*)-albuterol with an ee of 86% and in 15% yield.⁵⁸ More success has been attained in resolving advanced intermediates of albuterol.

The first preparation of optically pure (*R*)-albuterol was *via* resolution of the doubly benzylated methyl ester **10** with (+)-di-*O*-toluoyltartaric acid which gave a 30% chemical yield in 97% ee.⁵² Reduction of the resolved base with lithium aluminium hydride, followed by catalytic debenylation gave (*R*)-albuterol which was characterised as an acetate salt. Other intermediates resolved include the benzyloxyarylethanolamine ester **11** with (+)-di-*O*-benzoyltartaric acid (37% yield, 95% ee on the resolution step),⁵⁸ arylethanolamine ester **12** with (+)-di-*O*-toluoyltartaric acid (30% yield, >99% ee)⁶⁰ and benzylated albuterol **13** with (+)-di-*O*-benzoyltartaric acid (37% yield, >99% ee).⁶¹ A process based on the last of these resolutions has been used by Sepracor to prepare multikilo quantities of (*R*)-albuterol hydrochloride for clinical trial purposes.



Resolution of albuterol *via* salt formation with a metal complex was reported in 1973.⁶² This involved the addition of (+)-Ba[CoEDTA]₂ to a solution of (*rac*)-albuterol in dilute H₂SO₄. After filtration to remove precipitated BaSO₄, the desired diastereomeric salt was precipitated by the addition of EtOH and Et₂O. (*R*)-Albuterol was recovered as the hydrochloride salt by addition of BaCl₂ to a solution of the diastereomeric salt in H₂O followed by precipitation of the resolving agent to leave the product which was then precipitated from the solution.

1.5.3 Determination of Enantiomer Composition of Albuterol

Apart from the traditional optical rotation measurements, other more recent approaches to the analysis of the enantiomer composition of albuterol have been reported.

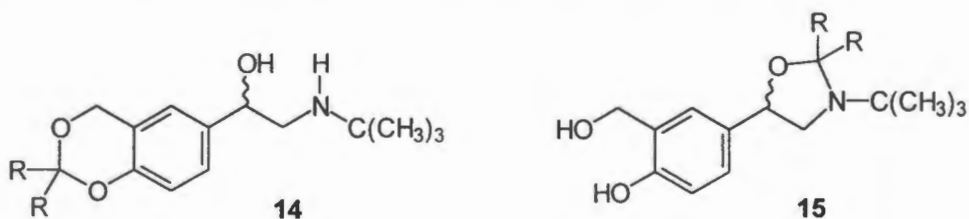
Analytical Separations have been performed by HPLC and capillary electrophoresis on chiral stationary phases. High performance liquid chromatographic separation has been achieved on a chiral α_1 -acid glycoprotein column⁶³ as well as a Pirkle-brush column.⁶⁴ The electrophoretic separation was accomplished using a cyclodextrin stationary phase.⁶⁵

NMR techniques used include the addition of either a lanthanide shift reagent⁶⁶ or *O*-acetylmandelic acid (as a chiral solvating agent)⁶⁷ to allow the discrimination of the enantiomers of albuterol, which are quantified by the integration of suitable peaks in the spectra produced.

1.6. The Approach taken in this work

The objective of this work was to produce (*R*)-albuterol using crystallisation techniques. As is evident from Scheme 1.8, the chiral centre is introduced late in the industrial syntheses of albuterol. The classical resolutions discussed in Section 1.5.2 are on intermediates other than those found in the routine synthesis of (*rac*)-albuterol. Producing these intermediates requires selective reduction of a suitably protected carbonyl compound with lithium aluminium hydride to give one of compounds **10** - **13**. These are then resolved and deprotected, as in the last step in Scheme 7, resulting in (*R*)-albuterol. The strategy adopted in this work was to produce a resolution target by the derivatisation of readily available (*rac*)-albuterol, rather than altering the routine synthesis of the drug. In order to compete with the resolutions described above the target sought needed to be produced in a single step with economically viable reagents. The same holds for the conversion of the resolved target back to (*R*)-albuterol. In selecting a target, the criteria used as a guide by ten Hoeve and Wynberg in the design of synthetic resolving agents⁶⁸ were considered, in particular the preference for rigidity in the compound.

In order to introduce rigidity into albuterol, the ketal **14** or oxazolidine **15**, were selected as resolution targets. Such protection reactions require symmetrical ketones such as acetone ($R = \text{CH}_3$) or benzophenone ($R = \text{Ph}$) in the presence of an acid catalyst whilst the deprotection is usually an acid hydrolysis. Both sets of conditions are cheap and amenable to large scale reactions.

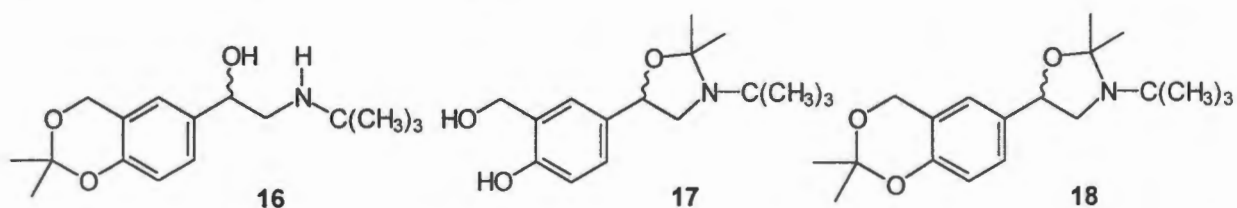


The work described in this thesis investigates the formation of a target derivative and the resolution thereof. Further synthetic and structural work performed in order to verify the absolute configuration of the resolved derivative is also described.

CHAPTER 2 DERIVATISATION AND RESOLUTION STUDIES

2.1 Derivatisation of Albuterol

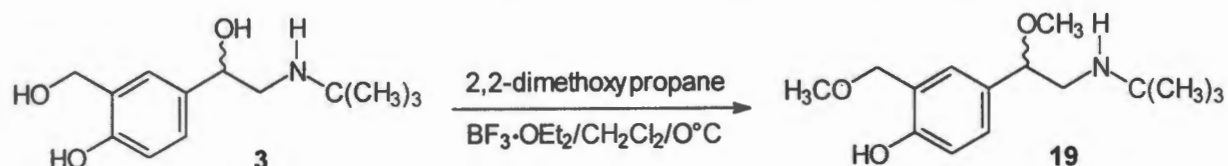
The isopropylidene derivatives of albuterol, **16** and **17** were those first targeted. Since both acetonide and oxazolidine formations utilise the same reaction conditions, it was hoped that the nature of the substrate would allow some chemoselectivity. Although formation of the diprotected adduct, **18** would lead to further reduction in the conformational freedom of the molecule, it would also block all functionality capable of hydrogen bonding. This was considered undesirable since intermolecular hydrogen bonding is a major contributor to the stability of the lattice in crystalline compounds.⁶⁹ It was rationalised that oxazolidine formation was more likely than ketalisation due to the superior nucleophilicity of an amine nitrogen in comparison to that of a hydroxyl oxygen.



Protections of this nature are traditionally carried out using dry acetone in the presence of an acid catalyst.⁷⁰ Refluxing of (rac)-albuterol in an excess of acetone with *p*-toluenesulfonic acid did not produce any reaction. Since a molecule of water is formed in the protection reaction, some means of dehydration is required. Azeotropic removal of water with toluene or benzene was not possible due to the insolubility of the polar starting material in these solvents and the low boiling point of acetone. An alternative method for isopropylidene ketal formation involving acetal exchange using 2,2-dimethoxypropane, was attempted. In this process, two moles of methanol are liberated with the equilibrium usually favouring complete product formation.⁷¹ No change, however, was observed in the reaction with albuterol.

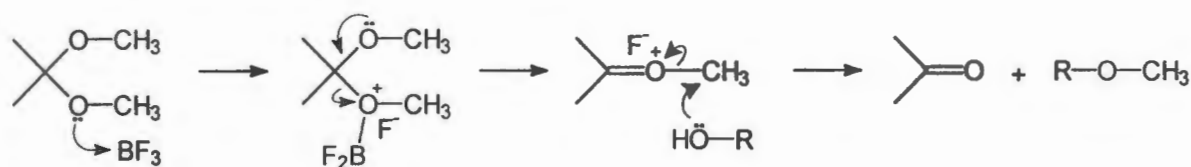
The use of a Lewis acid activator, $\text{BF}_3 \cdot \text{OEt}_2$, which would consume water or methanol produced, was thus introduced. In an excess of 2,2-dimethoxypropane, an inseparable mixture of products was produced, but a major product, **19**, could be isolated from the reaction between albuterol and 3 equivalents each of acid and 2,2-dimethoxypropane in dichloromethane (Scheme 2.1). The ^1H NMR shifts (3.16 and 3.44 ppm) for the new methyl protons of the product indicated that

methylation of both benzylic hydroxyl groups as opposed to the phenol or amine moieties (Ar-OCH_3 $\delta \approx 3.8$ ppm, N-CH_3 $\delta \approx 2.3$ ppm)⁷² had taken place.



Scheme 2.1

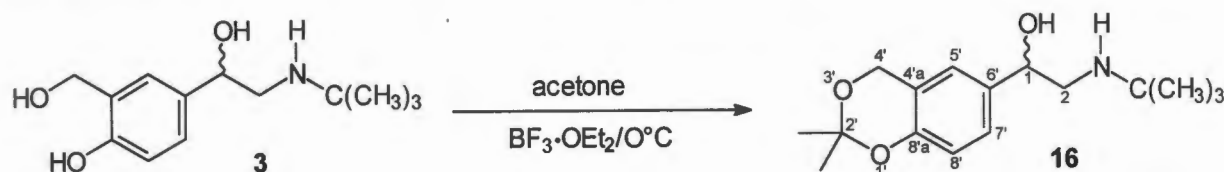
The observed methylation was a surprising result since, according to literature precedent, under acidic conditions, heteroatom attack at the ketal carbon of dimethoxypropane was expected. A plausible explanation for the methylation outcome is that methyl transfer from the methylated oxocarbenium ion, as shown in Scheme 2.2, took place. The chemoselectivity of methylation can be rationalised in terms of the relative hardnesses of the nucleophiles concerned. The harder oxygen nucleophile is preferred by the relatively hard methylating agent to the nitrogen nucleophile which is, in any event, quite sterically hindered. Clearly, of the three oxygen sites, the phenolic centre is of a much reduced nucleophilicity due to resonance. The issue of O versus N chemoselectivity re-emerges in Chapter 3.



Scheme 2.2

By comparison, the $\text{BF}_3 \cdot \text{OEt}_2$ catalysed condensation of acetone and albuterol yielded a single product which was identified as the isopropylidene ketal of albuterol, **16** (Scheme 2.3). The ^1H NMR spectrum revealed two singlets integrating for 3 protons each at 1.505 and 1.510 ppm respectively which confirmed the presence of diastereotopic methyl groups as expected from the formation of an isopropylidene derivative. The *t*-butyl methyl and benzylic methylene protons which both give rise to singlets, and the assignment of other protons was made on the basis of the coupling present. The geminal protons 2- H_A and 2- H_B constituted the AB portion of an ABX system with 1-H, and both resonated as double doublets at 2.56 and 2.80 ppm respectively ($J_{\text{A,B}} = 11.7$ Hz, $J_{\text{A,X}} = 9.0$ Hz, $J_{\text{B,X}} = 3.5$ Hz). The doublet of doublets for 1-H was located further downfield at 4.50 ppm. The aromatic protons 7'-H and 8'-H showed vicinal coupling (J 8.3 Hz), while an expected W-coupling was observed between 7'-H and 5'-H (J 1.6 Hz). These coupling

motifs were used to aid assignments in the spectra of all albuterol-based compounds synthesised in this work. ^{13}C - ^1H correlation spectroscopy (HETCOR) was used to assist in the assignment of the ^{13}C spectrum. The expected chemical shift for the acetal carbon in a 2,2-dimethyl-1,3-oxazolidine is ~ 81 ppm whilst that in the analogous 1,3-dioxane is ~ 99 ppm.⁷³ The observed shift for C-2', 99.5 ppm, thus indicated acetonide formation. The crystal structure of (+)-**16** confirmed the integrity of the acetonide (See Section 3.3). Since the reaction is under thermodynamic control, this unexpected chemoselectivity is ascribed to the thermodynamic preference for the 6-membered 1,3-dioxane over the oxazolidine in which some severe steric interactions, notably *t*-butyl *versus* the phenyl ring and dimethyl substituents, exist.



Scheme 2.3

Acetonide formation was also achieved when reacting acetone and albuterol in the presence of H_2SO_4 . A series of experiments were conducted on a 4 mmol scale and at 0°C in order to optimise the conditions for both the Lewis acid and mineral acid catalysed reactions. The results of these are summarised in Table 2.1.

Table 2.1: Optimisation of albuterol acetonide formation

Exp.	Acid	Equiv. ^a	Dehydrating agent	Equiv.	Rxn Time (min)	Yield (%) ^b	Impurities ^c
1	$\text{BF}_3\cdot\text{OEt}_2$	2	-	-	10	87	$\sim 3\%$
2	$\text{BF}_3\cdot\text{OEt}_2$	2	-	-	60	95	$< 1\%$
3	$\text{BF}_3\cdot\text{OEt}_2$	3	-	-	10	90	$\sim 5\%$
4	H_2SO_4	1	-	-	60	100	$\sim 3\%$
5	H_2SO_4	2	-	-	60	104	$\sim 5\%$
6	H_2SO_4	2	CuSO_4	2	10	102	$\sim 1\%$
7	H_2SO_4	1.5	CuSO_4	0.5	30	100	$\sim 3\%$
8	H_2SO_4	3	CuSO_4	1	30	109	$\sim 10\%$

a equivalents = moles acid used per mole albuterol

b based on mass of crude material

c as by-products and/or starting material which were demonstrated by tlc and quantitated by ^1H NMR of crude material

From Table 2.1 it can be concluded that greater than one equivalent of H_2SO_4 with CuSO_4 does not drastically increase the yield. Where more than two equivalents of acid were used, the impurity migrated on tlc as a less polar spot. This impurity could not be isolated cleanly for full characterisation, but ^1H NMR indicated the presence of the diprotected adduct, **18**. Although chromatographic purification was used in the experiments quoted in the experimental section, Chapter 5, no impurities could be detected by tlc or ^1H NMR after a single recrystallisation of the crude material from acetone or acetonitrile.

All efforts to produce the 2',2'-diphenyl analogue of albuterol isopropylidene ketal by condensation of albuterol with benzophenone were unsuccessful. This was probably because of the reduced electrophilicity of the carbonyl carbon due to resonance, as well as the additional steric crowding of the ketone by the phenyl substituents.

2.2 Space Group Determination of Albuterol Acetonide, **16**

Of the two main approaches to resolution using crystallisation techniques, direct crystallisation is preferred over diastereomeric salt formation since no resolving agent is required in the resolution process. In order to decide if direct crystallisation was applicable to the resolution of (rac)-**16**, it was necessary to determine whether the material was crystallising as a conglomerate or a racemic compound. The comparative methods mentioned in Section 1.2.1 could not be used since no resolved material was available for comparison to the racemate. This necessitated the use of X-ray methods to determine the space group of (rac)-**16**, which allowed distinction between a conglomerate and a racemic compound.

The first oscillation photograph of a single crystal of this compound, grown from acetone, showed the presence of a mirror plane. Reflections in the zero level Weissenberg showed two further mutually orthogonal mirror planes and from these two photographs, which indicated *mmm* Laue symmetry, the crystal system was established to be orthorhombic. In addition to extensive precession photography, cone-axis photographs were recorded. These yielded the following preliminary cell constants:

$$a = 25.3 \text{ \AA} \quad b = 41.1 \text{ \AA} \quad c = 6.0 \text{ \AA}$$

Photographs of the general layers showed the condition: $h + k = 2n$ which is consistent with a C-centred lattice. The photographs also revealed the following conditions limiting possible reflections:

0kl	(k = 2n)
h0l	(h = 2n)
hk0	h = 2n, k = 2n
h00	(h = 2n)
0k0	(k = 2n)

These data are indicative of two possible space groups, Cmma (No. 67⁷⁴) and Cm2a (a non-standard setting of Abm2, No. 39⁷⁴), with the former group being centric and the latter acentric. An intensity data collection was performed and the intensity statistic ($|E^2 - 1|$) compared to theoretical values in an attempt to assign the space group present as either centric or acentric:

Data	Theoretical - Centric	Theoretical - Acentric
0.896	0.968	0.736

No unambiguous conclusions about the centricity of the crystal could be made from these values. Attempts to elucidate the structure in either space group using direct methods failed, despite many trials with the program SHELX-86⁷⁵ using both default and modified approaches. This failure was ascribed to the presence of pseudosymmetry which manifested itself in some unusual features on the X-ray photographs. Firstly, diffuse streaking was noted in alternate reciprocal lattice rows running parallel to the b^* axis. Secondly, the additional condition $h = 4n$ was noted on the $h0l$ photograph as well as $k = 4n$ along $0k0$. These conditions do not relate to any orthorhombic space group and are thus ascribed to the presence of pseudosymmetry. However, although assignment of the correct space group was not completed, both of the possible space groups contain mirror planes, thus necessitating the presence of both enantiomers of a chiral molecule in the crystal. The crystalline material was thus established to be a true racemate and resolution *via* diastereomeric salt formation was the necessary approach.

2.3 Diastereomeric Salt Formation

Owing to the lack of predictability of the resolution step, the crystallisation array strategy advocated by Wilen *et al*³³ was followed. The following components were included in the pilot study:

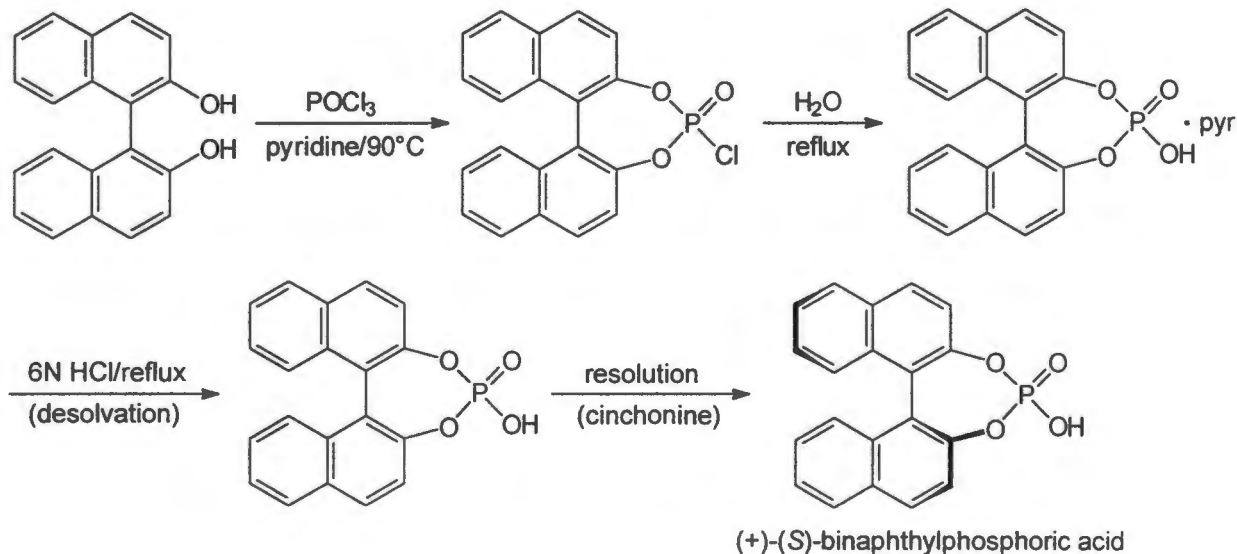
(i) Resolution substrates (bases): albuterol **3** and albuterol acetonide **16**.

Parallel arrays were performed on both bases in order to confirm the reported lack of success in resolving albuterol.

(ii) Resolving agents (acids): The acids listed below were available

(1 <i>R</i>)-(-)-Camphor-10-sulfonic acid	(CSA)
(2 <i>R</i> ,3 <i>R</i>)-(-)-Di- <i>O</i> -benzoyltartaric acid monohydrate	(DOBT)
(<i>S</i>)-(-)-Malic acid	(MA)
(2 <i>R</i> ,3 <i>R</i>)-(+)-Tartaric acid	(TA)
(<i>S</i>)-(+)-Mandelic acid	(MDA)

In addition, (*S*)-(+)-1,1'-Binaphthylphosphoric acid (BNP) was prepared in 85% yield and 98% ee from racemic binaphthol using the method of Jaques and Fouquey⁷⁶ (Scheme 2.4).



Scheme 2.4

(iii) Solvents: methanol, ethanol, acetone and ethyl acetate.

A statistical analysis by Jaques *et al*²⁴ of solvents used in over 800 resolutions showed that alcohols, acetone, water and mixtures of solvents containing alcohols were used in 90% of the cases. Water could not be used here due to the insolubility of **16**, so ethyl acetate, as the next most prevalent solvent, was included.

Crystallisation was induced by slow cooling followed by slow evaporation of the solvent. Where suitable material was obtained, the melting point was measured and compared to the melting point of the components to give an indication of the formation of a new species. The results of the trial arrays are summarised in Tables 2.2 and 2.3 and the notes which follow.

Table 2.2: Experiments with albuterol (3) as base

Acid	Methanol	Ethanol	Ethyl acetate	Acetone
(+)-BNP	Paste	Paste	Insoluble	Paste
(-)-DOBT	Oil	Oil	Insoluble	Oil
(-)-CSA	Oil	Paste	Insoluble	Paste
(-)-MA	Oil	Oil	Insoluble	Insoluble
(+)-TA	Oil	Crystalline (a)	Insoluble	Insoluble
(+)-MDA	Oil	Oil	Insoluble	Insoluble

Table 2.3: Experiments with albuterol acetonide (16) as base

Acid	Methanol	Ethanol	Ethyl acetate	Acetone
(+)-BNP	Paste	Paste	Crystalline (b)	Paste
(-)-DOBT	Crystalline (c)	Crystalline (d)	Powder	Powder
(-)-CSA	Oil	Paste	Paste	Crystalline (e)
(-)-MA	Oil	Paste	Insoluble	Oil
(+)-TA	Oil	Paste	Insoluble	Crystalline (f)
(+)-MDA	Oil	Oil	Oil	Oil

- (a) A few crystals were obtained on slow evaporation of the solvent. These melted at 99°C which is unique. Attempts to repeat this experiment resulted in the formation of oils.
- (b) The crystals obtained on slow evaporation decomposed from 290°C. These are likely to be crystals of the resolving agent (lit. mp 300°C dec.).
- (c), (d) Fine crystals formed on cooling which melted at 185-195°C which is unlikely to be either resolving agent (lit. mp 90°C) or base (mp 91°C).
- (e) Crystals were obtained on complete solvent evaporation and these decomposed from 190°C which is similar to the melt of the resolving agent (lit. mp 198°C dec.).
- (f) Crystallisation occurred on solvent evaporation. The melt at 90°C coincided with that of 16 (91°C)

The DOBT/16 series of experiments appeared most worthy of further investigation and that in methanol was repeated on a larger scale, using the non-hydrated resolving agent, in order to allow further characterisation of the solid material obtained. Salt formation between (2*R*,3*R*)-(-)-di-*O*-toluoyltartaric acid (DOTT) and 16 was also attempted and proceeded in a similar fashion.

A recent study on the diastereomers formed between pipercolic acid anilides and DOBT shows that for 50% of the species studied, the diastereomers formed were complexes as opposed to salts.⁷⁷ In addition, when salts were formed, the acid and base were present in a 1:2 ratio whereas the ratio for complexes was 1:1. The infrared spectra for the DOBT and DOTT diastereomers formed here showed a broad band centred around 2700 cm⁻¹ and a strong band at 1640 cm⁻¹ which were assigned as ammonium N-H and carboxylate C-O stretching frequencies respectively. Those in the non-ionised species would have absorbed at ~3400 and 1720 cm⁻¹ respectively, thus confirming that the species formed were, indeed, salts. The ¹H NMR spectra were run in DMSO and that for the DOBT salt has been reproduced in Fig. 2.1 on page 24. Comparison of the integrals for the peak assigned to the *t*-butyl methyl protons (1.13 ppm) and the DOBT methine proton (5.66 ppm) gives a 9:1 ratio of protons. This is consistent with a 1:2 acid:base salt. Microanalysis confirmed this result for the salts of both acids. These results were in contrast to DOBT or DOTT resolutions of other protected albuterol derivatives^{52,58-61} in which, although no experimental evidence is presented, the implication from diagrams is that 1:1 salts were formed. The 1:2 ratio is advantageous industrially since a maximum of 0.5 equivalents of resolving agent is required in the resolution.

Further resolution experiments were performed with the acid and base being combined in 1:2 proportions. The solvent was removed from the mother liquors of a crystallisation experiment with each salt and the resulting material dried under vacuum to give a colourless solid. Optical rotations of the precipitates and mother liquors were determined:

Table 2.4: Optical rotations of material from salt formation experiments.

Resolving Agent	Precipitate [α] _D	Mother Liquor [α] _D	Resolving Agent [α] _D
(-)-DOBT	-30°	-60°	-116°
(-)-DOTT	-39°	-73°	-138°

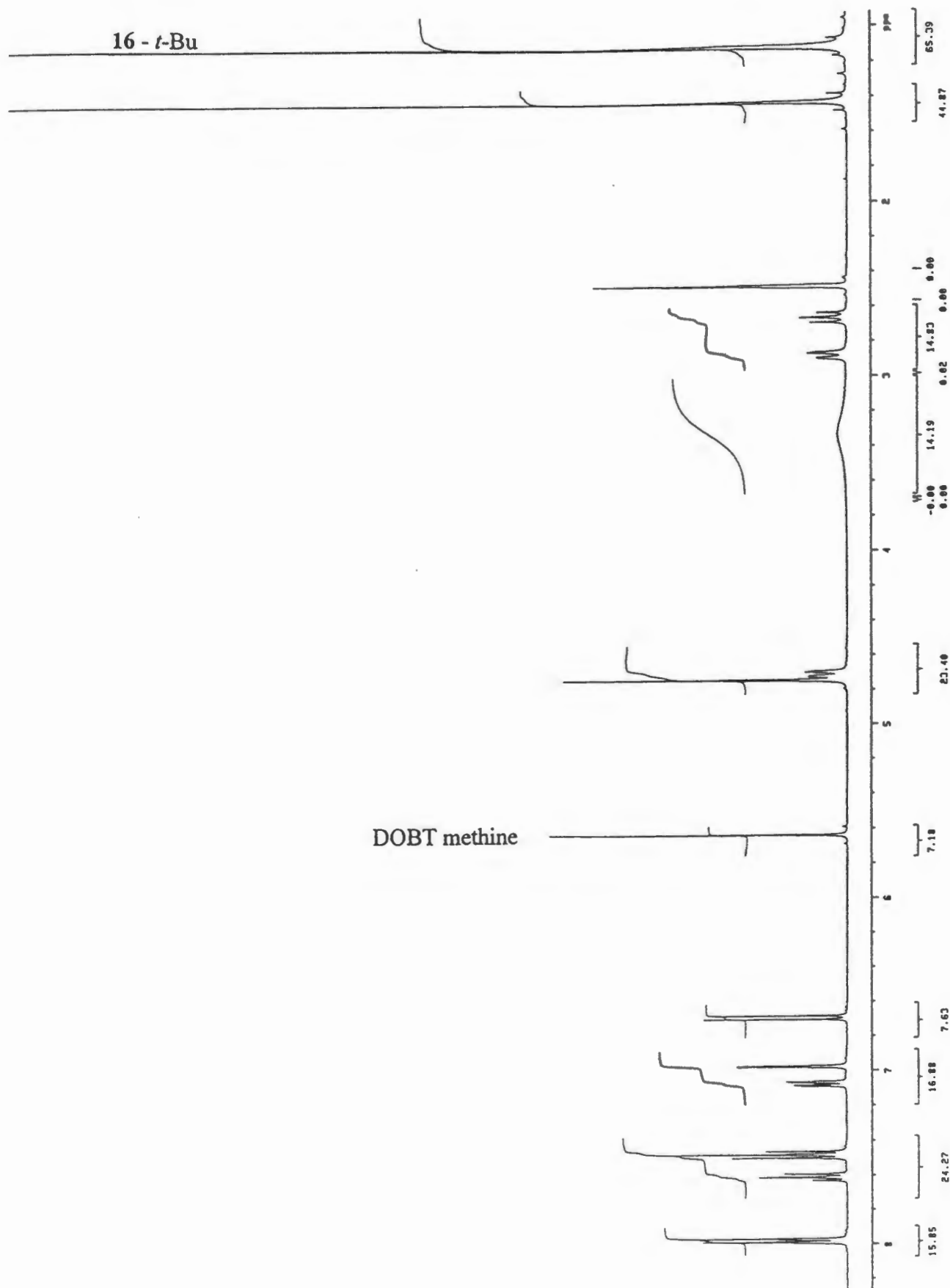


Figure 2.1: ¹H NMR Spectrum of DOBT-albuterol acetonide salt

Two conclusions could be drawn from these results: firstly, the disparity between the rotations of the mother liquor and the precipitate indicated that some enantiomeric enrichment had taken place and secondly, because the precipitate rotation was less negative, that the (+)-16/(-)-acid salt, *i.e.* the n-salt was that precipitating.

The enriched ketal was extracted in very high yield from each of the precipitates in a basic work-up procedure to give an optical rotation of $+16^\circ$ in each case. Since the absolute rotation of either enantiomer of 16 was unknown, alternative means of evaluating resolution efficiency was required and those applied are discussed in Section 2.4. Acidification of the aqueous phase from the ketal recovery allowed extraction of the resolving agent into ethyl acetate. Both resolving agents were recovered in high yields ($>95\%$) and optical purity ($>97\%$ ee).

The absolute configurations of the enantiomers of 16 were also unknown when these experiments were started. A series of experiments on the resolved material were undertaken in order to establish this and these are described in Chapter 3. Hydrolysis of this material (see Section 2.6) gave rise to (*S*)-(+)-albuterol acetate. Since the (*R*)-enantiomer is that desired, further resolution work was undertaken using (2*S*,3*S*)-(+)-DOBT and (2*S*,3*S*)-(+)-DOTT and the salts referred to in the remainder of this work are (*R*)-16/(2*S*,3*S*)-DOBT, 20 and (*R*)-16/(2*S*,3*S*)-DOTT, 21 (Fig 2.2). The (2*S*,2*S*)-resolving agents are derivatives of unnatural tartaric acid which are more expensive than those of the natural (2*R*,3*R*)-isomer. They are, however, also the enantiomers required in the aforementioned resolutions of compounds 10-13. A recent resolution of DOBT by preferential crystallisation of its calcium salt-methoxyethanol complex⁷⁸ provides a route that should lead to cheaper sources of these resolving agents.

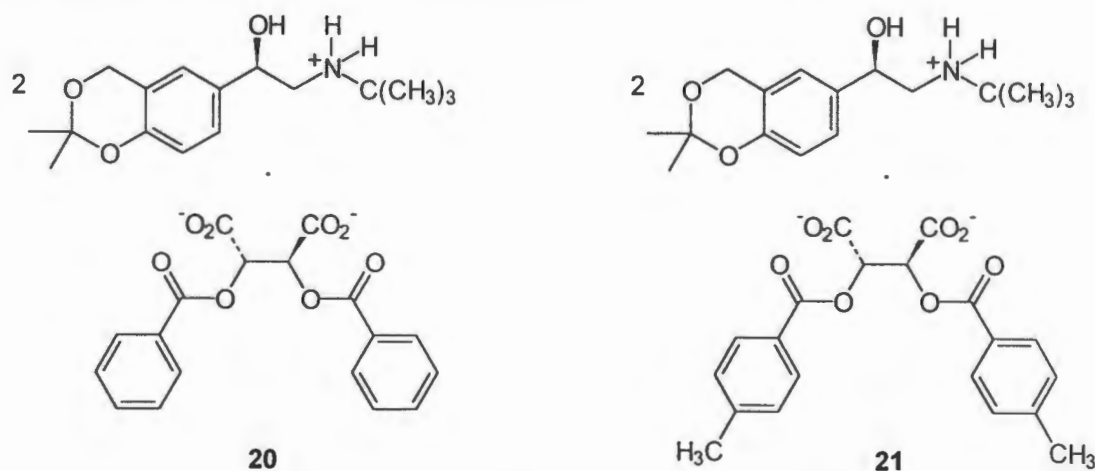


Figure 2.2: DOBT and DOTT n-salts of 16

2.4 Determination of Enantiomeric Purity

2.4.1 ¹H-Nuclear Magnetic Resonance

(*R*)- or (*S*)-*O*-acetylmandelic acid (OAM) forms soluble diastereomeric salts with a wide range of chiral amines and amino alcohols, thus permitting a direct measure of their enantiomeric composition by NMR spectroscopy.⁶⁷ The spectrum for (rac)-**16** with (*R*)-OAM in CDCl₃ was recorded at 0°C (400 MHz) and is reproduced in Fig. 2.3 on page 27. The expansions shown indicate a number of areas where chemical shift non-equivalence is observed for the diastereomers. In the literature report on OAM, the peaks for the methylene group α- to the amine in albuterol were simplified by simultaneous irradiation of the adjacent methine proton, and the integrals determined. In the spectrum obtained here, the obvious peaks to use for quantitative work were those of the *t*-butyl methyl protons (δ~1.2 ppm) since they were uncomplicated singlets, and because of the increased sensitivity achieved by integrating for a higher number of protons. A spectrum for a resolution sample of (*R*)-**16** (~80% ee) is shown in Fig. 2.4 on page 28.

Although the shift non-equivalence was found to be higher at 0°C (Δδ = 0.10 ppm), the spectra run at room temperature showed suitable resolution (Δδ = 0.05 ppm) of the peaks being used. Use of this method was, however, limited by a lack of sensitivity due to: (i) the enantiomeric purity of the OAM used (98% ee) and (ii) the inherent limits of quantitative NMR for which limit of detection is estimated to be approximately 2%.¹³

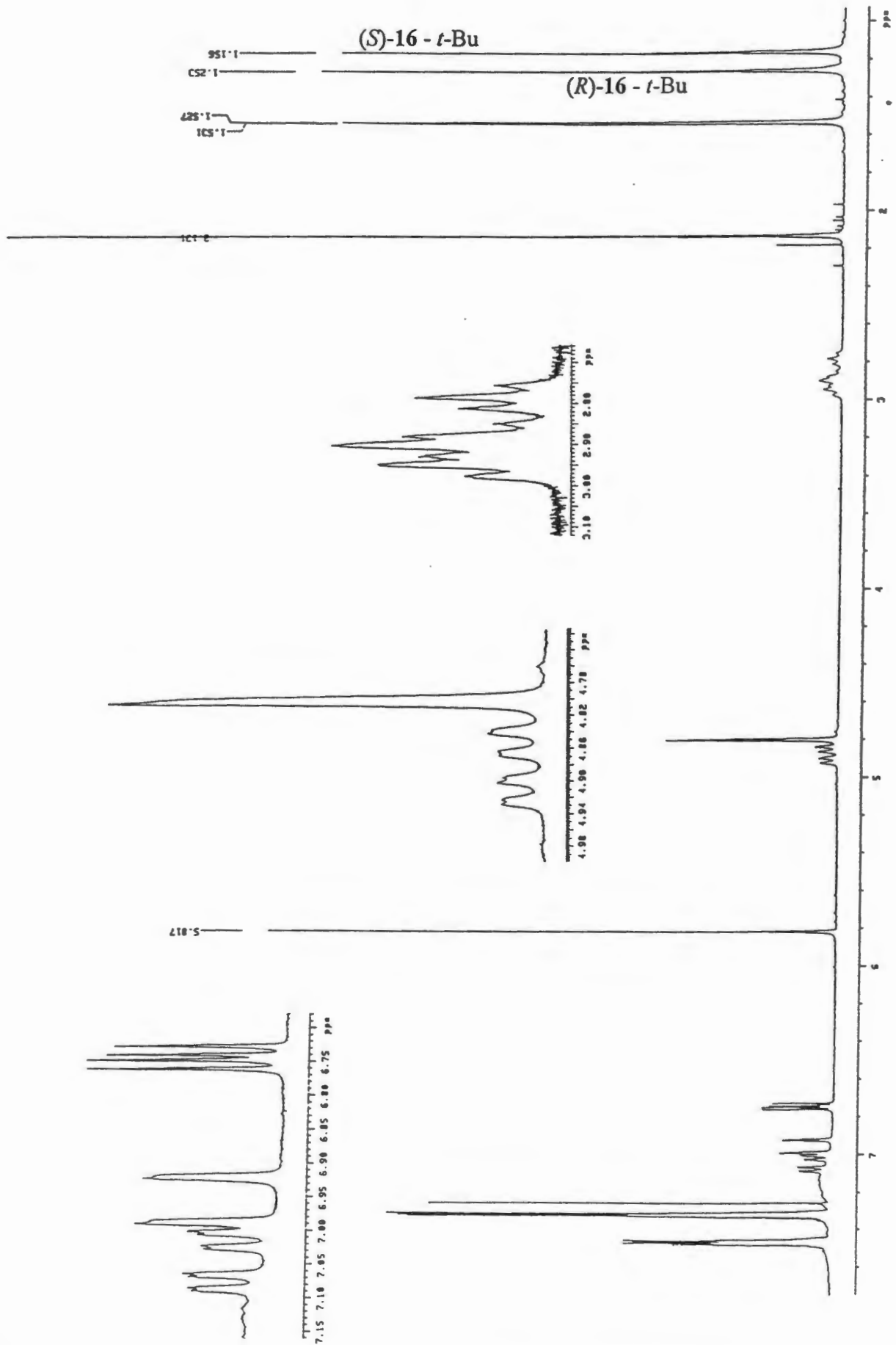


Figure 2.3: ¹H NMR spectrum of (rac)-16 with (R)-OAM in CDCl₃

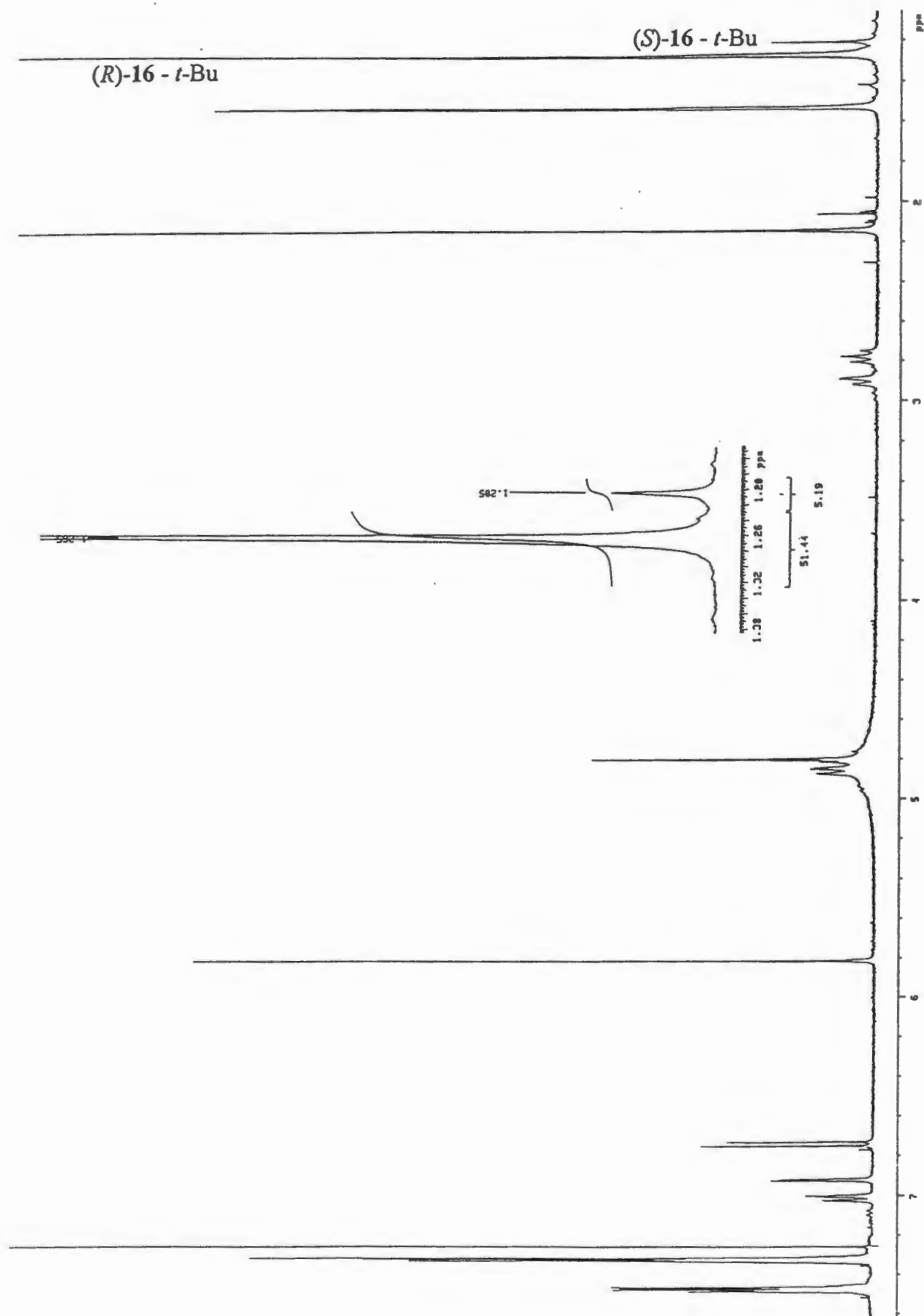


Figure 2.4: ^1H NMR spectrum of $(R)\text{-16}$ with $(R)\text{-OAM}$ in CDCl_3

2.4.2. High Performance Liquid Chromatography

Separation of the enantiomers of albuterol by a commercially available Pirkle-type chiral stationary phase formed by a urea linkage between (*R*)-1-(α -naphthyl)ethylamine and (*S*)-indoline-2-carboxylic acid, and which is grafted onto silica gel, has been demonstrated.⁶⁴ The likely stereoselective sites of interaction of this stationary phase are illustrated in Fig. 2.5.⁷⁹ Apart from the reduced number of sites for hydrogen bonding, the interactions of 16 with this phase should be similar to those of albuterol.

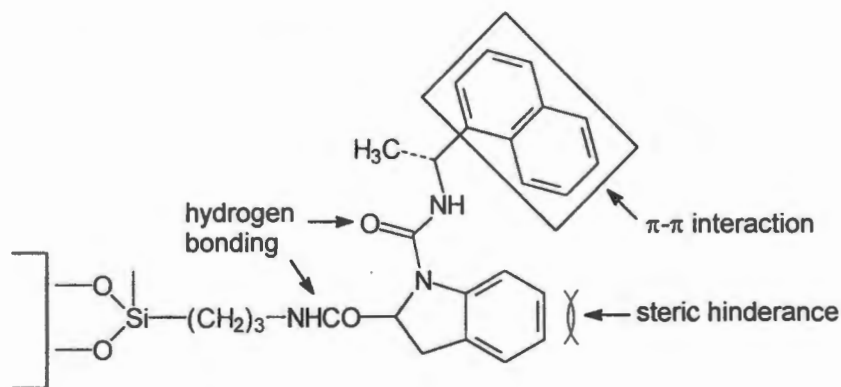


Figure 2.5: Possible stereoselective sites of interaction on the chiral stationary phase used

Separation of the enantiomers of 16 was achieved on this column using a less polar mobile phase than that used for albuterol. A typical chromatogram for a racemate sample is reproduced on page 31 (Fig. 2.7(a)). The earlier eluting peak is that of the (*S*)-enantiomer (retention time 10.7 min) while (*R*)-16 elutes at 12.5 min. This order of elution is desirable since, if it were reversed, (*S*)-16 as the small impurity peak would elute on the tail of the major (*R*) peak in sample solutions.

Samples were initially prepared by dissolution in the mobile phase (hexane/1,2-dichloroethane/methanol/trifluoroacetic acid 240/140/7.5/1), but decomposition was noted over a 12 hour period. The solutions were stable when trifluoroacetic acid was removed from the solvent.

A series of standards of the racemate were prepared and injected in order to determine the limit of quantitation and ensure linearity of the response. The results (areas of the (*S*)-peak) are presented in Table 2.5. At concentrations lower than $0.044 \text{ mg}\cdot\text{cm}^{-3}$ the reproducibility of integration was unsatisfactory. A concentration of $0.044 \text{ mg}\cdot\text{cm}^{-3}$ of the racemate gives 0.022

$\text{mg}\cdot\text{cm}^{-3}$ of either enantiomer which relates to an ee of 99.56% when a $10 \text{ mg}\cdot\text{cm}^{-3}$ sample solution is injected. The limit was thus set at 99.5% ee for samples of this concentration. Linear regression analysis of the results produced a satisfactory calibration curve (Fig. 2.6).

Table 2.5:

Concentration ($\text{mg}\cdot\text{cm}^{-3}$)	Mean Area	Relative Standard Deviation (%)
1.100	2412531	0.23
0.440	971840	0.45
0.088	198830	0.47
0.044	101707	1.97

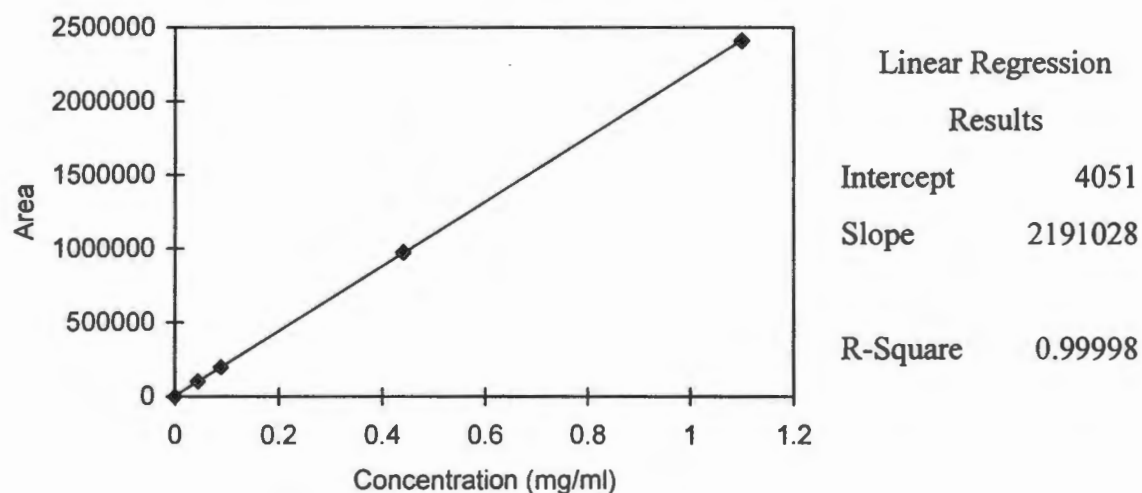


Figure 2.6: Calibration curve for (S)-16

In the sample determinations, the areas of the enantiomer peaks were compared in order to determine ee as an alternative to use of the calibration curve to determine the actual content of (S)-16 in the sample. The reasons for this were twofold: (i) the solutions were prepared in very small volumes (1 cm^3) and the relative proportion of each enantiomer present is independent of this volume which is likely to have a degree of error attached and (ii) the purpose of the determination was to evaluate resolution efficiency and not overall purity. A typical sample chromatogram is reproduced in Fig. 2.7(b) overleaf.

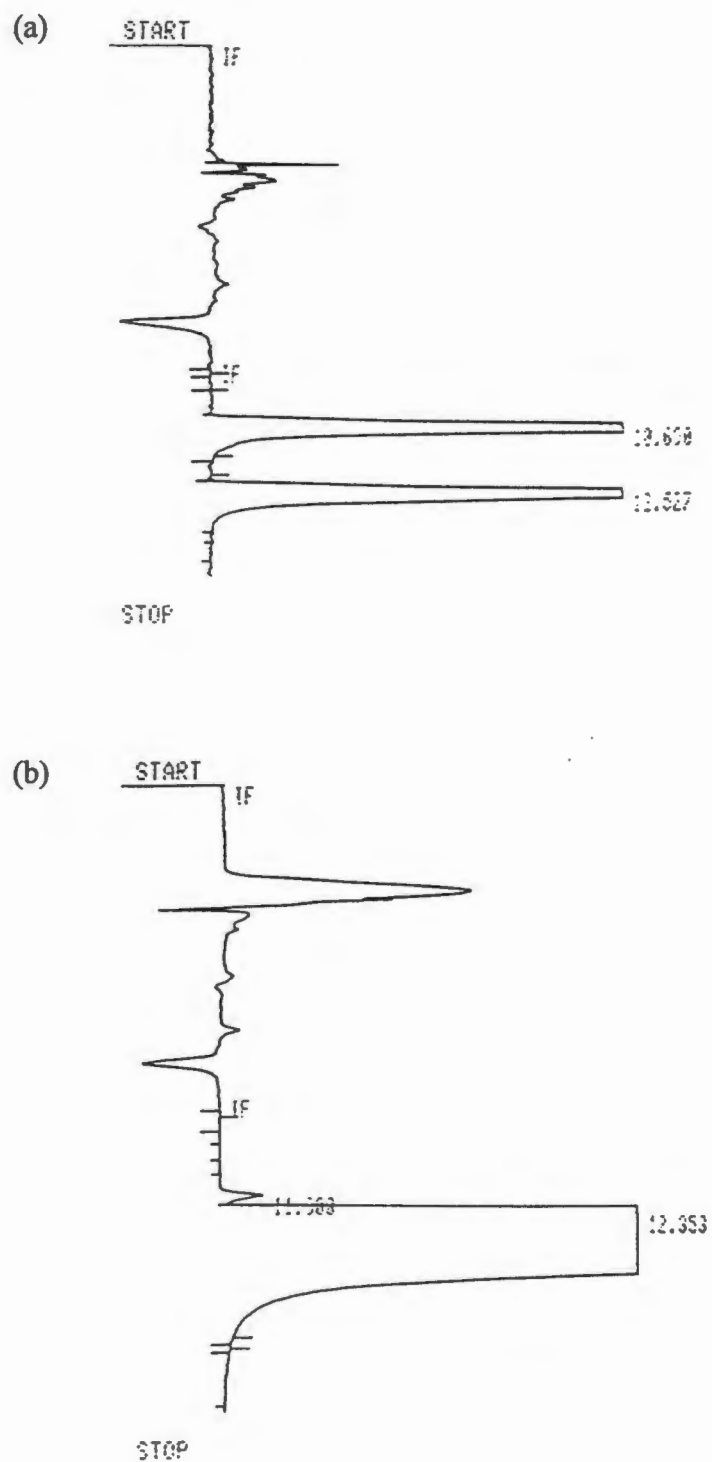


Figure 2.7: Chromatograms showing the separation of the enantiomers in:

(a) a 0.440 mg.cm⁻³ solution of (rac)-16

(b) a sample of (R)-16 (>99.5% ee).

Once a sample of 100% (*R*)-**16** had been produced, the $[\alpha]_D$ for the compound in methanol was determined as -18.9° and rotation could then be used as a preliminary measure of enantiomeric purity.

The calibration exercise undertaken for **16** was repeated on (*rac*)-albuterol. The retention times for the peaks, which eluted in the same order as **16**, were 16.9 and 19.9 min respectively. The material was insoluble in the sample solvent and was thus dissolved in a minimum of methanol and then diluted with sample solvent. The sample concentrations had to be reduced since a high methanol content resulted in poor chromatography. The quantitation limit was set at 0.023 mg.cm^{-3} racemate which gave a 99.5% ee limit for a 5 mg.cm^{-3} solution. Regression again revealed a linear relationship ($R^2 = 0.99997$). The treatment of sample data was as for **16**.

2.5 Resolution studies

^1H NMR shift experiments on the initial resolutions performed showed the enantiomeric excesses to be approximately 90%. This increased to 97% after a single recrystallisation of resolved **16**. These positive results led to further investigation of the resolution by both acids. With suitable means of evaluation in place, a number of experiments were attempted in order to determine the effect of certain variables on the resolutions. In each case **16** was extracted from the salts (either **20** or **21**) and the enantiomeric purity of the crude extract determined by the method indicated. Yields are those based on 100% being the full recovery of a single enantiomer.

Parallel resolution experiments with DOBT in ethanol were performed on the crude material isolated from both $\text{BF}_3\cdot\text{OEt}_2$ and H_2SO_4 catalysed preparations of **16**, and compared to the resolution of a recrystallised sample. As is evident from the table below, the chemical yield, more than the optical purity, was affected by the sample purity.

Table 2.6: Effect of purity of **16** on DOBT resolution (optical rotation)

	$\text{BF}_3\cdot\text{OEt}_2$	H_2SO_4	recrystallised
Yield (%)	78	86	91
ee (%)	80	81	85

Since the above resolutions from ethanol were considerably poorer than those from methanol, DOBT resolution was investigated for solvent dependence. The acid and base were each dissolved in warm solvent and the acid solution added to the base to give a 20 mg.cm^{-3} solution with respect to **16**. The precipitate produced from ethyl acetate was so fine that any filter used clogged and no meaningful results could be obtained. The other results are summarised in Table 2.7.

Table 2.7: Solvent dependence of DOBT resolution (optical rotation)

	Methanol	Ethanol	Ethanol/H ₂ O (95/5)
Yield (%)	34	96	78
ee (%)	99	67	89

Although the results for these resolutions were encouraging, the reproducibility between sets of experiments was unsatisfactory. It was felt that the temperature of the component solutions being added together, the rate of addition, and the rate of cooling of the diastereomer mixtures were also influencing the outcome of the resolutions. The optimisation of all these parameters, since demanding in terms of both material and time, was not undertaken in this study.

As a comparison of the DOBT and DOTT resolutions, parallel experiments as described in Chapter 5 (synthesis of **20** and **21**) were performed, with extreme care being taken to keep the aforementioned variables constant. These results are tabulated below.

Table 2.8: Comparison of DOBT and DOTT resolutions of **16** (hplc)

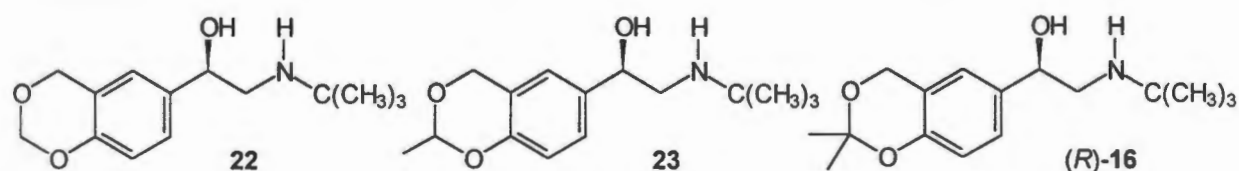
Resolution Stage		DOBT	DOTT
First precipitation of salt	Yield	70	90
	ee (%)	89.5	92.1
Recrystallised salt	Yield	63	80
	ee (%)	>99.5	95.5

The DOTT resolution was more successful in the initial stage but purification by recrystallisation of the salt was not successful due to the insolubility of **21** in most organic solvents. The sample here was slurried rather than recrystallised. The concentration of salt in the recrystallisation solvent was maintained for **20** in order to allow comparison with **21**, although a lower volume of

solvent was maintained for **20** in order to allow comparison with **21**, although a lower volume of methanol would have sufficed for complete dissolution. The recrystallisation of **20** provided a notable improvement in optical purity but the yield was low. The use of a less polar solvent or a smaller volume of methanol may provide an optimised result. The (*R*)-**16** obtained from the DOTT resolution was recrystallised three times from acetone, resulting in the following improvement to the ee: 95.5 → 99.5 → >99.5 → no (*S*)-**16** detected. The construction of ternary phase diagrams (described in Chapter 1) for the DOBT and DOTT salts in likely resolution and recrystallisation solvents, as well as for the enantiomers of **16** in recrystallisation solvents would allow determination of: (i) the optimum conditions of the resolution, and (ii) the stage in the procedure at which to purify resolved material.

2.6 Hydrolysis of Albuterol Acetonide **16**

In a recent publication by Effenburger and Jäger,¹⁷ difficulties in the acid hydrolysis of the (*R*)-albuterol ketals **22** and **23** was described. When HCl was the acid used, racemisation and decomposition were noted. They also reported several failed attempts to hydrolyse under neutral conditions.

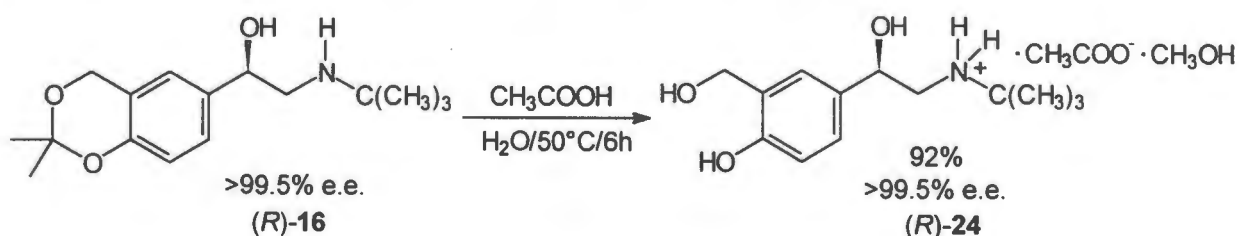


As a protecting group for 1,2 and 1,3 diols the isopropylidene ketal in **16** is usually preferred to the methylene or ethylidene equivalents in **22** and **23**, because it is the most reactive towards acid hydrolysis. It is thus surprising that synthesis of (*R*)-**16** was not attempted in the Effenburger study.

Hydrolysis of isopropylidene ketals at mild temperatures has been achieved with acetic acid.⁸⁰ A number of reaction conditions were explored in the acetic acid hydrolysis of **16** and complete reaction was only achieved in those in which acetic acid/water 50/50 was used in a 20-fold excess as the solvent for the reaction. When heated to reflux, the reaction was complete in 1.5 hours. The reaction time increased to 6 hours when the solution was stirred at 50°C. In both cases decomposition products were only detected well after completion of the reaction.

Isolation of the hydrolysed product from the reaction proved problematic. Since albuterol is soluble in water, standard basic work-up conditions to isolate the free base were not viable. It was thus decided to isolate the albuterol as an acetate salt, as in the first separation of the enantiomers of albuterol.⁵² Attempted azeotropic removal of the excess reagents with toluene resulted in decomposition of the product when low volumes were reached. Vacuum distillation at 40°C allowed removal of the reagents without any decomposition of albuterol. The oil formed was taken up in methanol and addition of ethyl acetate prompted precipitation of the product, albuterol acetate monomethanolate **24**, in 92% yield.

Hplc was used to determine the effect of the hydrolysis conditions on the enantiomeric purity of the material. A (*R*)-albuterol ketal sample of >99.5% ee was hydrolysed at 50°C as described above. Once reaction was complete, an aliquot of the reaction mixture was taken and most of the water removed by azeotropeing with isopropyl alcohol. The sample was then diluted as for solid samples. Hplc analysis revealed the enantiomeric excess of the material to be unchanged. The reaction mixture was then refluxed for 2 hours. Hplc showed the presence of some early eluting impurities, as well as a decrease in the ee to 97.7%, thus demonstrating that higher temperatures are required in order to effect racemisation by acetic acid. A sample of (*R*)-**16** of lower enantiomeric purity (95.5% ee) was similarly hydrolysed in order to determine the effect of the isolation procedure on ee. The enantiomeric excess of the crystalline (*R*)-**24** isolated was determined at 97.0% ee. Recrystallisation of **24** thus provides another opportunity for optimisation of the optical purity of the product and, as before, the construction of a phase diagram in order to determine the eutectic of **24** in various recrystallisation solvents would allow evaluation of this as a purification step. The optimised hydrolysis procedure is illustrated in Scheme 2.5.



Scheme 2.5: Hydrolysis of (*R*)-**16**

Characterisation of (*R*)-24 was not straightforward owing to its crystallisation as a methanol solvate. Inconsistent microanalytical results were obtained due to partial desolvation on drying. Thermogravimetric analysis (Fig. 2.8) of a sample freshly removed from the mother liquor showed a mass loss of approximately 10% over the range 80-140°C which is as expected for the inclusion of one molecule of methanol per salt formula unit (Theoretical mass loss = 9.7%). This is followed by mass loss due to decomposition of the salt after melting of the desolvated crystal at 144°C. The trace produced by differential scanning calorimetry over the same temperature range, also reproduced in Figure 2.8, shows two endotherms confirming these two events (desolvation and melting). ¹H NMR of the same sample shows a peak at $\delta = 3.17$ ppm which integrates for 3 protons and corresponds to that expected for the methyl protons on methanol, thus confirming the presence of a 1:1 methanol solvate. Microanalysis was performed on a sample dried at 120°C overnight and gave the correct analysis for the desolvated salt. Optical rotation measurements were also made on the dried salt.

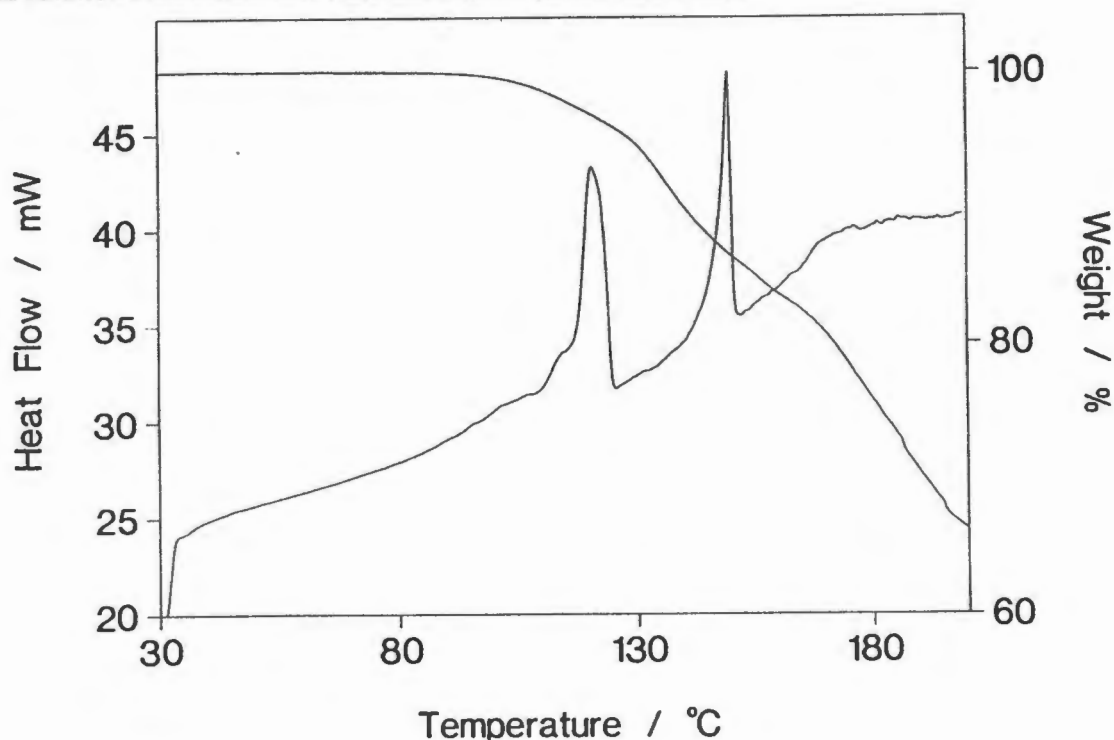


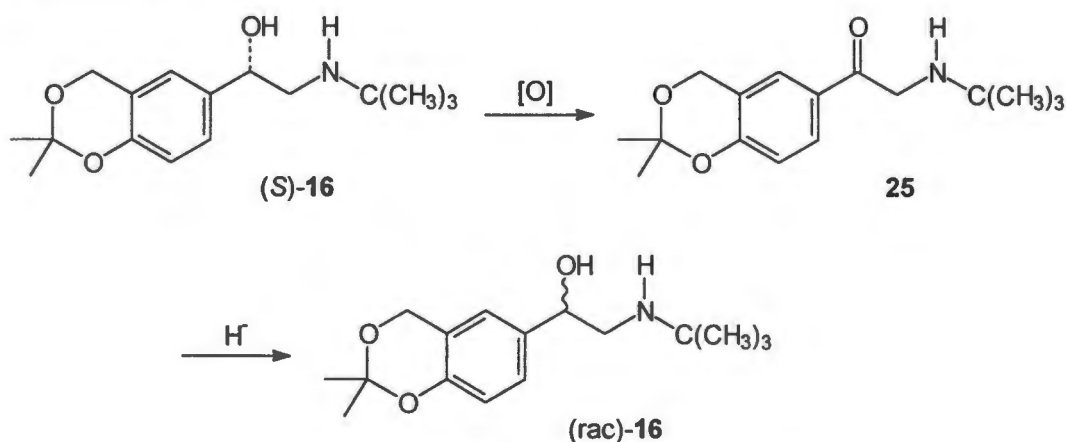
Figure 2.8: Thermogravimetric and differential scanning calorimetric analysis of (*R*)-24

A study of the cleavage of acetals using a sulfonic acid-based polystyrene cation exchange resin, Amberlyst-15, has been documented.⁸¹ It is an attractive means of catalysing the hydrolysis because the work-up is exceedingly simple. When molecules with no basic functionality are hydrolysed, the resin is simply filtered off and the solvent removed to leave the crude product. With an amine such as 16, the product would be retained on the resin and elution with a basic

solvent would be required. The route is additionally attractive in the case of albuterol because the elution would allow isolation of (*R*)-albuterol as a free base as opposed to the acetate salt. Tlc showed the hydrolysis to be complete after stirring a solution of **16** in methanol/water, with the resin, at room temperature overnight. When acetone was the reaction solvent (as used by Coppola⁸¹), decomposition was noted by TLC prior to completion of the reaction. Elution of the product from the resin was only partially achieved with 50% methanol/triethylamine or methanol/ammonia (prepared by passing a stream of ammonia through methanol for 20 min). Owing to the poor recoveries, this method was not pursued. Other strong cationic exchange resins with differing elution properties could be investigated, although epimerisation in the strongly acidic conditions may be problematic.

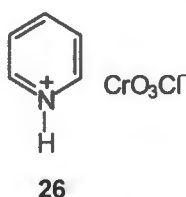
2.7 Racemisation Studies

The economic viability of resolution procedures frequently depends on the ability to racemise and recycle the unwanted enantiomer. The initial racemisation route envisaged here was *via* oxidation of (*S*)-**16** to the α -amino ketone **25** followed by hydride reduction to give (*rac*)-**16** as depicted in Scheme 2.6.



Scheme 2.6: Envisaged racemisation of (*S*)-**16**

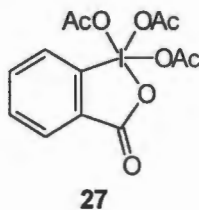
The most common species used for the oxidation of secondary alcohols to ketones is hexavalent chromium which is available in various reagents such as pyridinium chlorochromate (PCC) **26**.⁸²



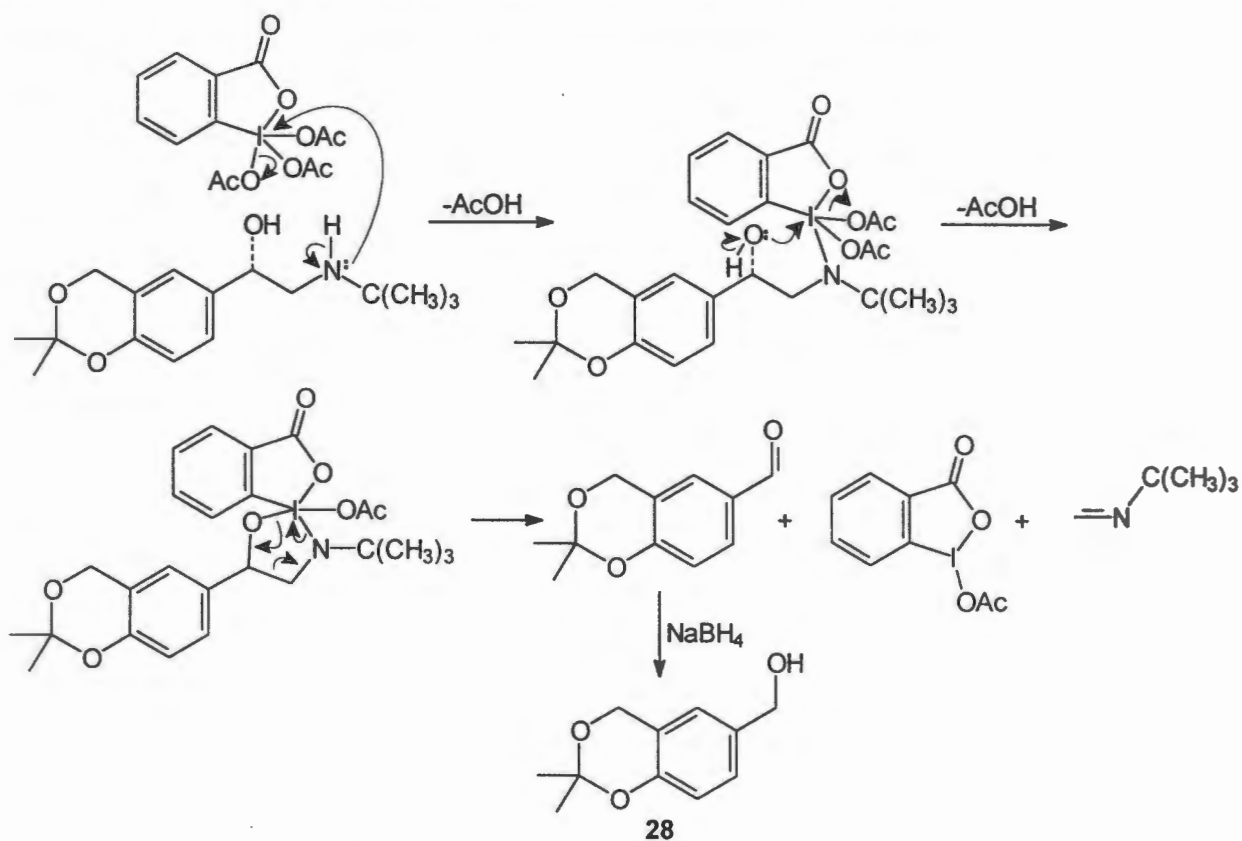
The presence of the acid-sensitive acetonide group on **16** meant that the use of PCC-alumina was advisable. In this reagent, the acidic nature of PCC is diminished by adsorption onto alumina which acts as a buffer. In addition, work-up and removal of chromium-containing by-products is often difficult and alumina here acts as an adsorbent for the by-products of the reaction resulting in the work-up only requiring filtration and concentration. PCC-alumina was freshly prepared⁸³ and reacted with **16** in a ten-fold excess at room temperature. Tlc showed complete reaction to a single product after 5 hours. Filtration and evaporation of the solvent, however, delivered very little material. Attempts to recover additional material by washing the alumina with ethyl acetate/methanol mixtures failed. Similar difficulties with product recovery have been reported in the oxidation of β -amino alcohols and have been ascribed to the formation of strong chelates between the α -amino carbonyl compound and the chromium by-products of the reaction.⁸⁴ This may be avoided by protection of the amine as an amide, or *via* the more attractive option of using an oxidant containing no cationic metal species.

Dimethyl sulfoxide (DMSO) may be used to oxidise alcohols to carbonyl compounds under mild conditions. It is used in conjunction with an activating species of which oxalyl chloride appears to be the most effective.⁸⁵ These Swern oxidation conditions have been successfully applied to the oxidation of β -amino alcohols, although rapid polymerisation of the isolated product *via* intermolecular Schiff base formation is a problem in many cases.⁸⁶ The oxidation, using triethylamine as base, and work-up conditions as described for a successful isolation of an α -amino carbonyl product⁸⁶ were applied in the reaction with **16** but a complex mixture of products (by TLC) was obtained. In order to avoid the polymerisation associated with isolation of the amino-ketone, the Swern oxidation of a β -amino alcohol followed by in-situ reduction with a Grignard reagent has been described in an approach to the taxotere side chain.⁸⁷ This approach was followed by performing the oxidation of **16** in THF, followed by the addition of an excess of lithium aluminium hydride. Unfortunately, the recovery of material was poor and the product consisted of an inseparable mixture of compounds.

A more recently introduced reagent for the oxidation of primary and secondary alcohols under mild conditions ($\text{CH}_2\text{Cl}_2/\text{RT}$) is the Dess-Martin "periodinane", **27**.⁸⁸



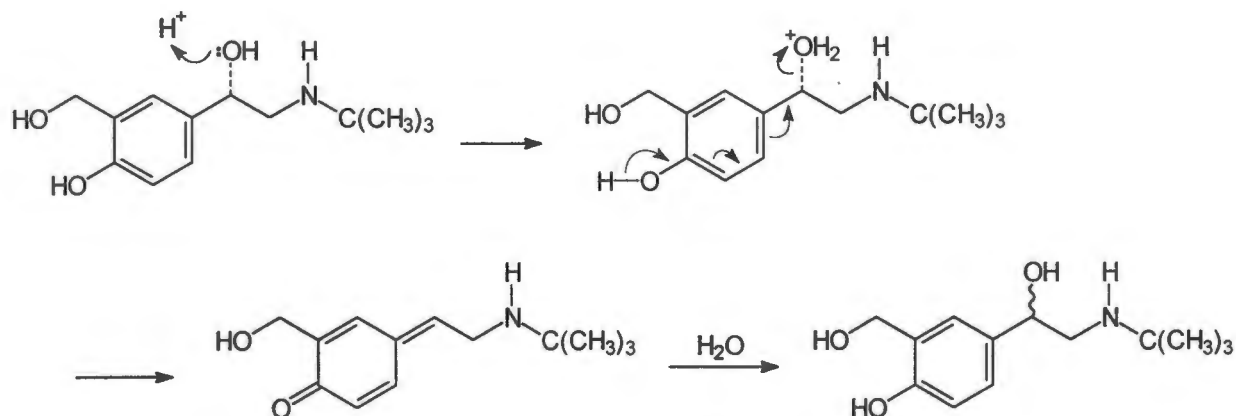
Tlc of the crude material from the Dess-Martin oxidation of **16** indicated the formation of a major product. The crude material was reduced with sodium borohydride without any further purification and the major product isolated by column chromatography. NMR evidence indicated the presence of alcohol **28**, the formation of which is rationalised by the mechanism shown in Scheme 2.7. No further characterisation of the product was undertaken.



Scheme 2.7: Dess-Martin oxidation of **16**

The possibility of using HCl catalysis, which proved problematic in the hydrolysis step, to the racemisation of albuterol was also briefly investigated. Acid catalysts have the potential of generating carbocations at chiral centres, provided suitable leaving groups as well as appropriate carbocationic stabilisation are available. In the case of albuterol, the benzylic carbocation would be stabilised by mesomeric release from the phenol moiety. The resulting intermediate would be

planar and reaction with an achiral reagent (H_2O) would thus result in a racemate. This is illustrated for albuterol in Scheme 2.8.



Scheme 2.8: Acid catalysed racemisation of albuterol

Hydrochloric acid-catalysed hydrolysis experiments were undertaken on (*S*)-**16** recovered from the mother liquors of resolution. In order to monitor the progress of the racemisation, an aliquot of the reaction solution was withdrawn and the optical rotation measured. The reactions were also monitored by tlc. When methanol or ethanol was used as the reaction solvent, decomposition was detected prior to consumption of all the starting material. Heating at 50°C in a less polar solvent, tetrahydrofuran, resulted in complete conversion of **16** to albuterol, but the sample still showed significant optical rotation. When this completely hydrolysed sample was left to stir at room temperature overnight, no significant change to the optical rotation occurred and a small amount of decomposition was noted. When the solution was refluxed, a substantial decrease in optical rotation, which corresponded to $\sim 80\%$ racemisation, was achieved. Complete racemisation was not, however, achieved without some decomposition. No further work was performed on this reaction, but other acids that are applied to the hydrolysis of ketals and the racemisation of alcohols, *e.g.* sulfuric or trifluoroacetic acid, should be investigated on this system.

CHAPTER 3 DETERMINATION OF ABSOLUTE CONFIGURATION

3.1 Introduction

The absolute configuration of albuterol was assigned by Hartley and Middlemiss⁵² in 1971, on the basis of a negative Cotton effect in the circular dichroism spectrum of the (-)-enantiomer. This effect coincided with that shown by (*R*)-octopamine, which is also a phenylethanolamine, and the (-)-enantiomer of albuterol was thus assigned as having the (*R*)-configuration. From the outset of this project, a search of the Cambridge Structural Database⁸⁹ revealed no crystallographic studies on homochiral albuterol or derivatives thereof. Although the absolute configurations of the enantiomers of **16** were later inferred from the optical rotation of compound **24** obtained on hydrolysis, the lack of structural work in this area led us to use crystallographic means in order to establish the absolute configuration of the enantiomer of **16** precipitating in the n-salts with DOBT and DOTT. From the documented optical rotation of **24**, (+)-**16** was shown to be the (*S*)-enantiomer and the enantiomers of **16** are illustrated with these inferred configurations in the following report describing the confirmation of this assignment.

3.2 The DOBT and DOTT salts of Albuterol Acetonide

Since the absolute stereochemistry of the stereogenic centres in these resolving agents is known, either stereocentre could serve as a reference for assigning the absolute configuration of **16** in a crystal structure solution of a diastereomeric salt. In addition, solution and inspection of the crystal structures of both the p and n diastereomeric salts would allow some rationalisation of the efficiency of the resolution.⁹⁰ The n-salts, **20** and **21**, which precipitated from resolution experiments were crystalline, but very insoluble in all but the most polar organic solvents. In spite of extensive efforts, no crystals of **20** or **21** with dimensions suitable for X-ray intensity data collection could be produced. Attempts to obtain crystalline material from the mother liquors of the resolution experiments by slow evaporation from various solvents resulted in oils. Solid material could only be obtained from the mother liquors when all solvent was removed under reduced pressure. The X-ray powder diffraction patterns of the DOBT salts of **16** were collected and are reproduced in Fig. 3.1. The sample obtained from the mother liquors, that is the p-salt, showed the expected contamination by the n-salt, but had no unique peaks in the pattern, which is an indication of the amorphous nature of the material.

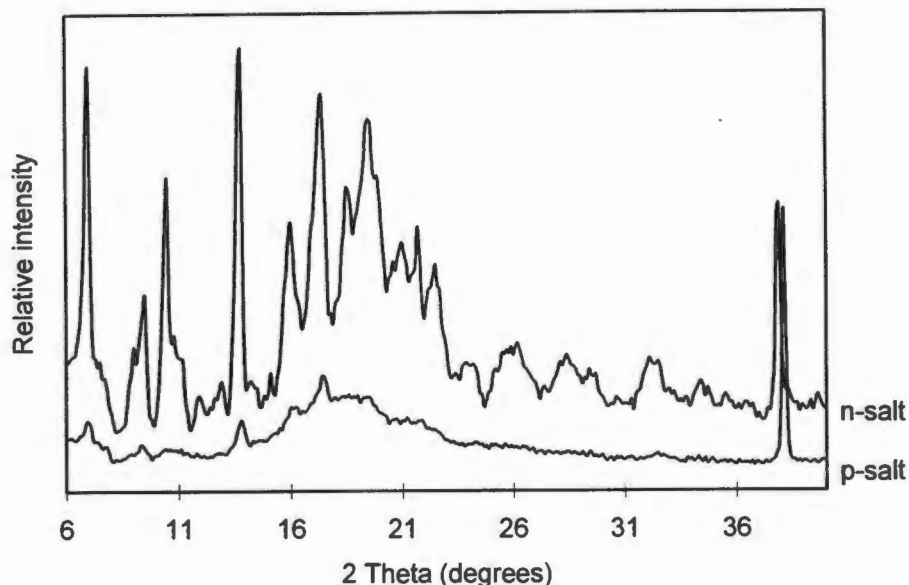


Figure 3.1: X-ray Powder Diffraction Patterns for the salts of **16** and (2*R*, 3*R*)-DOBT

3.3 Structure determination of (+)-Albuterol Acetonide, (+)-**16**

Calculation of the Flack absolute structure parameter⁹¹ indicates whether a refined absolute structure is correct or should be inverted. With MoK α radiation, as used here, the collection of high resolution data including Friedel opposites may allow the calculation of the Flack parameter to within a suitable standard deviation. Crystals suitable for the structure determination of (+)-**16** isolated from initial resolution experiments were grown from acetone.

Oscillation and Weissenberg photography revealed *mmm* Laue symmetry, indicating the orthorhombic system. The lack of any systematic absences among the general reflections on the Weissenberg photographs of the upper levels indicated the presence of a primitive lattice. There were no conditions on $0kl$, $h0l$ and $hk0$ reflections, but conditions on $h00$ and $0k0$ ($h = 2n$ and $k = 2n$ respectively) were observed. From this information, the space group was tentatively assigned as $P2_12_12_1$ (No. 19⁷⁴) which is common amongst homochiral organic molecules. Further photographs were not taken to confirm this, but the third condition, $00l$ ($l = 2n$) was found on inspection of the intensity data, thus confirming the presence of this space group. All non-hydrogen atoms were located using direct methods and successful structure refinement, as described in Section 5.4.2, followed.

The value of the Flack parameter calculated with data collected at room temperature was inconclusive, so the data were recollected at -50°C and including higher θ values. The final structure refinement was performed on these low temperature data. The high estimated standard deviation (1.6) of the Flack parameter in comparison to the parameter itself (1.8) after the final refinement calculation meant that no meaningful conclusions on the absolute configuration of (+)-16 could be made. The structure solution did however confirm the presence of the isopropylidene ketal, as was inferred from ^{13}C NMR data in Section 2.1.

The structure of the molecule with the atomic numbering used is shown in Fig. 3.2. Details of the crystal data and structure refinement appear in Table 3.1. Fractional atomic co-ordinates, anisotropic displacement parameters, bond lengths, bond angles and torsion angles appear in tables A1 to A6 in Appendix 1 and structure factor data are included on diskette in Appendix 3.

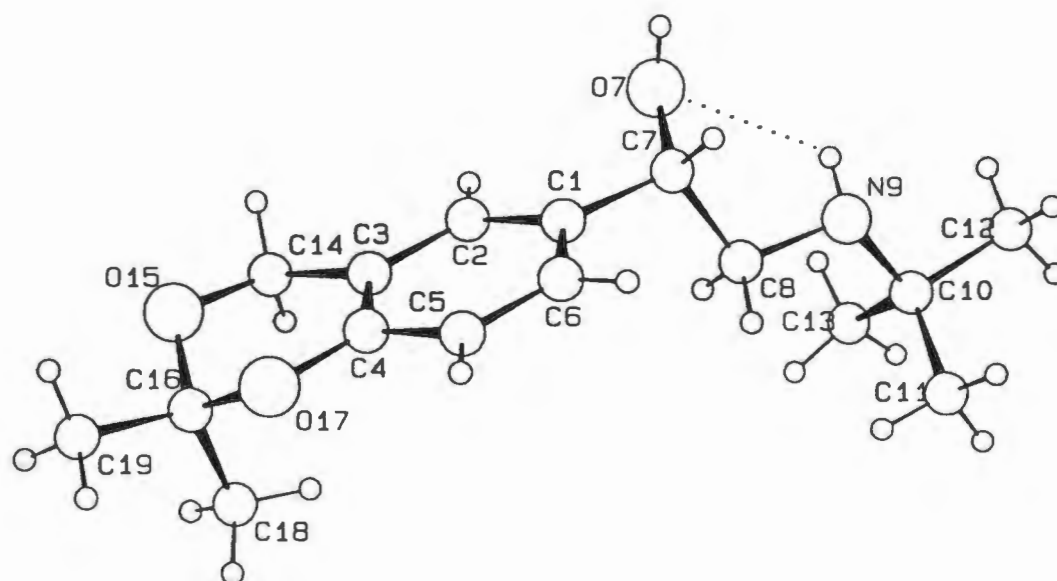


Figure 3.2: Molecular structure of (+)-16 showing atom labelling and intramolecular hydrogen bonding

Both inter- and intramolecular hydrogen bonding are present. In the intramolecular case, illustrated on Fig. 3.2, it is an N-H \cdots O bond with the following parameters: (e.s.d's in parentheses)

N9 -H9A	N9 ... O7	H9A ...O7	N9 -H9A ...O7
0.909(2) Å	2.844(2) Å	2.387(2) Å	111.1(1)°

The structure is stabilised the single O-H \cdots N intermolecular H-bonds with

O7 -H7A	O7 ...N9 ^a	H7A ...N9 ^a	O7 -H7A ...N9 ^a
0.820(6) Å	2.900(2) Å	2.081(5) Å	175.8(1)°

where 'a' denotes symmetry related position $x + \frac{1}{2}, -y + \frac{1}{2}, -z + 2$.

The intermolecular H-bonding scheme is illustrated by dotted lines in the stereoscopic packing diagram, Fig. 3.3. The albuterol acetone molecules, propagated by a 2-fold screw axis, are located in spirals which run parallel to [100].

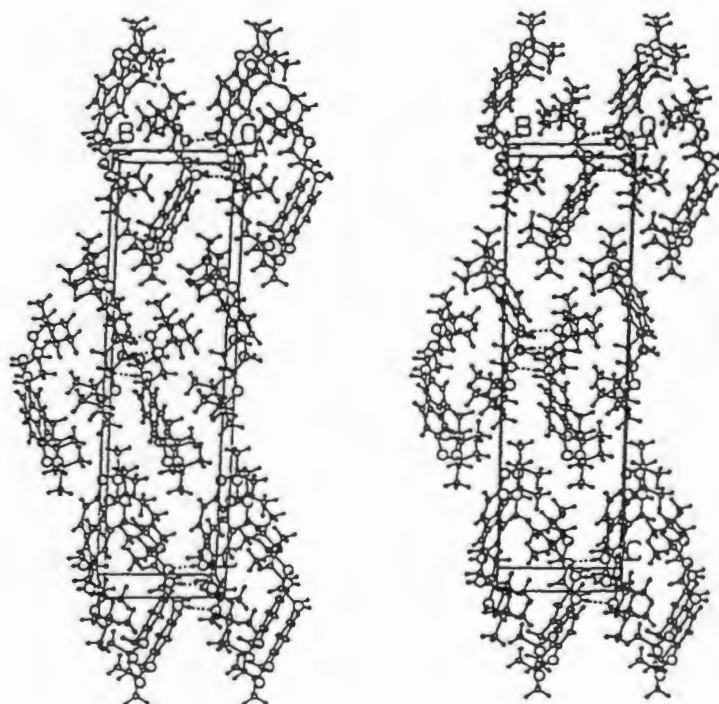


Figure 3.3: Stereoscopic view of crystal packing in (+)-16

Table 3.1: Crystal data and structure refinement for (+)-16

Empirical formula	C ₁₆ H ₂₅ NO ₃
Formula weight	279.38 g.mol ⁻¹
Temperature	223 K
Wavelength	0.7107 Å
Crystal system	Orthorhombic
Space group	P2 ₁ 2 ₁ 2 ₁
Unit cell dimensions	a = 5.958(1) Å b = 8.716(2) Å c = 30.481(3) Å
Volume	V = 1582.9(4) Å ³
Z	4
Density (calculated)	1.172 g.cm ⁻³
F(000)	608
Crystal size	0.2 x 0.4 x 0.3 mm
θ range for data collection	1° to 30°
Index ranges	-8 ≤ h ≤ 8 -12 ≤ k ≤ 12 -42 ≤ l ≤ 36
Reflections collected	4612
Independent reflections	3977 [R(int) = 0.0286]
Independent reflections [I > 2σ(I)]	2507
Data/restraints/parameters	3950 / 2 / 185
Final R indices [I > 2σ(I)]	R ₁ = 0.0488 wR ₂ = 0.3352
Largest difference peak and hole	0.28 and -0.26 e.Å ⁻³

The failed refinement of the Flack parameter is ascribed to the low scattering ability of the atoms present *i.e.* C, H, N and O. The presence a heavier atom such as bromine in a crystal containing (+)-16 would increase the likelihood of successful absolute structure determination. Inclusion of *p*-bromophenol has aided the crystal structure determination of several steroid molecules.^{92,93} Attempts to grow crystals from solutions containing various proportions of (+)-16 and *p*-bromophenol were unsuccessful. The HBr salt of (+)-16 was prepared by the dropwise addition of dry ethanol to cold stirring phosphorus tribromide under nitrogen. The hydrogen bromide

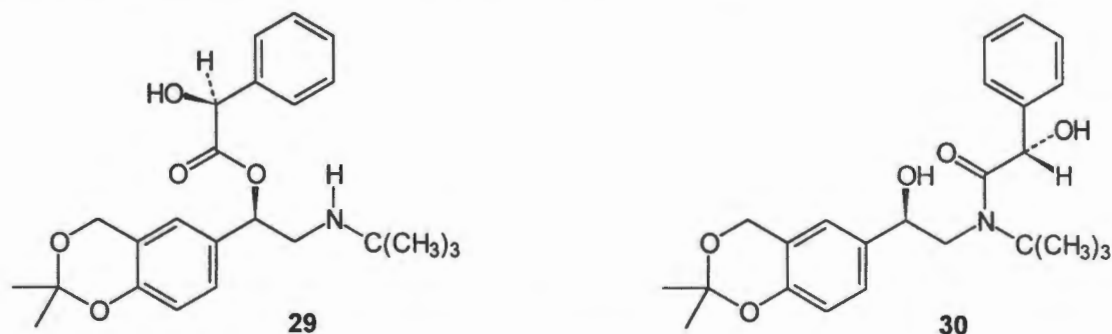
generated was bubbled through a cold solution of (+)-16 in ether, resulting in the precipitation of the salt. Crystals of the salts could not be grown since attempts to isolate and redissolve the fine precipitate resulted in decomposition.

3.4 Covalent Diastereomer Formation

Since no success was achieved using the Flack approach to assign the absolute configuration, it was decided to prepare a covalent diastereomer by derivatising (-)-16 with a homochiral reagent of known absolute stereochemistry. The nucleophilic hydroxy and amino functional groups present in 16 were targeted as the positions at which to derivatise and a reagent bearing electrophilic reactivity was thus sought. Of the chiral pool materials, the chiral acids, which already bore the suitable carbonyl functionality, were the obvious starting point.

3.4.1 Mandelate derivatives of (-)-Albuterol Acetonide, (-)-16

Condensation of (*S*)-Mandelic acid with (-)-16 could have resulted in the formation of either the mandelate ester 29 or the amide 30. The isolation of either of these products, or the diprotected version, as a crystalline compound was considered suitable for this study.



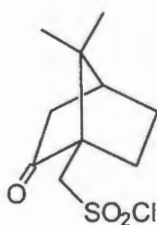
The formation of an ester or amide using a carboxylic acid is not spontaneous and a coupling agent is usually required. The reagent of choice,⁹⁴ dicyclohexylcarbodiimide, DCC, activates the acid by formation of an *O*-acylurea. The urea is then displaced by the hydroxyl or amino nucleophile resulting in the formation of an ester or amide and dicyclohexylurea which precipitates from the reaction mixture. The reaction is, however, hampered by the spontaneous rearrangement of the *O*-acylurea intermediate to an *N*-acylurea which does not undergo any further reaction. The use of an acylation catalyst eliminates this problem, with the preferred catalyst for ester formation being 4-(dimethylamino)-pyridine⁹⁵ (DMAP) and 1-hydroxybenzotriazole⁹⁶ (HOBt) for amide formation. The DCC/HOBt conditions were applied

and a complex mixture of products was obtained. In order to avoid possible interference by the mandelic acid hydroxyl functionality, the reaction was repeated using (*R*)-*O*-acetylmandelic acid, but a similar result was obtained. Attempted chromatographic isolation of the major products resulted in decomposition on the silica. Difficulty in the coupling of *N*-alkylated amines has been reported⁹⁷ and more exotic coupling agents⁹⁸ are frequently required in order to achieve suitable reaction.

The use of an activated carboxyl moiety such as an acid chloride negates the need for a coupling agent. It is, however, usually avoided in cases where the acid chloride contains an α -chiral centre which is tertiary, as in the case of mandelic acid, since abstraction of the tertiary carbon proton can lead to racemisation *via* an enol form. This is particularly true for mandelic acid in which the proton in question is also benzylic and thus has enhanced acidity. For this reason, the next derivatisation reagent chosen from the chiral pool was based on camphorsulfonic acid in which racemisation is not an issue.

3.4.2 Camphorsulfonyl derivatives of (-)-Albuterol Acetonide, (-)-16

A chiral acid in which the chiral centre is remote from the acidic functionality can be used in an activated form without the aforementioned racemisation problem. (1*R*)-Camphor-10-sulfonyl chloride, **31**, is an example of such a reagent and reacts with both alcohols and amines to give sulfonate esters and sulfonamides respectively. The reaction usually involves mixing a solution of the alcohol or amine in dichloromethane with camphorsulfonyl chloride in the presence of a base such as pyridine. Successful derivatisation of a secondary alcohol⁹⁹ and a secondary amine¹⁰⁰ have been achieved under these mild conditions.



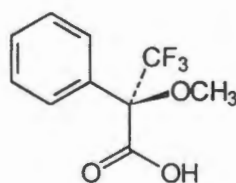
31

The procedure of Bartlett and Knox¹⁰¹ involving reaction of the sulfonic acid with phosphorus pentachloride was followed in order to prepare **31**. Minimal conversion of (-)-**16** occurred under the sulfonylation conditions described above. After the addition of DMAP and dimethylformamide¹⁰² to the reaction mixture, a number of products were detected by tlc but

after work-up, largely unreacted **16** remained. Of the other material present, only the major product was isolated. Although the material showed most of the ^1H NMR resonances characteristic of **16**, it was not the desired adduct and further characterisation was not undertaken. Derivatisation of a secondary alcohol with **31** has also been achieved using *n*-butyllithium as the base¹⁰³ and this approach was attempted. Again, **16** was not consumed, but in this reaction all of **31** was converted to one major product, with ^1H NMR indicating that it contained two residues of **31**. A plausible rationalisation for this is that deprotonation of the amino group of (-)-**16** by *n*-butyllithium, resulted in an amide anion which itself behaved as a hindered base as opposed to a nucleophile in removing an acidic proton (α - to the carbonyl or sulfonyl groups) from **31**. The resulting anion then reacted with an electrophilic site in another molecule of **31** to give the product. Although this reactivity is interesting, it did not achieve the objective of the study being undertaken and was not pursued.

3.4.3 Mosher's Ester of (-)-Albuterol Acetonide, (-)-**16**

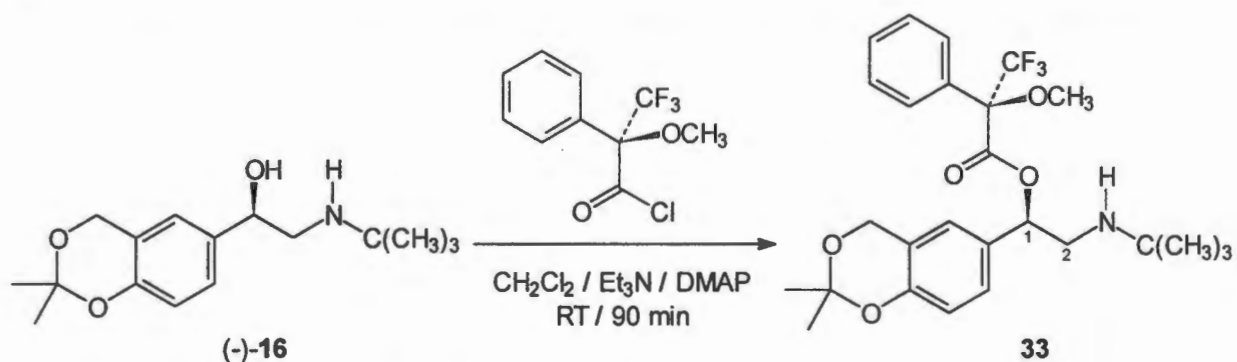
Methoxytrifluoromethylphenylacetic acid (MTPA), or Mosher's acid (whose (*R*)-enantiomer is illustrated as **32** below) is one of the more popular chiral derivatising agents since the quaternary nature of its chiral centre suppresses the risk of racemisation described in Section 3.4.1. It is most frequently used for the determination of the enantiomeric purity of chiral alcohols and amines by the preparation of diastereomeric esters or amides which are then assayed using chromatographic or spectroscopic methods.¹⁰⁴ The preparative use of MTPA has been limited, possibly due to its high cost in comparison to that of other naturally occurring chiral acids. The absolute configuration of alcohols and amines, in which the heteroatom is attached to the stereocentre, has been determined using the ^{19}F ¹⁰⁵, and, more commonly, ^1H NMR¹⁰⁶ shifts of their MTPA derivatives.



32

A literature method¹⁰⁷ was followed to convert commercially available **32** to the more reactive acid chloride (*R*)-MTPACl, which was purified by Kugelrohr distillation. This was reacted with (-)-**16** in the presence of triethylamine and DMAP to produce a single product in high yield after

90 min at room temperature. The NMR spectra of the product were assigned by comparison with the spectra of **16** and by a further 2D NMR (HMQC) experiment. The product was assigned as the ester **33** as opposed to the amide on the basis of the significant downfield shift of the signal for 1-H (5.87 ppm) in the ^1H NMR spectrum from a value of $\delta = 4.80$ ppm for **16**. This is substantiated by a similar comparison of the signals for C-1 in the ^{13}C spectrum in which the shift was from 72.0 to 79.0 ppm. If an amide had been formed, a degree of deshielding of the quaternary tertiary butyl carbon by the carbonyl would have been expected but the shift of this atom remained unchanged at 50.3 ppm. The infrared spectrum for **33** displayed a carbonyl absorption band at 1748 cm^{-1} which corresponds to that expected for an ester whilst that for an amide would be expected below 1700 cm^{-1} . The transformation is illustrated in Scheme 3.1.



Scheme 3.1: Derivatisation of (-)-**16** with (*R*)-MTPACl

The isolation of **33** as an oil was disappointing in that no X-ray structural studies could be carried out. The chemoselectivity demonstrated in the above reaction was again ascribed to the hardness of the carboxylic acid chloride electrophile which preferred to react with the harder oxygen nucleophile. Steric crowding of the nitrogen nucleophile by the *t*-butyl substituent could also have played a role. It was a fortuitous result in that ^1H NMR could be used to gain more insight into the absolute stereochemistry of the parent alcohol. Mosher analysis involves the preparation of diastereomeric Mosher esters and comparison of the chemical shifts of proton resonances from the groups attached to the asymmetric carbon (C-1) in each of the esters. A correlation between the chemical shifts and the conformation of the ester is made in order to assign the absolute configuration at the unknown chiral centre.

The analogous derivatisation of (*rac*)-**16** was performed and the proton NMR spectrum of the resulting mixture of diastereomers recorded. By comparison of the latter with the spectrum of **33**, the signals of the diastereomer arising from (+)-**16**, **34**, were extracted and the chemical shifts of the two diastereomers examined. These chemical shift data are presented in Table 3.2.

Table 3.2: ^1H Chemical shift data for the (*R*)-Mosher esters of (+)- and (-)-16

Proton	34 δ (ppm)	33 δ (ppm)	$\Delta\delta = \delta_{34} - \delta_{33}$ (ppm)
<i>t</i> -Bu	0.98	1.06	-0.08
2x2'-CH ₃	1.52	1.53	-0.01
2-H _A	2.75	2.83	-0.08
2-H _B	2.99	3.00	-0.01
2''-OCH ₃	3.43	3.54	-0.11
4'-H _A	4.78	4.72	+0.06
4'-H _B	4.84	4.79	+0.05
1-H	5.92	5.87	+0.05
8'-H	6.79	6.75	+0.04
5'-H	6.99	6.83	+0.16
7'-H	7.18	7.07	+0.11
other Ar-H	7.2-7.5	7.2-7.5	-

As illustrated in Fig. 3.4(a), **33** can thus be considered as having two substituents on the chiral carbon: L1 in which protons are deshielded relative to **34**, and L2 in which they are relatively shielded. The preferred conformation^{106,108} of **33** in which the C-1 - H bond is *gauche* to the O - C-1'' bond, the C-1 - O bond is *trans* to C-1'' - C-2'' and the C-2'' - CF₃ and C=O bonds are almost *syn* periplanar is shown in the sawhorse diagram Fig. 3.4(b) and the Newman projection 3.4(c) along C-1'' - C-2'' and C-1 - O. This information is related to the absolute configuration of the molecule with the aid of a Newman projection along C-1 - C-2'' (Fig. 3.4(d)).

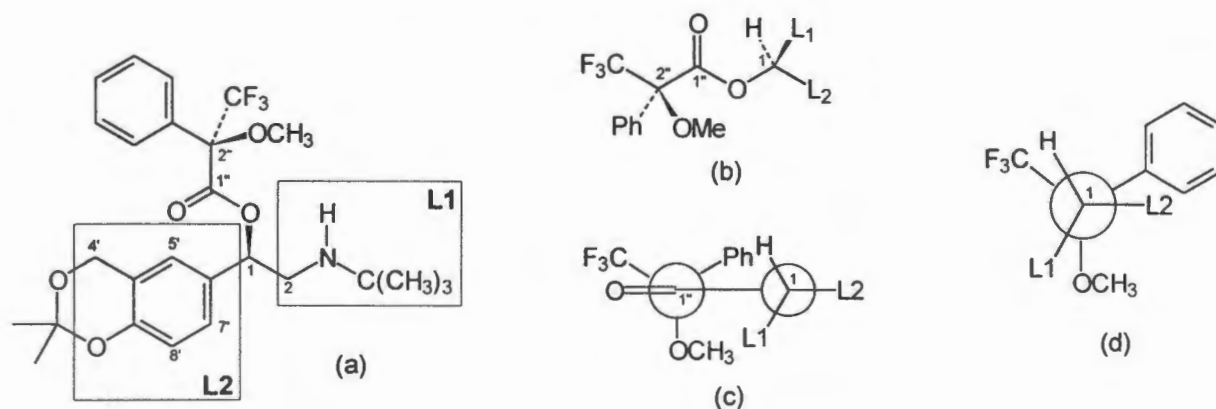
Figure 3.4: Stereochemical projections of the preferred conformation of **33**

Fig. 3.4(c) indicates that, with the absolute configuration and conformation shown, the protons on L2 in **33** should be subjected to aromatic shielding by the MTPA phenyl substituent and thus found upfield relative to the equivalent protons on **34** (the Newman projection for **34** would have the positions of L1 and L2 reversed). Similarly, the protons on L1 should be found further downfield than those of **34** due to the shielding of those on **34** by the MTPA phenyl moiety. Both of these trends are followed by the experimental NMR data, thus providing additional evidence that the absolute configuration of (-)-**16** is (*R*)-, as was concluded from the hydrolysis studies. In addition, the NMR data show the MTPA methoxy protons to be further downfield in **33** than in **34**. L2 is aromatic in nature and will shield the methoxy protons when the two are juxtaposed, which occurs when the absolute configuration at C-1 is (*S*)- as in **34**.

Some unexpected ^1H NMR results for the Mosher esters of alcohols have been reported^{109,110}. A recent computational study¹¹¹ shows that, contrary to the conformational model applied above, three low energy conformations of the esters may exist, each of which has a different shielding effect on either L1 or L2 (Fig. 3.5).

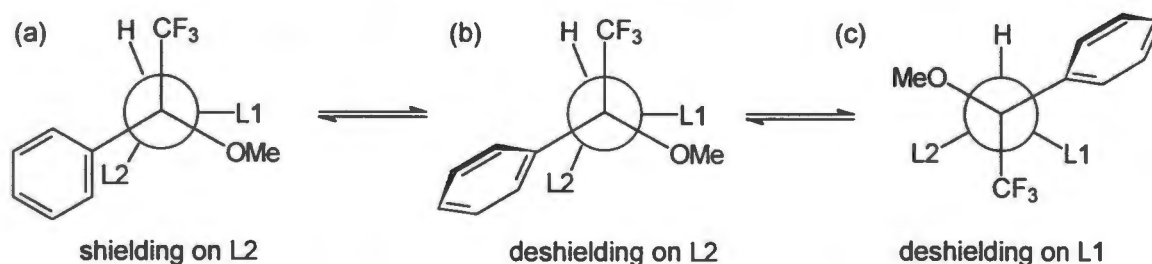


Figure 3.5: Low energy conformers of (*R*)-MTPA esters

The small $\Delta\delta$ values can be explained by the mutual cancellation of the aromatic anisotropic effects on L2 in (a) and (b), and the fact that the magnitude of deshielding as provided by (c) is usually smaller than shielding. The relative populations of each conformer, as well as the degree of shielding or deshielding contributed by each would have to be calculated for the ester concerned before the absolute configuration determined in this manner could be quoted with certainty. It was shown in the same study that, in the equivalent methoxyphenylacetic acid esters, one conformer is more populated and thus, if the racemisation problems are overcome, a more reliable determination of absolute configuration is provided. The equivalent modelling studies on Mosher amides¹¹² show rotamer (a) to be lowest in energy thus also allowing reliable predictions.

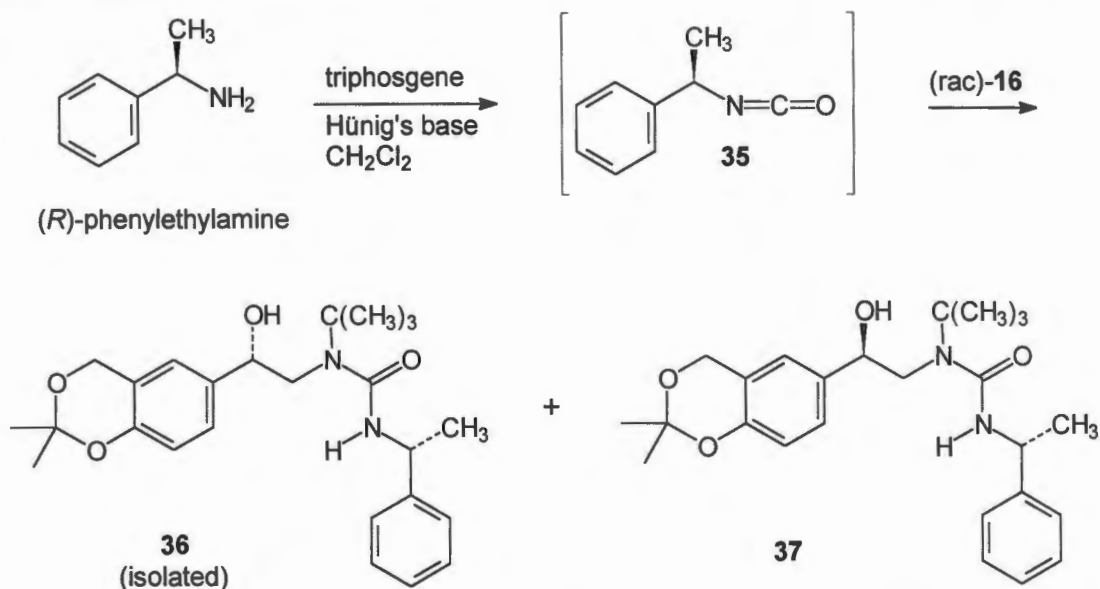
3.4.4 Phenylethylurea derivatives of (+)-and (-)-Albuterol Acetonide

In the light of the aforementioned doubts shed on the Mosher analysis, structural evidence for the assigned absolute configurations was still sought and this led to the preparation of (*R*)-phenylethylamine derivatives of **16**. Alkyl isocyanates, R-N=C=O, are reactive species which derivatise alcohols and amines under mild conditions to give carbamate esters (or urethanes) and ureas respectively. (*S*)-phenylethyl isocyanate has been used to form a urethane on a marine epoxyquinol to allow X-ray crystallographic determination of the absolute stereochemistry of the molecule.¹¹³ Isocyanates are usually prepared by reaction of the parent amine with phosgene (COCl₂).¹¹⁴ The toxicity of phosgene, however, makes this methodology unattractive and triphosgene (Cl₃COCO₂CCl₃) has become a popular commercial alternative.¹¹⁵ The preparation of asymmetrically substituted ureas in a one-pot method utilising triphosgene and two amino acid esters has been reported.¹¹⁶ This procedure was applied to the formation of (*R*)-phenylethyl isocyanate **35** from (*R*)-phenylethylamine, followed by in-situ derivatisation of (-)-**16**. Tlc showed the formation of a major product with a single impurity of similar polarity. The impurity could not be removed by chromatography on silica gel, but a ¹H NMR spectrum of the impure oil indicated the formation of the desired urea or urethane. The reaction was repeated using (rac)-**16** as substrate and two products, assumed to be the two diastereomers, were obtained (as well as the earlier impurity). The diastereomer arising from (+)-**16**, **36**, was isolated, crystallised and characterised. Although the chemoselectivity of **16** was expected to be as for Mosher ester formation, *i.e.* to give a carbamate ester *via* attack at the benzylic hydroxyl group, a comparison of relevant chemical shifts (Table 3.3) did not support this outcome.

Table 3.3: Comparison of selected ¹H and ¹³C NMR chemical shifts of **16** and **36**

Atom	16 δ(ppm)	36 δ(ppm)
<i>t</i> -Bu C(CH ₃) ₃	1.07	1.40
2-H _A	2.56	3.23
2-H _B	2.80	3.44
1-H	4.50	4.76
<i>t</i> -Bu C(CH ₃) ₃	29.1	29.1
C-2	50.3	54.4
<i>t</i> -Bu C(CH ₃) ₃	50.3	55.9
C-1	72.0	76.7

The unexpected formation of the (*R*)-phenylethylurea of (+)-**16**, (Scheme 3.2) was revealed on crystal structure solution (discussed in Section 3.4.5). The carbonyl carbon in the reacting isocyanate moiety is a softer electrophilic centre than that in an acid chloride. It is thus suggested that the softer amino nucleophile was preferred to the hydroxyl nucleophile in this reaction. Although **36** is a urea, it has been named and numbered as a derivative of **16** for the purposes of continuity.



Scheme 3.2: Urea formation with in-situ generation of (*R*)-phenylethyl isocyanate

As (-)-**16** gave rise to the desired (*R*)-albuterol on hydrolysis, the preferred diastereomer for crystal structure determination was that synthesised from this enantiomer, *i.e.* **37**. Owing to the aforementioned experimental problems, the derivatisation of (-)-**16** was performed in two steps. The first step in the one-pot method was performed and this was followed by a fast, cold aqueous work-up procedure¹¹⁷ to isolate **35** which was purified by Kugelrohr distillation. The infra-red spectrum showed a strong band with ν_{\max} 2250 cm⁻¹ corresponding to isocyanate formation. The reaction with (-)-**16** proceeded as expected and the (*R*)-phenylethylurea of (-)-**16**, *i.e.* compound **37**, was isolated. Although full characterisation of **37** was carried out, no crystals of this material suitable for X-ray analysis could be produced. The crystal structure determination on **36**, which provided the stereochemical information sought equally well, was thus undertaken.

3.4.5 Crystal structure of (*R*)-Phenylethylurea of (+)-Albuterol Acetonide, 36

The oscillation, and de Jong-Bouman photographs revealed the presence of *mmm* Laue symmetry, thus indicating the orthorhombic crystal system. Comparison of upper layers revealed no systematic absences in the general reflections and the lattice was thus established to be primitive. There were no conditions on $0kl$, $h0l$ and $hk0$. However conditions of $h = 2n$, $k = 2n$ and $l = 2n$ for observed reflections on $h00$, $0k0$ and $00l$ respectively led to the deduction of $P2_12_12_1$ space group symmetry.

The structure was solved by direct methods and successfully refined, giving a final *R* value of 0.0396. The data for the collection and refinement are given in Table 3.4 and fractional atomic co-ordinates, anisotropic displacement parameters, bond lengths, bond angles and torsion angles have been reproduced in tables B1 to B6 in Appendix 2, and structure factor data are included on diskette in Appendix 3.

The relative stereochemistry of the chiral centres (labelled as C7 and C22 respectively) is clearly defined in the molecular structure (Fig. 3.6) and, since the absolute configuration at C22 was known to be (*R*)-, that at C7 was unambiguously assigned as (*S*)-. Since this centre originates from (+)-16, the assignment made on the basis of the optical rotation of the hydrolysis products was confirmed.

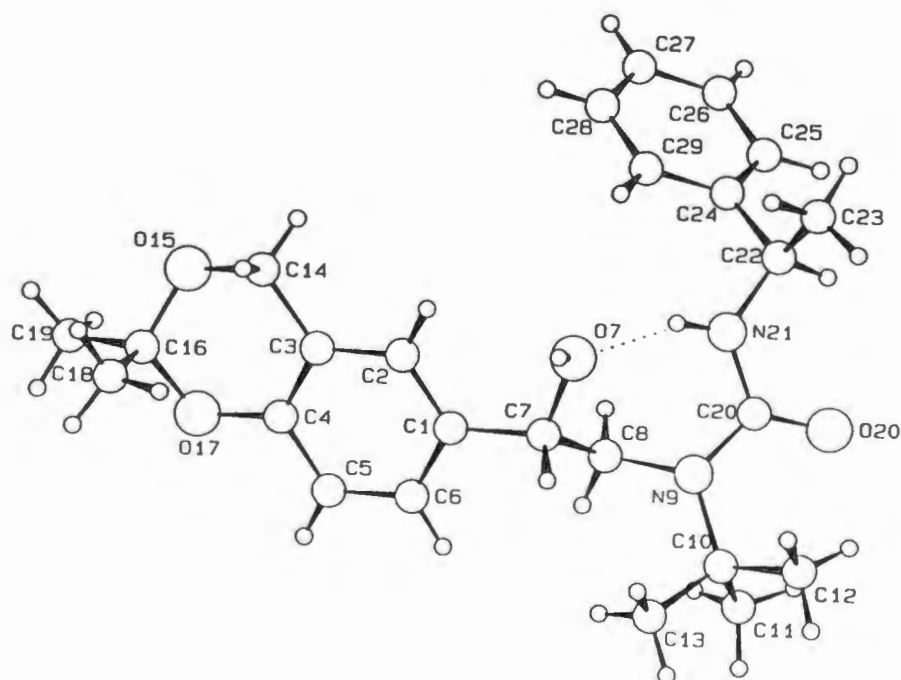


Figure 3.6: Molecular structure of the (*R*)-phenylethylurea of (+)-16

The intramolecular hydrogen bond illustrated in Fig 3.6 has the following parameters:

N21 -H21	N21 ...O7	H21 ...O7	N21 -H21 ...O7
0.860(2) Å	2.867(2) Å	2.079(2) Å	152.1(1)°

Single intermolecular H-bonds between a hydroxyl donor and carbonyl acceptor were found:

O7 -H7A	O7 ...O20 ^a	H7A ...O20 ^a	O7 -H7A ...O20 ^a
0.820(13) Å	2.728(1) Å	1.950(12) Å	158.0(1.1)°

where 'a' denotes symmetry related position $x + 1, y, z$.

This results in an infinite ribbon of hydrogen bonding running through the structure parallel to [100], as can be seen on the stereoscopic packing diagram below.

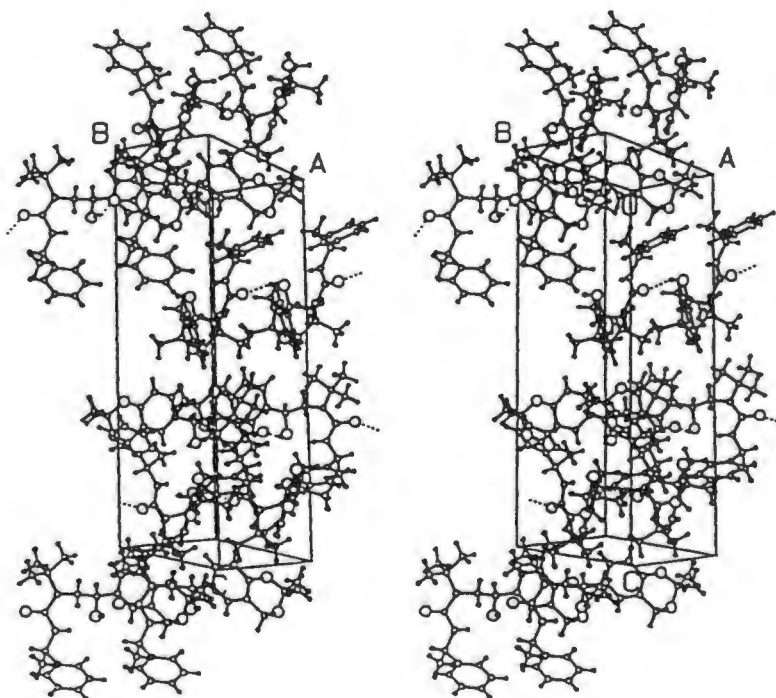


Figure 3.7: Stereoscopic packing diagram of 36

Table 3.4: Crystal data and structure refinement for 36

Empirical formula	$C_{25}H_{34}N_2O_4$
Formula weight	426.56 g.mol ⁻¹
Temperature	273 K
Wavelength	0.7107 Å
Crystal system	Orthorhombic
Space group	P2 ₁ 2 ₁ 2 ₁
Unit cell dimensions	a = 6.749(1) Å b = 13.860(2) Å c = 25.628(3) Å
Volume	V = 2397.3(4) Å ³
Z	4
Density (calculated)	1.182 g/cm ³
F(000)	920
Crystal size	0.3 x 0.4 x 0.4 mm
θ range for data collection	3° to 28°
Index ranges	0 ≤ h ≤ 8 0 ≤ k ≤ 18 -33 ≤ l ≤ 33
Reflections collected	5919
Independent reflections	5750 [R(int) = 0.0244]
Independent reflections [I > 2σ(I)]	4765
Data/restraints/parameters	5749 / 2 / 290
Final R indices [I > 2σ(I)]	R ₁ = 0.0396 wR ₂ = 0.1173
Largest difference peak and hole	0.17 and -0.17 e.Å ⁻³

The primary objective of this work was to produce (*R*)-albuterol using crystallisation techniques. This has been achieved by performing a low cost, high yielding protection of (*rac*)-albuterol and resolving the resulting acetonide *via* diastereomeric salt formation with (*2S,3S*)-di-*O*-benzoyltartaric acid and (*2S,3S*)-di-*O*-toluoyltartaric acid. (*R*)-Albuterol was obtained as its acetate salt in high yield and optical purity by acid hydrolysis of the resolved acetonide derivative. The efficiency of the resolution step as well as the simplicity of the protection and deprotection steps make this an attractive industrial alternative to the present resolution methods in which, although albuterol precursors are resolved, the protection and deprotection steps required are less amenable to large scale syntheses. Existing chiral hplc and ¹H NMR methods were adapted, optimised and applied to the determination of optical purity of the resolved intermediate to allow in-process monitoring. In order for this process to be truly competitive industrially, further work on the racemisation of the intermediate, towards obtaining a 100% theoretical yield of (*R*)-albuterol, is required. In addition, the application of ion exchange methodology to the isolation of (*R*)-albuterol as a free base should be investigated. Construction and comparison of solubility phase diagrams for the diastereomeric salt pairs as well as the final product is also suggested in order to determine the optimal stage in the production process at which to apply recrystallisation to increase optical and chemical purity.

The successful structure elucidation of the (*R*)-phenylethylurea derivative of (*S*)-albuterol acetonide is the first structural evidence available for confirmation of the assignment of the absolute configuration of the enantiomers of albuterol first proposed on the basis of circular dichroism studies. This was further corroborated by the preparation and ¹H NMR analysis of the (*R*)-Mosher esters of the enantiomers of albuterol acetonide. The synthetic work involved in producing the various diastereomeric derivatives of the acetonide has also provided some insight into the reactivity of the *N*-alkylated β-amino alcohol structural moiety of the system.

CHAPTER 5

EXPERIMENTAL

5.1 General

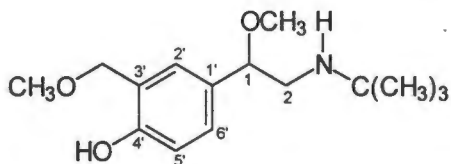
Melting points were measured using a Reichert-Jung Thermovar hot-stage microscope and are uncorrected. Optical rotations were measured on a Perkin-Elmer 141 polarimeter. Infrared spectra were recorded using a Perkin-Elmer Paragon 1000 FT-IR spectrometer over the range 4000-600 cm^{-1} . Microanalyses were determined using a Fisons EA 1108 CHNS-O instrument. Mass spectra were recorded on a VG micromass 16F spectrometer operating at 70 eV with an accelerating voltage of 4kV. Accurate masses were determined on a VG-70E spectrometer at the Cape Technikon. $^1\text{H-NMR}$ spectra were recorded on a Varian VXR-200 (200MHz) or a Varian Unity Spectrometer (400MHz). $^{13}\text{C-NMR}$ spectra were recorded on the same instruments at 50 or 100MHz. The relevant solvent peak (CHCl_3 or DMSO) was used as an internal standard in each case. Thermal gravimetric analysis and differential scanning calorimetry were performed on a Perkin Elmer PC7 Series thermal analysis system. High performance liquid chromatography was performed on a Hewlett Packard 1090 system with a diode array detection and a Hewlett Packard 3393A integrator.

Thin layer chromatography was performed on aluminium backed silica gel 60 F_{254} plates. The plates were visualised under ultraviolet light and by spraying with ceric ammonium sulphate in 8 mol.dm^{-3} sulfuric acid and baking at 200°C. Column chromatography was conducted with Merck Kieselgel 60, 70-230 mesh.

Acetone was distilled from Drierite (anhydrous CaSO_4) and stored over 4Å molecular sieves. Dichloromethane was freshly distilled from P_2O_5 prior to use. Solvents used for hplc were BDH HiperSolv grade. Albuterol was supplied by South African Druggists, Port Elizabeth, South Africa. The major optically active reagents used were purchased as follows:

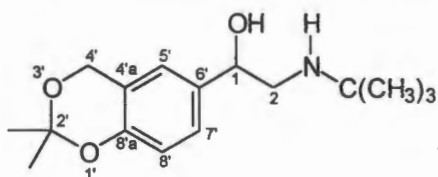
(2 <i>S</i> ,3 <i>S</i>)-Di- <i>O</i> -benzoyltartaric acid (99%)	Merck
(2 <i>S</i> ,3 <i>S</i>)-Di- <i>O</i> -benzoyltartaric acid monohydrate (99%)	Merck
(2 <i>S</i> ,3 <i>S</i>)-Di- <i>O</i> -toluoyltartaric acid (97%)	Aldrich
(<i>R</i>)- and (<i>S</i>)- <i>O</i> -Acetylmandelic acid (99%)	Aldrich

5.2 Syntheses

2-(*N*-*tert*-Butylamino)-1-(4-hydroxy-3-methoxymethyl-1-phenyl)-1-methoxyethane 19

To a stirred slurry of albuterol (1.036 g, 4.3 mmol) in CH_2Cl_2 (10 cm^3) at 0°C was added 2,2-dimethoxypropane (1.6 cm^3 , 1.37g, 13.1 mmol) and $\text{BF}_3 \cdot \text{OEt}_2$ (1.6 cm^3 , 1.85g, 13.0 mmol). The solution was stirred at room temperature for 12 h after which time the reaction was quenched with aqueous Na_2CO_3 . The mixture was extracted into CH_2Cl_2 , dried (MgSO_4) and the solvent removed under reduced pressure to give an oily residue (1.32 g). The residue was chromatographed on silica gel with methanol/ethyl acetate (30/70) to furnish 19 (790 mg, 3.0 mmol, 68%), mp $109\text{--}110^\circ\text{C}$ (acetone); Found C, 67.4; H, 9.8; N, 5.2; $\text{C}_{15}\text{H}_{25}\text{NO}_3$ requires C, 67.4; H, 9.4; N, 5.2%; ν_{max} (CHCl_3)/ cm^{-1} 3374 (O-H), 2960 ($-\text{CH}_2-$), 2832 ($-\text{OCH}_3$), 1501 (aromatic C-C), 1365 (C-N), 1232 (phenolic C-O), 1097 (dialkyl C-O); δ_{H} (200MHz, CDCl_3) 1.08 (9H, s, *t*-Bu), 2.56 (1H, dd, J 11.5 and 3.7 Hz, 2- H_A), 2.80 (1H, dd, J 11.5 and 9.3 Hz, 2- H_B), 3.16 (3H, s, $-\text{OCH}_3$), 3.44 (3H, s, $-\text{OCH}_3$), 4.19 (1H, dd, J 9.3 and 3.7 Hz, 1-H), 4.60 (1H, br s, NH), 4.61 (2H, s, 3'- CH_2OCH_3), 6.83 (1H, d, J 8.3 Hz, 5'-H), 7.02 (1H, d, J 1.7Hz, 2'-H), 7.12 (1H, dd, J 8.3 and 1.7 Hz, 6'-H); δ_{C} (50MHz, CDCl_3) 28.8 (*t*-Bu $-\text{CH}_3$), 49.8 (C-2), 50.1 (*t*-Bu $-\text{C}(\text{CH}_3)_3$), 56.4 (O- CH_3), 58.3 (O- CH_3), 73.1 (C-1), 83.2 (3'- CH_2-), 116.2 (C-5'), 122.9 (C-3'), 126.7 (C-2'), 127.7 (C-5'), 131.4 (C-1'), 155.8 (C-4'), (Found M^+ , 267, $\text{C}_{15}\text{H}_{25}\text{NO}_3$ requires M, 267).

2-(*N*-*tert*-Butylamino)-1-(2,2-dimethyl-1,3-benzodioxin-6-yl)ethanol 16



(a) $\text{BF}_3 \cdot \text{OEt}_2$ procedure

Freshly distilled $\text{BF}_3 \cdot \text{OEt}_2$ (2.7 cm³, 3.1 g, 22.0 mmol) was added dropwise to a stirred mixture of albuterol (2.39 g, 10.0 mmol) in dry acetone (50 cm³) under nitrogen at 0°C. The solution was stirred at 0°C for 60 min after which it was slowly poured into 50 cm³ cold aqueous Na_2CO_3 . The excess acetone was removed under reduced pressure and the mixture extracted into ethyl acetate. The combined organic phases were dried (MgSO_4) and the solvent removed *in vacuo* to give a crystalline crude product (2.70 g). Column chromatography on silica gel with ethyl acetate/ petroleum ether/triethylamine (50/45/5) afforded **16** as a colourless crystalline product (2.67 g, 9.6 mmol, 96%), mp 91-92°C (acetone); Found C, 68.9; H, 9.3; N, 5.0; $\text{C}_{16}\text{H}_{25}\text{NO}_3$ requires C, 68.8, H, 9.0; N, 5.0%; ν_{max} (CHCl_3)/cm⁻¹ 3402 (O-H), 2969 (-CH₂-), 1501 (aromatic C-C), 1118 (C-O); δ_{H} (400MHz, CDCl_3) 1.07 (9H, s, *t*-Bu), 1.505 (3H, s, 2'-CH₃), 1.510 (3H, s, 2'-CH₃), 2.56 (1H, dd, *J* 11.7 and 9.0 Hz, 2-H_A), 2.75 (2H, br s, OH/NH), 2.80 (1H, dd, *J* 11.7 and 3.5 Hz, 2-H_B), 4.50 (1H, dd, *J* 9.0 and 3.5 Hz, 1-H), 4.81 (2H, s, 4'-H₂), 6.76 (1H, d, *J* 8.3 Hz, 8'-H), 6.99 (1H, d, *J* 1.6 Hz, 5'-H), 7.11 (1H, dd, *J* 8.3 and 1.6 Hz, 7'-H); δ_{C} (100MHz, CDCl_3) 24.6 and 24.8 (2'-CH₃) 29.1 (*t*-Bu -CH₃), 50.3 (C-2), 50.3 (*t*-Bu -C(CH₃)₃), 61.0 (C-4'), 72.0 (C-1), 99.5 (C-2'), 116.8 (C-8'), 119.2 (C-4'a), 122.0 (C-5'), 125.7 (C-7'), 134.9 (C-6'), 150.5 (C-8'a), (Found M^+ , 279, $\text{C}_{16}\text{H}_{25}\text{NO}_3$ requires M , 279).

(b) $\text{CuSO}_4/\text{H}_2\text{SO}_4$ procedure:

Acetone (50 cm³) was added to a flask containing albuterol (2.39 g, 10.0 mmol) and anhydrous copper sulphate (1.65 g, 10.0 mmol) and the resulting mixture cooled to 0°C under nitrogen. Concentrated sulfuric acid (1.3 cm³, 22.0 mmol) was added dropwise and the solution stirred for 60 min at 0°C. The work-up procedure as used above resulted in 2.70 g crude material which was purified in an identical manner to yield crystalline **2** (2.65 g, 9.5 mmol, 95%).

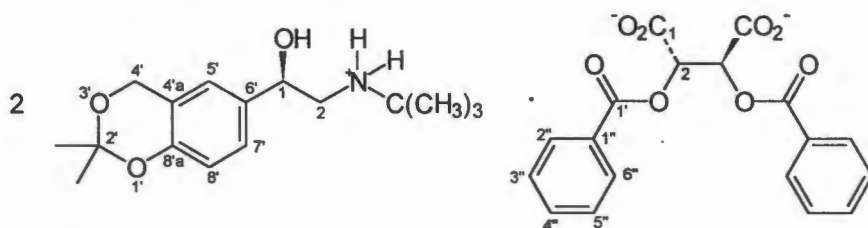
Diastereomeric Salt formation

Pilot Study

Bases	Acids	Solvents
(rac)-Albuterol	(<i>S</i>)-(+)-Binaphthylphosphoric acid	Ethanol
(rac)-Isopropylidene ketal of Albuterol 16	(1 <i>R</i>)-(-)-Camphor-10-sulfonic acid	Methanol
	(2 <i>R</i> ,3 <i>R</i>)-(-)-Di- <i>O</i> -benzoyltartaric	Ethyl acetate
	(<i>S</i>)-(-)-Malic acid	Acetone
	(2 <i>R</i> ,3 <i>R</i>)-(+)-Tartaric acid	
	(<i>S</i>)-(+)-Mandelic acid	

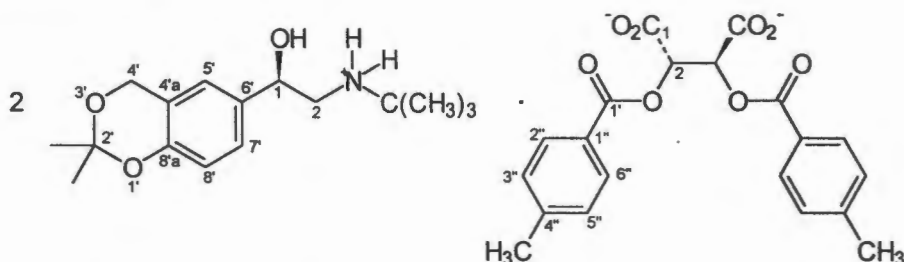
General procedure:

0.2 mmol of each of the relevant acid and base was weighed into a glass vial. 1 cm³ of the required solvent was added and the solution heated sufficiently to allow dissolution of all solids (not achieved in all cases). The vials were stoppered and left to stand at room temperature. Where no precipitate was observed after 24 h, the lids were removed to allow slow evaporation. In each case either an oil, paste or crystalline material was obtained. Where solid crystalline material was obtained, the melting point was compared to that of the parent acid and base to indicate formation of a new species.

(2*S*,3*S*)-Di-*O*-benzoyl tartrate salt of (*R*)-16 20

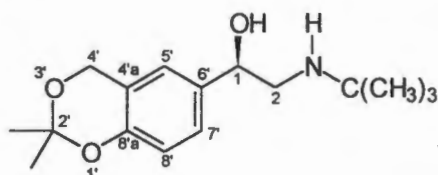
To a refluxing solution of (*rac*)-16 (1.90 g, 6.8 mmol) in methanol (15 cm³) was added a hot solution of (2*S*,3*S*)-di-*O*-benzoyltartaric acid monohydrate (1.32 g, 3.5 mmol) in methanol (10 cm³). Heating was discontinued and the solution stirred until a solid cake of precipitate formed. A further 20 cm³ methanol was added and the solution refluxed for a further 10 min whereafter it was stirred at room temperature for 2 h. The resulting precipitate was isolated by filtration, washed with ethyl acetate and dried under vacuum to yield the diastereomeric salt **20** (1.10 g, 1.20 mmol, 71% yield as a single enantiomer, 93.9% de*). A portion of this salt (0.80 g, 0.87 mmol) was further purified by redissolving it in boiling methanol (70 cm³) followed by stirring at 0°C overnight. The salt was isolated and dried as above (0.50 g, 0.55 mmol, 63% for this step, 45% overall yield as a single enantiomer, >99.5% de*), mp 188-190°C (methanol); [α]_D +24.6° (c 0.19 methanol); Found C, 65.5; H, 7.1; N, 3.0; C₅₀H₆₄N₂O₁₄ requires C, 65.5, H, 7.0; N, 3.1%; ν_{max} (KBr)/cm⁻¹ 3411 (O-H), 2900-2400 (N⁺-H), 1723 (C=O ester), 1641 (C=O carboxylate (s)), 1504 (C=O carboxylate (as)), 1118 (2° C-O); δ_H (400MHz, DMSO-d₆) 1.13 (9H, s, *t*-Bu), 1.44 (6H, s, 2x2'-CH₃), 2.68 (1H, dd, *J* 11.9 and 10.3 Hz, 2-H_A), 2.90 (1H, dd, *J* 11.9 and 2.4 Hz, 2-H_B), 3.36 (2H, br s, NH), 4.72 (1H, dd, *J* 10.3 and 2.4 Hz, 1-H), 4.76 (2H, s, 4'-H₂), 5.66 (1H, s, DOBT 2-H), 6.71 (1H, d, *J* 8.4 Hz, 8'-H), 7.00 (1H, d, *J* 1.9 Hz, 5'-H), 7.10 (1H, dd, *J* 8.4 and 1.9 Hz, 7'-H); 7.50 (1H, m, DOBT 3''-H and 5''-H), 7.63 (1H, m, DOBT 4''-H), 8.00 (1H, dd, *J* 7.8 and 1.4 Hz, DOBT 2''-H and 6''-H); δ_C (100MHz, DMSO-d₆) 24.4 and 24.5 (2'-CH₃) 25.1 (*t*-Bu -CH₃), 48.1 (C-2), 54.7 (*t*-Bu -C(CH₃)₃), 60.0 (C-4'), 68.2 (C-1), 74.9 (DOBT C-2), 99.1 (C-2''), 116.0 (C-8'), 119.0 (C-4'a), 122.4 (C-5'), 125.5 (C-7'), 128.3 (DOBT C-3'' and C-5''), 129.1 (DOBT C-2'' and C-6''), 130.6 (DOBT C-1''), 132.8 (DOBT C-4''), 134.1 (C-6'), 149.9 (C-8'a), 165.1 (DOBT C-1'), 170.2 (DOBT C-1).

* Note: Diastereomeric excesses of the above salt was determined by liberation of **16** from the salt as outlined below and subsequent chiral hplc determination (described in 5.3.3) of the enantiomeric excess in the crude extract obtained.

(2*S*,3*S*)-Di-*O*-toluoyl tartrate salt of (*R*)-16 21

(*rac*)-16 (7.50 g, 26.9 mmol) was dissolved in methanol (60 cm³) and heated to reflux. A hot solution of (*2S,3S*)-di-*O*-toluoyltartaric acid (5.30 g, 3.7 mmol) in methanol (40 cm³) was slowly added to the refluxing solution. Precipitation started during the addition and a solid cake formed on complete addition of the resolving agent. A further 100 cm³ methanol was added and the resulting slurry refluxed for 10 min followed by stirring at room temperature for 2 h. The precipitate was filtered off, washed with ethyl acetate and dried under vacuum to yield **21** (5.75 g, 6.1 mmol, 91% as a single enantiomer, 90.0% de*). This salt (5.25 g, 5.6 mmol) was added to boiling methanol (450 cm³) and stirred at 0°C overnight. The solid material was again isolated by filtration, washed with ethyl acetate and vacuum dried (4.19 g, 4.4 mmol; 80% for this step, 73% overall yield as a single enantiomer, 95.2% de*), mp 191-192°C (methanol); [α]_D +38.5° (c 0.15 methanol); Found C, 65.8; H, 7.3; N, 2.9; C₅₂H₆₈N₂O₁₄ requires C, 66.1, H, 7.2; N, 3.0%; ν_{max} (KBr)/cm⁻¹ 3409 (O-H), 2900-2400 (N⁺-H), 1721 (C=O ester), 1641 (C=O carboxylate (s)), 1503 (C=O carboxylate (as)), 1123 (2° C-O); δ_H (400MHz, DMSO-d₆) 1.14 (9H, s, *t*-Bu), 1.45 (6H, s, 2x2'-CH₃), 2.37 (3H, s, DOTT 4''-CH₃), 2.67 (1H, dd, *J* 12.0 and 10.4 Hz, 2-H_A), 2.89 (1H, dd, *J* 12.0 and 2.2 Hz, 2-H_B), 3.35 (2H, br s, NH), 4.71 (1H, dd, *J* 10.4 and 2.2 Hz, 1-H), 4.76 (2H, s, 4'-H₂), 5.61 (1H, s, DOTT 2-H), 6.71 (1H, d, *J* 8.4 Hz, 8'-H), 6.99 (1H, d, *J* 2.0 Hz, 5'-H), 7.09 (1H, dd, *J* 8.4 and 2.0 Hz, 7'-H); 7.29 (1H, d, *J* 8.2 Hz, DOTT 3''-H and 5''-H), 7.87 (1H, d, *J* 8.2 Hz, DOTT 2''-H and 6''-H); δ_C (100MHz, DMSO-d₆) 21.1 (DOTT 4''-CH₃), 24.4 and 24.5 (2'-CH₃) 25.0 (*t*-Bu -CH₃), 48.1 (C-2), 54.7 (*t*-Bu -C(CH₃)₃), 60.0 (C-4'), 68.2 (C-1), 74.8 (DOTT C-2), 99.1 (C-2'), 116.0 (C-8''), 118.9 (C-4'a), 122.4 (C-5'), 125.5 (C-7'), 128.0 (DOTT C-1''), 128.8 (DOTT C-3'' and C-5''), 129.2 (DOTT C-2'' and C-6''), 134.1 (C-6'), 142.9 (DOTT C-4''), 149.9 (C-8'a), 165.2 (DOTT C-1'), 170.6 (DOTT C-1).

* Note: Diastereomeric excess of **21** was determined as for **20**.

(R)-2-(N-tert-Butylamino)-1-(2,2-dimethyl-1,3-benzodioxin-6-yl) ethanol (R)-16

To a vigorously stirring mixture of ethyl acetate (200 cm³) and aqueous Na₂CO₃ (200 cm³) was added **21** (4.19 g, 4.4 mmol). Stirring was continued until no solid material remained. The organic layer was removed and the aqueous phase extracted twice with equal volumes of ethyl acetate. The combined organic phases were dried (MgSO₄) and the solvent removed under reduced pressure to yield a colourless crystalline solid (2.43 g, 8.7 mmol, 98%). Recrystallisation from acetone was used to improve the optical purity as follows (by chiral hplc - see 5.3.3):

SAMPLE	enantiomeric excess (%)
Crude extract	95.2
Recrystallisation 1	99.5
Recrystallisation 2	>99.5
Recrystallisation 3	100

mp 102-103°C (acetone); $[\alpha]_D -18.9^\circ$ (*c* 1.5 methanol); Found C, 68.5; H, 9.6; N, 5.1; C₁₆H₂₅NO₃ requires C, 68.8; H, 9.0; N, 5.0%; δ_H (400MHz, CDCl₃) 1.11 (9H, s, *t*-Bu), 1.53 (3H, s, 2'-CH₃), 1.54 (3H, s, 2'-CH₃), 2.56 (1H, dd, *J* 11.7 and 9.1 Hz, 2-H_A), 2.12 (2H, br s, OH/NH), 2.87 (1H, dd, *J* 11.7 and 3.5 Hz, 2-H_B), 4.51 (1H, dd, *J* 9.0 and 3.5 Hz, 1-H), 4.84 (2H, s, 4'-H₂), 6.79 (1H, d, *J* 8.4 Hz, 8'-H), 7.01 (1H, d, *J* 1.5 Hz, 5'-H), 7.13 (1H, dd, *J* 8.4 and 1.5 Hz, 7'-H).

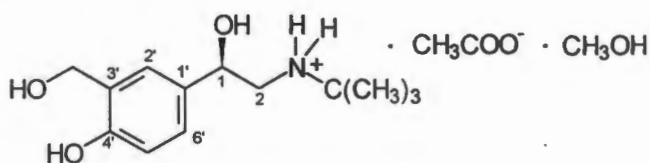
Liberation of (*R*)-**16** from the analogous Di-*O*-benzoyltartrate salt was performed in an identical fashion and the same % yield was achieved.

(2*S*,3*S*)-Di-*O*-benzoyltartaric acid recovery

The pH of the basic aqueous phase remaining after extraction of (*R*)-16 from the salt 20 (2.00 g, 2.2 mmol) was adjusted to about 4 with 1M HCl. The resulting solution was extracted three times with equal volumes of ethyl acetate. The combined organic phases were dried (MgSO₄) and the solvent removed *in vacuo* to produce a clear oil which solidified during vacuum drying (0.76 g, 2.1 mmol, 97%), [α]_D +114° (*c* 1.9 methanol) (lit. +116°).

(2*S*,3*S*)-Di-*O*-toluoyltartaric acid recovery

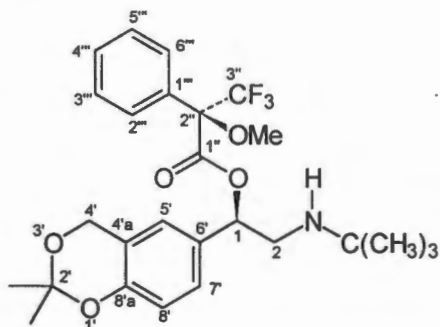
After liberation of (*R*)-16 from its di-*O*-toluoyltartrate salt, (4.19 g, 4.4 mmol) the remaining aqueous phase was acidified, extracted and dried as above. On addition of toluene to the oil and subsequent removal under reduced pressure, a crystalline solid was obtained (1.70 g, 4.4 mmol, 99%), [α]_D +135° (*c* 1 methanol) (lit. =138°).

(R)-Albuterol acetate monomethanolate (R)-24

Glacial acetic acid (0.4 cm³, 7.2 mmol) was added to a mixture of (*R*)-16 (90 mg, 0.32 mmol, 95.5% ee*) in H₂O (0.4 cm³, 0.4 g, 22 mmol). The resulting solution was stirred at 60°C for 5h. The solvents were removed by vacuum distillation to leave a colourless tacky oil which was taken up in methanol and chilled. Ethyl acetate was added to this solution resulting in the precipitation of (*R*)-24 (98 mg, 0.30 mmol, 92%, 97.0% ee*), mp 143-144°C (methanol/ethyl acetate) (lit. 144.3°C); δ_{H} (400MHz, DMSO) 1.15 (9H, s, *t*-Bu), 1.82 (3H, s, CH₃COO⁻), 2.66 (1H, dd, *J* 11.7 and 9.6 Hz, 2-H_A), 2.75 (1H, dd, *J* 11.7 and 3.4 Hz, 2-H_B), 3.17 (3H, s, CH₃OH), 4.48 (2H, s, 3'-CH₂OH), 4.60 (1H, dd, *J* 9.6 and 3.4 Hz, 1-H), 5.22 (3H, br s, OH/NH), 6.73 (1H, d, *J* 8.1 Hz, 5'-H), 7.03 (1H, dd, *J* 8.1 and 1.9 Hz, 6'-H), 7.27 (1H, d, *J* 1.9 Hz, 2'-H), δ_{C} (200MHz, DMSO) 23.5 (CH₃COO⁻), 27.6 (*t*-Bu -CH₃), 49.2 (CH₃OH), 50.2 (C-2), 53.1 ((*t*-Bu - C(CH₃)₃), 59.0 (3'-CH₂OH), 71.1 (C-1), 114.8 (C-5'), 125.5 (C-6'), 125.7 (C-2'), 128.7 (C-3'), 134.1 (C-1'), 154.1 (C-4'), 174.5 (CH₃COO⁻). Since desolvation of the salt occurred on drying at room temperature, the following analyses were performed on the fully desolvated material: $[\alpha]_{\text{D}} -37.9^{\circ}$ (*c* 0.5 methanol); Found C, 60.4; H, 8.6; N, 4.7; C₁₅H₂₅NO₅ requires C, 60.2, H, 8.4; N, 4.7%.

* Note: Enantiomeric excesses determined by hplc (5.3.3).

(1*R*,2'*R*)-2-(*N*-*tert*-Butylamino)-1-(2,2-dimethyl-1,3-benzodioxin-6-yl)ethyl-(2-methoxy-2-trifluoromethyl)phenylacetate 33



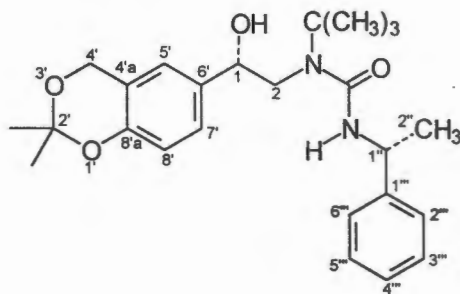
To a solution of (*R*)-**16** (280 mg, 1.0 mmol) in dichloromethane (5 cm³) at room temperature and under nitrogen was added *N,N*-dimethylaminopyridine (127 mg, 1.0 mmol), triethylamine (0.7 cm³, 511 mg, 5.0 mmol), and (*R*)-(2-methoxy-2-trifluoromethyl) phenylacetyl chloride (0.23 cm³, 311 mg, 1.2 mmol). The resulting yellow solution was stirred for 90 min followed by quenching with aqueous Na₂CO₃. The mixture was extracted into dichloromethane and the combined organic phases dried (MgSO₄) and the solvent removed under reduced pressure giving an oil (500 mg) which was adsorbed onto silica and chromatographed using ethyl acetate/petroleum ether (20/80) as eluent to give the product **33** as an oil (416 mg, 0.8 mmol, 84%), [α]_D 1.7° (*c* 1.5 methanol); ν_{\max} (CHCl₃)/cm⁻¹ 1748 (C=O ester), δ_{H} (400MHz, CDCl₃) 1.06 (9H, s, *t*-Bu), 1.53 (6H, s, 2x2'-CH₃), 2.83 (1H, dd, *J* 12.3 and 4.1 Hz, 2-H_A), 3.01 (1H, dd, *J* 12.3 and 9.3 Hz, 2-H_B), 3.55 (3H, s, 2''-OCH₃), 4.72 (1H, d, *J* 15.0Hz, 4'-H_A), 4.79 (1H, d, *J* 15.0Hz, 4'-H_B), 5.87 (1H, dd, *J* 9.3 and 4.1 Hz, 1-H), 6.75 (1H, d, *J* 8.5 Hz, 8'-H), 6.83 (1H, d, *J* 2.2 Hz, 5'-H), 7.07 (1H, dd, *J* 8.5 and 2.2 Hz, 7'-H); 7.2-7.4 (3H, m, 3'''-H, 4'''-H, 5'''-H), 7.46 (2H, d, *J* 7.4 Hz, 2'''-H, 6'''-H); δ_{C} (100MHz, CDCl₃) 24.6 and 24.7 (2'-CH₃) 28.8 (*t*-Bu -CH₃), 47.8 (C-2), 50.3 (*t*-Bu -C(CH₃)₃), 55.5 (2''-OCH₃), 60.7 (C-4'), 79.0 (C-1), 84.6 (q, 2''-CF₃), 99.6 (C-2'), 117.0 (C-8'), 119.2 (C-4'a), 123.3 (C-5'), 126.6 (C-7'), 127.5 (C-2''', C-6''')128.2 (C-3''', C-5'''), 129.4 (C-4'''), 129.6 (C-1'''), 132.3 (C-6'), 151.3 (C-8'a), 165.7 (C-1''); (HRMS: Found M⁺ 495.2226, C₂₆H₃₂NO₅F₃ requires M, 495.2231).

(1*R*,2''*R*)-2-(*N*-*tert*-Butylamino-1-(2,2-dimethyl-1,3-benzodioxin-6-yl)ethyl-(2-methoxy-2-trifluoromethyl)phenyl)acetate, 33 and its (1*S*,2''*R*)-diastereomer, 34

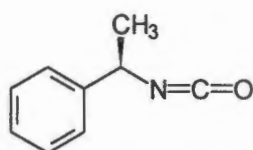
Reaction of (rac)-16 under the conditions described above resulted in an inseparable mixture of diastereomers. These were purified as above and analysed by ¹HNMR.

33		34		Multiplicity	Assignment
δ (ppm)	<i>J</i> (Hz)	δ (ppm)	<i>J</i> (Hz)		
1.06	-	0.98	-	s	<i>t</i> -Bu
1.53	-	1.52	-	s	2x2'-CH ₃
2.83	12.3 and 4.1	2.75	12.3 and 3.9	dd	2-H _A
3.00	12.3 and 9.5	2.99	12.3 and 9.3	dd	2-H _B
3.54	-	3.43	-	s	2''-OCH ₃
4.72	15.2	4.78	15.0	d	4'-H _A
4.79	15.2	4.84	15.0	d	4'-H _B
5.87	9.5 and 4.1	5.92	9.3 and 3.9	dd	1-H
6.75	8.6	6.79	8.4	d	8'-H
6.83	2.2	6.99	2.1	d	5'-H
7.07	8.6 and 2.2	7.18	8.4 and 2.1	dd	7'-H
7.2-7.5	-	7.2-7.5	-	m	other Ar-H

(1*S*,1'*R*)-2-[*N*-*tert*-Butyl-*N*-(1-phenethylamido)amino]-1-(2,2-dimethyl-1,3-benzodioxin-6-yl)ethanol 36

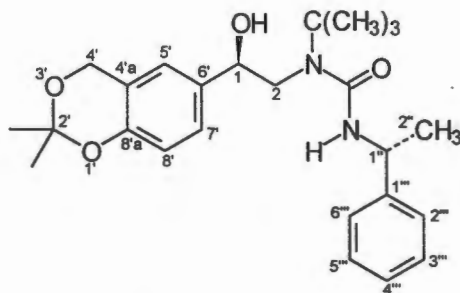


A solution of triphosgene (220 mg, 0.7 mmol) in dichloromethane (4 cm³) was stirred at room temperature under nitrogen while a solution of (*R*)-phenylethylamine (0.26 cm³, 247 mg, 2.0 mmol) and *N,N*-diisopropylethylamine (0.40 cm³, 296 mg, 2.3 mmol) in dichloromethane (3.5 cm³) was added over 45 min. The resulting solution was stirred for a further 10 min followed by the addition of a solution of (*rac*)-**16** (558 mg, 2.0 mmol) in dichloromethane (4 cm³). After 10 min stirring the solution was evaporated to dryness under reduced pressure and the residue taken up in ethyl acetate (100 cm³), washed with equal volumes of 10% NaHCO₃ and brine and dried (MgSO₄). The solvent was removed under reduced pressure to produce 768 mg crude material (largely comprising two major products and starting material). The material was adsorbed onto silica and chromatographed using a mixture of ethyl acetate and petroleum ether (10/90 followed by 20/80) as eluent. Only the more polar of the products could be isolated cleanly to give **36** (156 mg, 0.4 mmol, 37% as a single diastereomer), mp 149-150°C (ethyl acetate/hexane); [α]_D -3.5° (*c* 1.1 methanol); Found C, 70.1; H, 8.6; N, 6.7; C₂₅H₃₄N₂O₄ requires C, 70.4; H, 8.0; N, 6.6%; ν_{max} (CHCl₃)/cm⁻¹ 1652 (C=O urea); δ_H (400MHz, CDCl₃) 1.40 (9H, s, *t*-Bu), 1.47 (3H, d, *J* 6.8 Hz, 2''-H), 1.54 (6H, s, 2x2'-CH₃), 3.23 (1H, dd, *J* 16.3 and 2.3 Hz, 2-H_A), 3.44 (1H, dd, *J* 16.3 and 9.6 Hz, 2-H_B), 4.76 (1H, dd, *J* 9.6 and 2.3 Hz, 1-H), 4.82 (2H, s, 4'-H₂), 4.94 (1H, m, 1''-H), 6.60 (1H, d, *J* 7.4 Hz, 1''-NH), 6.80 (1H, d, *J* 8.4 Hz, 8'-H), 6.93 (1H, d, *J* 1.9 Hz, 5'-H), 7.09 (1H, dd, *J* 8.4 and 1.9 Hz, 7'-H), 7.2-7.4 (5H, m, 2'''-6'''-H); δ_C (100MHz, CDCl₃) 23.3 (C-2''), 24.7 and 24.8 (2'-CH₃) 29.1 (*t*-Bu -CH₃), 49.9 (C-1'''), 54.4 (C-2), 55.9 (*t*-Bu -C(CH₃)₃), 60.9 (C-4'), 76.7 (C-1), 99.7 (C-2'), 117.3 (C-8'), 119.7 (C-4'a), 121.9 (C-5'), 125.5 (C-7'), 126.0, 126.7 and 128.5 (C-2'''-C-6'''), 134.1 (C-6'), 145.3 (C-1'''), 151.1 (C-8'a), 160.7 (C=O); (HRMS: Found M⁺, 426.2507, C₂₅H₃₄N₂O₄ requires M, 426.2518).

(R)-Phenylethylisocyanate 35

Triphosgene (2.96 g, 10 mmol) was dissolved in dichloromethane (50 cm³) and stirred at room temperature and under nitrogen. A solution of (*R*)-phenylethylamine (3 cm³, 3.15 g, 26 mmol) and *N,N*-diisopropylethylamine (5 cm³, 3.71 g, 29 mmol) in dichloromethane (80 cm³) was added over 2 h via a dropping funnel. The mixture was then cooled to 0 °C and added to a mixture of 0.5M HCl (100 cm³) and ice (100 cm³) and the organic layer removed. This acid wash step was repeated and the combined aqueous phases were extracted with dichloromethane (50 cm³). The combined organic phases were washed with a brine/ice mixture and concentrated by rotary evaporation to afford a yellow oil (3.05g, 77%). The product was purified by Kugelrohr distillation to give a colourless oil [α]_D +12° (undiluted, lit. +13°); ν_{\max} (CHCl₃)/cm⁻¹ 2250 (N=C=O).

(1*R*,1'*R*)-2-[*N*-*tert*-Butyl-*N*-(1-phenethylamido)amino]-1-(2,2-dimethyl-1,3-benzodioxin-6-yl)ethanol 37



To a stirred solution of (*R*)-16 (140 mg, 0.5 mmol) in dichloromethane (2.5 cm³) at room temperature and under nitrogen was added 35 (0.10 cm³, 0.105 g, 0.7 mmol). The mixture was stirred overnight and then adsorbed onto silica gel. Elution with ethyl acetate/petroleum ether (20/80) yielded 37 (186 mg, 0.4 mmol, 87%), mp 122-125°C (ethyl acetate/hexane); [α]_D -58.0° (c 1.0 methanol); Found C, 70.3; H, 8.4; N, 6.6; C₂₅H₃₄N₂O₄ requires C, 70.4; H, 8.0; N, 6.6%; ν_{\max} (CHCl₃)/cm⁻¹ 1640 (C=O urea); δ_{H} (400MHz, CDCl₃) 1.41 (9H, s, *t*-Bu), 1.45 (3H, d, *J* 6.8 Hz, 2''-H), 1.54 (6H, s, 2x2'-CH₃), 1.67 (1H, br s, OH), 3.27 (1H, dd, *J* 16.0 and 2.2 Hz, 2-H_A), 3.49 (1H, dd, *J* 16.0 and 9.5 Hz, 2-H_B), 4.75 (1H, dd, *J* 9.5 and 2.2 Hz, 1-H), 4.84 (2H, s, 4'-H₂), 4.92 (1H, m, 1''-H), 6.46 (1H, d, *J* 7.7 Hz, 1''-NH), 6.81 (1H, d, *J* 8.4 Hz, 8'-H), 6.98 (1H, d, *J* 2.2 Hz, 5'-H), 7.12 (1H, dd, *J* 8.4 and 2.2 Hz, 7'-H), 7.2-7.4 (5H, m, 2'''-6'''-H); δ_{C} (100MHz, CDCl₃) 23.3 (C-2''), 24.6 and 24.8 (2'-CH₃) 29.3 (*t*-Bu -CH₃), 50.0 (C-1''), 54.4 (C-2), 55.8 (*t*-Bu -C(CH₃)₃), 60.9 (C-4'), 77.2 (C-1), 99.7 (C-2'), 117.3 (C-8'), 119.6 (C-4'a), 121.9 (C-5'), 125.5 (C-7'), 125.9, 126.7 and 128.4 (C-2'''-C-6'''), 134.2 (C-6'), 145.1 (C-1'''), 151.1 (C-8'a), 160.7 (C=O); (HRMS: Found M⁺, 426.2505, C₂₅H₃₄N₂O₄ requires M, 426.2518).

5.3 Analyses

5.3.1 X-ray Powder Diffraction Patterns

These were measured on a Philips PW 1050/80 goniometer with Ni-filtered CuK α radiation ($\lambda = 1.5418\text{\AA}$). The powder patterns were collected in the range $6^\circ \leq 2\theta \leq 40^\circ$ with step scans of $2\theta = 0.1^\circ$. Samples were coground to ensure particle sizes were less than $100\ \mu\text{m}$ and carefully packed into a $20 \times 14 \times 1\ \text{mm}$ aluminium holder so as to minimise preferred orientation effects.

5.3.2 NMR Determination of optical purity of (*R*)-Albuterol Acetonide, (*R*)-16

Typically, **16** (5 mg) and (*R*)- or (*S*)-*O*-Acetylmandelic acid (6 mg) were dissolved in CDCl₃ (1 cm³) and the ¹H-NMR spectra recorded (400MHz). Several of the protons in **16** gave well distinguished peaks for each diastereomer formed in solution and integration of these pairs (usually the *t*-Bu peaks) allowed determination of the optical purity.

Data for the 400 MHz ¹H-NMR spectrum obtained with (*R*)-*O*-Acetylmandelic Acid:

MAJOR [(<i>R</i>)-16]		MINOR [(<i>S</i>)-16]		Multiplicity	Assignment
δ (ppm)	<i>J</i> (Hz)	δ (ppm)	<i>J</i> (Hz)		
1.22	-	1.18	-	s	<i>t</i> -Bu
1.53	-	1.53	-	s	2x2'-CH ₃
2.81	12.2 and 10.2	obscured	-	dd	2-H _A
2.87	12.2 and 2.6	2.95	12.2 and 3.0	dd	2-H _B
4.80	-	4.80	-	s	4'-H ₂
4.89	10.2 and 2.6	4.96	3.0 and 10.2	dd	1-H
6.74	8.4	6.75	8.2	d	8'-H
6.94	2.0	7.00	1.7	d	5'-H
7.04	8.4 and 2.0	7.09	8.2 and 1.7	dd	7'-H

(*R*)-OAM: δ_{H} 2.13, 5.83, 7.30, 7.47 ppm

5.3.3 Chiral High Performance Liquid Chromatography on (*R*)-16 and (*R*)-24

Hplc parameters for (*R*)-16

Column:	Phenomenex Chirex 3022
Mobile Phase:	hexane/1,2-dichloroethane/methanol/trifluoroacetic acid (240/140/7.5/1)
Temperature:	ambient
Flow rate:	1.0 cm ³ .min ⁻¹
Detection λ:	254 nm
Injection volume:	25 μl
Sample solvent	hexane/1,2-dichloroethane/methanol (240/140/7.5)

Linearity and limit of quantitation

A set of standard solutions of (*rac*)-16 was prepared by dissolving 11.0 mg in 10 cm³ sample solvent and making the appropriate dilutions to give solutions of 1.100, 0.440, 0.088 and 0.044 mg.cm⁻³. Triplicate injections of each solution were made and a linear curve constructed. The limit of quantitation was taken as the lowest concentration at which reproducible integration of peak areas of the impurity (*S*)-16 could be achieved and was determined to be 0.044 mg.cm⁻³ of the racemic solution which relates to 0.022 mg.cm⁻³ of the single enantiomer.

Sample analysis

About 10 mg sample was accurately weighed into a vial and 1 cm³ sample solvent added. The solutions were injected in duplicate and the enantiomeric excess in each determined by:

$$\% ee = 100 \left(\frac{\text{Area } (R) - \text{Area } (S)}{\text{Area } (R) + \text{Area } (S)} \right)$$

Hplc parameters for (R)-24

Column:	Phenomenex Chirex 3022
Mobile Phase:	hexane/1,2-dichloroethane/methanol/trifluoroacetic acid (240/140/20/1)
Temperature:	ambient
Flow rate:	1.2 cm ³ .min ⁻¹
Detection λ :	280 nm
Injection volume:	25 μ l
Sample solvent	hexane/1,2-dichloroethane/methanol (240/140/7.5)

Linearity and limit of quantitation

231 mg (rac)-albuterol was dissolved in a minimum of methanol and diluted to 10 cm³ with the sample solvent used in the ketal determinations. Suitable dilutions with this solvent produced samples of 1.155, 0.462, 0.046 and 0.023 mg.cm⁻³ which gave a satisfactory calibration curve. The limit of quantitation under these conditions was determined to be 0.023 mg.cm⁻³ of the racemate which gives 0.012 mg.cm⁻³ in each enantiomer.

Sample analysis

5mg sample was accurately weighed, diluted to 1 cm³ and analysed as for 16

5.4 Crystal Structure Determinations

5.4.1 (rac)-Albuterol Acetonide, (rac)-16

Preliminary X-Ray photography

Oscillation and Weissenberg photographs were taken using a non-integrating Stoë goniometer. A Stoë Reciprocal Lattice Explorer was used to record de Jong-Bouman, Buerger precession and cone-axis photographs. The crystals were irradiated with Ni-filtered CuK α radiation ($\lambda = 1.5418$ Å) generated by Philips PW1120 and PW1140 X-ray generators. Space group data and preliminary cell parameters were determined from the photographs.

Intensity data collection

The data collection was performed at 293K on a Nonius KappaCCD using graphite monochromated 1kW Mo radiation ($\lambda = 0.7107$ Å). 474 exposures of 40s each were collected. 400 of these were in the $\chi = 0^\circ$ position with 0.5° rotation in ϕ per image. The remaining 74 exposures were collected with $\chi = -90^\circ$ and 0.5° rotation in ω per image. Data processing was performed by DENZO-SMN.¹¹⁸

Both default and modified approaches with the program SHELX-86⁷⁵ were applied in attempts to elucidate the structure using direct methods. These were not successful.

5.4.2 (R)-Albuterol Acetonide, (R)-16

Preliminary X-Ray photography

Space group data and preliminary cell parameters were determined from oscillation and Weissenberg photographs taken using the instrumentation and conditions described in Section 5.4.1.

Intensity data collections

Two intensity data collections were performed on an Enraf-Nonius CAD4 diffractometer using graphite-monochromated MoK α radiation ($\lambda = 0.7107 \text{ \AA}$) at 298 K and 223 K respectively. The unit cell was refined by least-squares analysis of the setting angles of 24 reflections collected in the θ range 16-17°. Data in the range $1^\circ \leq \theta \leq 25^\circ$ (298 K) and $1^\circ \leq \theta \leq 30^\circ$ (223 K) were collected in the ω -2 θ scan mode with a final acceptance limit of 20σ at 20°min^{-1} and a maximum scan time of 40s per reflection. The vertical aperture length was fixed at 4 mm, the aperture width varied according to $(1.12+1.05 \tan \theta)$ mm and the scan width as $\omega=(0.80+0.35 \tan \theta)^\circ$. In both cases, Friedel opposite reflections were collected. Intensity control was performed every hour by means of three reference reflections. Lorentz-polarisation corrections were applied to the data in addition to empirical absorption corrections.¹¹⁹

Structure analysis and refinement

Using the data collected at 298 K, all non-hydrogen atoms were found by direct methods using SHELX-86⁷⁵. The structures were refined by full-matrix least-squares on F^2 using SHELXL-93¹²⁰. Friedel opposites were not merged since it was intended to distinguish the absolute structure of the compound. All non-hydrogen atoms were treated anisotropically. Hydrogen atoms were located in difference electron density syntheses, placed in geometrically calculated positions and linked to a common temperature factor for chemically equivalent entities. In the final cycle of refinement, the Flack parameter⁹¹ was inspected but this failed to indicate the correctness of the handedness assigned to the structure. The refined parameters from the 298K data set were used as input for further refinement using the low temperature (223 K) intensity data. Inspection of the Flack parameter generated here led to the conclusion that the atoms present in the molecule (C, H, N, O) were insufficiently large to produce a significant difference between Friedel opposite reflections.

The residual indices based on F values (R_1) and F^2 (R_2) quoted in Table 3.1 are defined as:

$$R_1 = \frac{\sum ||F_o| - |F_c||}{\sum |F_o|} \quad wR_2 = \left(\frac{\sum (F_o^2 - F_c^2)^2}{\sum (F_o^2)} \right)^{1/2}$$

where w is the weighting scheme: $w = 1 / [\sigma^2(F_o^2) + (aP)^2 + bP]$

$$P = [\max(0, F_o^2) + 2F_c^2] / 3$$

(a and b refined for structure)

5.4.3 (*R*)-Phenylethylurea of (*S*)-Albuterol Acetonide, 36

Preliminary X-Ray photography

Oscillation, Weissenberg, de Jong-Bouman and precession photographs were taken as described for (rac)-16 (Section 5.4.1).

Intensity data collection

The data collection was performed at 293K on a Nonius KappaCCD using graphite monochromated 1kW Mo radiation ($\lambda = 0.7107 \text{ \AA}$). 237 exposures of 40s each were collected. 200 of these were in the $\chi = 0^\circ$ position with 1° rotation in ϕ per image. The remaining 37 exposures were collected with $\chi = -90^\circ$ and 1° rotation in ω per image. Data processing was performed by DENZO-SMN.¹¹⁸

Structure analysis and refinement

As before, all non-hydrogen atoms were found by direct methods using SHELX-86⁷⁵, and the structure was refined by full-matrix least-squares on F^2 using SHELXL-93¹²⁰. Non-hydrogen atoms were again treated anisotropically and location and treatment of hydrogen atoms was as for the previous structure. An extinction correction was applied in the final refinement step. The definition of the residual indices quoted in Table 3.4 is given in Section 5.4.2 on page 76.

REFERENCES

1. Jamali, F. in *Drug Stereochemistry*, Ed. I.W. Wainer, Marcel Dekker, New York, 1993.
2. Cushney, A.R., *J. Physiol.*, 1904, **30**, 193.
3. Blaschke, G., Kraft, H.P., Fickentscher, K., Koehler, F., *Arzneim-Forsch.*, 1979, **29**, 1640
4. Stinson, S.C., *C.&E.N.*, 1994, Sept 19, 38.
5. Stinson, S.C., *C.&E.N.*, 1997, Oct 20, 38.
6. Richards, A., McCague, R., *Chem. & Ind.*, 1997, June 2, 422.
7. *Guidelines for Submitting Supporting Documentation in Drug Applications for the Manufacture of Drug Substances*, Office of Drug Evaluation and Research, U.S. Food and Drug Administration, Rockville, 1987.
8. F.D.A.'s Policy statement for the Development of New Stereoisomeric Drugs, *Fed. Reg.*, 1992, **57**, 22249.
9. *Fed. Reg.*, 1997, **62**, 2167.
10. *Chirality in Industry*, Eds A.N. Collins, G.N. Sheldrake and J. Crosby, John Wiley & Sons, New York, 1994.
11. *Chirality in Industry*, Vol 2, Eds A.N. Collins, G.N. Sheldrake and J. Crosby, John Wiley & Sons, New York, 1997.
12. Sheldon, R.A., *Chirotechnology*, Marcel Dekker, New York, 1993
13. Federsel, H.-J., *Chemtech*, 1993, Dec, 24.
14. Federsel, H.-J., Högberg, T., Råmsby, S., Ström, P., PCT Application No. PCT/SE87/00246, 1987.
15. Giordiano, C., Castaldi, G., *Tetrahedron*, 1990, **45**, 4243.
16. Ohta, T., Takaya, H., Kitamura, M., Nagai, K., Noyori, R., *J. Org. Chem.*, 1987, **52**, 3174.
17. Effenberger, F., Jäger, J., *J. Org. Chem.*, 1997, **62**, 3867.
18. Sheldon, R.A., *J. Chem. Tech. Biotechnol.*, 1996, **67**, 1.
19. Matsumae, H., Furui, M., Shibatani, T., Tosa, T., *J. Ferment. Bioeng.*, 1994, **78**, 59.
20. Jacobson, E.N., *Science*, 1997, **277**, 936.
21. *Chiral Separations: Applications and Technology*, Ed. S. Ahija, American Chemical Society, Washington, DC, 1997.
22. Eliel, E.L., Wilen, S.H., *Stereochemistry of Organic Compounds*, John Wiley & Sons, New York, 1994.
23. Jaques, J., Leclercq, M., Brienne, M.-J., *Tetrahedron*, 1981, **37**, 1727.

24. Jaques, J., Collet, A., Wilen, S.H., *Enantiomers, Racemates and Resolutions*, John Wiley & Sons, New York, 1981.
25. Pasteur, L., *C. R. Acad. Sci.*, 1848, **26**, 535.
26. Reinhold, D.F., Firestone, R.A., Gaines, W.A., Chemerda, J.M., Sletzing, M.J., *J. Org. Chem.*, 1968, **33**, 1209.
27. Amiard, G., *Experientia*, 1959, **15**, 1.
28. Toda, F., *Jpn Chem. Week*, 1986, 20 Mar, 1.
29. Toda, F., *Top. Curr. Chem.*, 1987, **140**, 43.
30. Toda, F., Tanaka, K., Leung, C.W., Meetsma, A., Feringa, B.L., *J. Chem. Soc., Chem. Commun.*, 1994, 2371.
31. Pasteur, L., *C. R. Acad. Sci.*, 1853, **37**, 162.
32. Ugi, I., *Z. Naturforsch.*, 1965, **20b**, 405.
33. Wilen, S.H., Collet, A., Jaques, J., *Tetrahedron*, 1977, **33**, 2725.
34. Cannarsa, M.J., *Chem. & Ind.*, 1996, 20 May, 374.
35. Iwao, J., Oya, M., Kato, E., Watanabe, T., Jpn Kokai Tokyo, JP 54-151912, 1979.
36. Fogassy, E., Ács, M., Faigl, K.S., Rohonczy, J., Ecsery, Z., *J. Chem. Soc. Perkin Trans. II*, 1986, 1881.
37. Simon, K., Kozda, É., Böcskei, Z., Faigl, F., Fogassy, E., Reck, G., *J. Chem. Soc. Perkin Trans. II*, 1990, 1395.
38. Ács, M., *ACH-Models in Chemistry*, 1995, **132(3)**, 409.
39. Gould, R.O., Wakinshaw, M.D., *J. Am. Chem. Soc.*, 1984, **106**, 7840.
40. Zingg, S.P., Arnett, E.M., McPhail, A.T., Bothner-By, A.A., Gilkerson, W.R., *J. Am. Chem. Soc.*, 1988, **108**, 1565.
41. Ariaans, G.J.A., Leusen, F.J.J., Bruggink, A., *Proceedings of the Chiral '92 Symposium, Manchester, U.K.*, 1992, 99.
42. Leusen, F.J.J., Noordik, J.H., Karfunkel, H.R., *Tetrahedron*, 1993, **49(24)**, 5377.
43. Gavezzotti, A., *J. Am. Chem. Soc.*, 1989, **111**, 1835.
44. Gavezzotti, A., *J. Am. Chem. Soc.*, 1991, **113**, 4622.
45. Jaques, J., Gabard, J., *Bull. Soc. Chim. Fr.*, 1972, 342.
46. Pohland, A., Peters, L.R., Sullivan, H.R., *J. Org. Chem.*, 1963, **28**, 2483.
47. Reider, P.J., Davis, P., Hughes, L.D., Grabowski, E.J.S., *J. Org. Chem.*, 1987, **28**, 52, 955.
48. Yoshioka, R., Tohyama, M., Ohtsuki, O., Yamada, S., Chibata, I., *Bull. Chem. Soc. Japan*, 1987, **60**, 649.

49. Howarth, P.H., George, G.F., *Adverse Drug React. Acute Poisoning Rev.*, 1983, **2**, 25.
50. Kelly, H.W., Murphy, S., *Annu. Pharmacother.*, **26**, 81.
51. Lunts, L.H.C. in *Medicinal Chemistry: The Role of Organic Chemistry in Drug Research*, Eds S.M. Roberts and B.J. Price, Academic Press, London, 1985.
52. Hartley, D., Middlemiss, D., *J. Med. Chem.*, 1971, **14(9)**, 895.
53. Bakale, R.P., Wald, S.A., Butler, H.T., Gao, Y., Hong, Y., Nie, X., Zepp, C.M., *Clin. Rev. Allerg. Immunol.*, 1996, **14(1)**, 7.
54. Hoshiko, K.I., Kristersson, A., Morley, J., *J. Allergy Clin. Immunol.*, 1993, **91**, 909
55. Boulton, D.W., Fawcett, J.P., *Clin. Rev. Allerg. Immunol.*, 1996, **14(1)**, 115.
56. Perrin-Fayolle, M., Blum, P.S., Morley, J., Grosclaude, M., Chambe, M.T., *Clin. Rev. Allerg. Immunol.*, 1996, **14(1)**, 139.
57. Kleemann, Von A., Engel, J., *Pharmazeutische Wirkstoffe, Ergänzungsband, 1982-1987*, Georg Thieme Verlaak, Stuttgart.
58. Bakale, R.P., *Speciality Chem. Prod., Market Applic.*, 1995, **15**, 249.
59. Gao, Y., Hong, Y., Nie, X., Zepp, C.M., U.S. Patent # 5,442,118, 1995, August 15.
60. Gao, Y., Zepp, C.M., U.S. Patent # 5,399,765, 1995, March 21.
61. Gao, Y., Zepp, C.M., U.S. Patent # 5,545,745, 1996, August 13.
62. Hawkins, C.J., Klease, G.T., *J. Med. Chem.*, 1973, **16**, 856.
63. Tan, Y., Soldin, S.J., *J. Chromatog. Biomed. Applic.*, 1987, **422**, 187.
64. Adams, A., Stewart, J.T., *J. Liquid Chromatog.*, 1993, **16(17)**, 3863.
65. Heuermann, M., Blaschke, G., *J. Chromatog.*, 1993, **648**, 267.
66. Dewar, G.H., Kwakye, J.K., Parfitt, R.T., Sibson, R., *J. Pharm. Sci.*, 1982, **71(7)**, 802.
67. Parker, D., Taylor, R.J., *Tetrahedron*, 1987, **43(22)**, 5451.
68. ten Hoeve, W., Wynberg, H., *J. Org. Chem.*, 1985, **50**, 4508.
69. Jeffrey, G.A., *An Introduction to Hydrogen Bonding*, Oxford University Press, New York, 1997
70. Greene, T.W., Wutz, P.G.M., *Protective Groups in Organic Synthesis*, John Wiley & Sons, New York, 1991.
71. Kocienski, P.J., *Protecting Groups*, Georg Thieme Verlag, Stuttgart, 1994.
72. Williams, D.H., Fleming, I., *Spectroscopic Methods in Organic Chemistry*, 3rd Edⁿ, McGraw-Hill Book Co, UK, 1980.
73. Pihlaja, K., Kleinpeter, E., *Carbon-13 NMR Chemical Shifts in Structural and Stereochemical Analysis*, VCH Publishers, New York, 1994.

74. *International Tables for Crystallography*, Vol 1, Ed. T. Hahn, D. Riedel Publishing Company, Dordrecht, 1983
75. Sheldrick, G.M., SHELX-86, *Crystallographic Computing 3*, eds G.M. Sheldrick, C. Kruger, R. Goddard, Oxford University Press, 1985.
76. Jaques, J., Fouquey, C., *Organic Synthesis*, 1989, **67**, 1
77. Nemák, K., Ács, M., Jászay, Z.M., Kozma, D., Fogassy, E., *Tetrahedron*, 1996, **52**, 1637.
78. Mravik, A., Lepp, Z., Fogassy, E., *Tetrahedron: Asymmetry*, 1996, **7**, 2387.
79. *Chiral Separations by HPLC*, Ed. Krststulovic, A.M., Ellis Horwood Ltd, Chichester, 1989.
80. Lewbart, M.L., Schneider, J.J., *J. Org. Chem.*, 1969, **34**, 3505.
81. Coppola, G., *Synthesis*, 1984, Dec, 1021.
82. Hudlický, M., *Oxidations in Organic Chemistry*, American Chemical Society, Washington, DC, 1990.
83. *Encyclopedia of Reagents for Organic Synthesis*, Ed. Paquette, L.A., John Wiley & Sons, Chichester, 1995.
84. Lyle, R.E., Maloney, J.R., White, R.J., *Org. Prep. and Proced.*, 1980, **12**, 255.
85. Haines, A.H., *Methods for the Oxidation of Organic Compounds*, Academic Press, London, 1988.
86. Chrisman, W., Singaram, B., *Tetrahedron Letters*, 1997, **38**, 2053.
87. Denis, J.-N., Correa, A., Greene, A.E., *J. Org. Chem.*, 1991, **56**, 6939.
88. Dess, D.B., Martin, J.C., *J. Org. Chem.*, 1983, **48**, 4155.
89. Cambridge Structural Database and Cambridge Structural Database System Version 5.11 (April 1996), Cambridge Crystallographic Data Centre, University Chemical Laboratory, Cambridge, England.
90. K. Kinbara, K. Sakai, Y. Hashimoto, H. Nohira, K. Saigo, *J. Chem. Soc. Perkin Trans. II*, 1996, 2615.
91. Flack, H.D., *Acta Cryst.*, 1983, **A39**, 876.
92. Cooper, A., Kartha, G., Gopalakrishna, E.M., Norton, D.A., *Acta Cryst.*, 1969, **B25**, 2409.
93. Peck, D., Langs, D.A., Eger, C., Duax, W.L., *Cryst. Struct. Comm.*, 1974, **3**, 573.
94. Bodanszky, M., *Int. J. Peptide protein Res.*, 1985, **25**, 449.
95. Neises, B., Steglich, W., *Angew. Chem., Int. Ed. Engl.*, 1978, **17**, 522.
96. König, W., Geiger, R., *Chem. Ber.*, 1970, **103**, 788.
97. Tung, R.D., Rich, D.H., *J. Am. Chem. Soc.*, 1985, **107**, 4342.

98. Coste, J., Frérot, E., Jouin, P., *Tetrahedron Letters*, 1991, **32**, 1967.
99. Halterman, R.L., Vollhardt, K.P.C., Welker, M.E., *J. Am. Chem. Soc.*, 1987, **109**, 8105.
100. Dehmlow, E.V., Westerheide, R., *Synthesis*, 1992, Oct, 947.
101. Bartlett, P.D., Knox, L.H., *Org. Syn.*, 1965, **45**, 14.
102. Oppolzer, W., Chapius, C., Bernardinelli, G., *Tetrahedron Letters*, 1984, **25**, 5885.
103. Mori, K., Kisida, H., *Liebigs Ann. Chem.*, 1989, 35.
104. Dale, J.A., Dull, D.L., Mosher, H.S., *J. Org. Chem.*, 1969, **34**, 2543.
105. Sullivan, G.R., Dale, J.A., D.L., Mosher, H.S., *J. Org. Chem.*, 1975, **38**, 2143.
106. Dale, J.A., D.L., Mosher, H.S., *J. Am. Chem. Soc.*, 1973, **95**, 512.
107. Ward, D.E., Rhee, C.K., *Tetrahedron Letters*, 1991, **32**, 7165
108. Latypov, Sh.K., Seco, J.M., Quiñoá, E., Riguera, R., *J. Org. Chem.*, 1995, **60**, 504 and references cited therein.
109. Joshi, B.S., Newton, M.G., Lee, D.W., Barber, A.D., Pelletier, S.W., *Tetrahedron: Asymmetry*, 1996, **7**, 25.
110. Ohtani, I., Kusumi, T., Kashman, Yo., Kakisawa, H., *J. Org. Chem.*, 1991, **56**, 1296.
111. Latypov, Sh.K., Seco, J.M., Quiñoá, E., Riguera, R., *J. Org. Chem.*, 1996, **61**, 8569.
112. Seco, J.M., Latypov, Sh.K., Quiñoá, E., Riguera, R., *J. Org. Chem.*, 1997, **62**, 7569.
113. Carroll, A.R., Scheuer, P.J., *J. Org. Chem.*, 1990, **55**, 4426.
114. Goldschmidt, S., Wick, M., *Liebigs Ann. Chem.*, 1952, **575**, 217.
115. Eckert, H., Forster, B., *Angew. Chem., Int. Ed. Engl.*, 1987, **26**, 894.
116. Majer, P., Randad, R.S., *J. Org. Chem.*, 1994, **59**, 1937.
117. Nowick, J.S., Holmes, D.L., Noronha, G., Smith, E.M., Nguyen, T.M., Huang, S-L., *J. Org. Chem.*, 1996, **61**, 3929.
118. Otwinowski, Z., Minor, W. in "Processing of X-ray diffraction data Collected in Oscillation Mode", *Methods in enzymology*, **276**: Macromolecular crystallography, part A, 1997, 307, eds C.W. Carter, J and R.M. Sweet, Academic Press.
119. North, A.C.T., Phillips, D.C., Mathews, F.S., *Acta Crystallogr.*, 1968, **A24**, 351
120. Sheldrick, G.M., SHELXL-93: Programme for Crystal Structure Determination, unpublished work.

APPENDIX 1

CRYSTAL STRUCTURE DATA FOR (+)-16

Table A1: Atomic coordinates and equivalent isotropic displacement parameters, $U_{(eq)}$ ($\text{\AA}^2 \times 10^3$), with e.s.d.'s in parentheses. $U_{(eq)}$ is defined as one third of the trace of the orthogonalised U_{ij} tensor.

Atom	X/a	Y/b	Z/c	$U_{(eq)}$
C1	-0.0704(5)	0.0946(3)	0.9105(1)	29(1)
C2	0.0668(5)	0.0063(3)	0.8840(1)	30(1)
C3	-0.0004(5)	-0.0399(3)	0.8419(1)	31(1)
C4	-0.2092(5)	0.0066(3)	0.8269(1)	33(1)
C5	-0.3487(5)	0.0971(4)	0.8528(1)	40(1)
C6	-0.2794(5)	0.1384(3)	0.8941(1)	38(1)
C7	-0.0101(5)	0.1353(3)	0.9574(1)	29(1)
O7	0.2250(3)	0.1317(2)	0.9654(1)	34(1)
C8	-0.1208(2)	0.0202(2)	0.9881(1)	33(1)
N9	-0.0810(2)	0.0632(2)	1.0343(1)	29(1)
C10	-0.1466(2)	-0.0545(2)	1.0675(1)	33(1)
C11	-0.3994(2)	-0.0769(2)	1.0667(1)	49(1)
C12	-0.0746(8)	0.0089(4)	1.1117(1)	55(1)
C13	-0.0276(7)	-0.2078(4)	1.0598(1)	53(1)
C14	0.1427(5)	-0.1391(4)	0.8133(1)	43(1)
O15	0.0605(4)	-0.1417(3)	0.7694(1)	45(1)
C16	-0.1741(6)	-0.1621(4)	0.7660(1)	42(1)
O17	-0.2864(4)	-0.0334(3)	0.7859(1)	43(1)
C18	-0.2561(8)	-0.3078(4)	0.7873(2)	62(1)
C19	-0.2295(8)	-0.1530(5)	0.7179(1)	66(2)

Table A2: Anisotropic displacement parameters ($\text{\AA}^2 \times 10^3$), with e.s.d.'s in parentheses. The anisotropic displacement factor exponent takes the form:

$$-2\pi^2[h^2a^2U_{11} + \dots + 2hka^*b^*U_{12}]$$

Atom	$U_{(11)}$	$U_{(22)}$	$U_{(33)}$	$U_{(23)}$	$U_{(12)}$	$U_{(13)}$
C1	32(1)	29(1)	25(1)	-1(1)	0(1)	1(1)
C2	28(1)	35(1)	28(1)	0(1)	-1(1)	4(1)
C3	31(1)	33(1)	30(1)	-2(1)	-1(1)	2(1)
C4	36(2)	31(1)	31(1)	-2(1)	-6(1)	3(1)
C5	34(1)	43(2)	44(2)	-7(1)	-12(1)	13(1)
C6	34(1)	40(2)	39(2)	-8(1)	-2(1)	13(1)
C7	30(1)	29(1)	26(1)	-2(1)	3(1)	-1(1)
O7	31(1)	36(1)	34(1)	-3(1)	-2(1)	-4(1)
C8	39(2)	32(1)	29(1)	-2(1)	0(1)	-7(1)
N9	30(1)	29(1)	27(1)	1(1)	2(1)	-5(1)
C10	35(1)	31(1)	32(1)	4(1)	4(1)	-6(1)
C11	34(2)	54(2)	57(2)	11(2)	8(2)	-9(2)
C12	79(3)	55(2)	30(2)	11(1)	-4(2)	-22(2)
C13	52(2)	40(2)	66(2)	14(2)	10(2)	2(2)
C14	39(2)	56(2)	34(2)	-14(1)	-2(1)	11(2)
O15	44(1)	65(1)	28(1)	-12(1)	4(1)	-3(1)
C16	42(1)	49(2)	36(2)	-13(1)	-4(1)	1(1)
O17	48(1)	45(1)	36(1)	-8(1)	-13(1)	8(1)
C18	57(2)	43(2)	84(3)	-13(2)	7(2)	-7(2)
C19	70(3)	86(3)	40(2)	-17(2)	-13(2)	0(3)

Table A3: Bond Lengths (Å) with e.s.d.'s in parentheses.

Bond	Length	Bond	Length
C1 - C2	1.382(4)	C8 - N9	1.475(2)
C1 - C6	1.395(4)	N9 - C10	1.493(2)
C1 - C7	1.517(4)	C10 - C11	1.519(2)
C2 - C3	1.403(4)	C10 - C12	1.520(4)
C3 - C4	1.387(4)	C10 - C13	1.531(4)
C3 - C14	1.495(4)	C14 - O15	1.425(4)
C4 - C5	1.392(4)	O15 - C16	1.413(4)
C4 - O17	1.375(4)	C16 - O17	1.440(4)
C5 - C6	1.373(5)	C16 - C18	1.507(5)
C7 - O7	1.422(3)	C16 - C19	1.506(5)
C7 - C8	1.522(3)		

Table A4: Bond Angles (degrees) with e.s.d.'s in parentheses.

Bonds	Angle	Bonds	Angle
C6 - C1 - C7	119.1(2)	C8 - N9 - C10	115.4(1)
C2 - C1 - C7	122.7(2)	N9 - C10 - C13	112.1(2)
C2 - C1 - C6	118.1(3)	N9 - C10 - C12	106.1(2)
C1 - C2 - C3	121.7(2)	N9 - C10 - C11	109.8(1)
C2 - C3 - C14	122.5(3)	C12 - C10 - C13	108.7(2)
C2 - C3 - C4	118.4(3)	C11 - C10 - C13	110.2(2)
C4 - C3 - C14	119.2(3)	C11 - C10 - C12	109.9(2)
C3 - C4 - O17	121.8(3)	C3 - C14 - O15	111.2(2)
C3 - C4 - C5	120.9(3)	C14 - O15 - C16	114.3(2)
C5 - C4 - O17	117.4(3)	O15 - C16 - C19	106.4(3)
C4 - C5 - C6	119.3(3)	O15 - C16 - C18	113.2(3)
C1 - C6 - C5	121.7(3)	O15 - C16 - O17	109.3(3)
C1 - C7 - C8	108.8(2)	C18 - C16 - C19	113.2(3)
C1 - C7 - O7	112.9(2)	O17 - C16 - C19	105.6(3)
O7 - C7 - C8	107.9(2)	O17 - C16 - C18	108.9(3)
C7 - C8 - N9	110.4(1)	C4 - O17 - C16	115.2(2)

Table A5: Torsion Angles (degrees) with e.s.d.'s in parentheses.

Bonds	Angle	Bonds	Angle
C6 - C1 - C7 - O7	-160.2(2)	C3 - C4 - C5 - C6	-1.1(5)
C2 - C1 - C7 - O7	24.5(4)	C5 - C4 - O17 - C16	-161.6(3)
C6 - C1 - C7 - C8	80.0(3)	O17 - C4 - C5 - C6	179.3(3)
C2 - C1 - C7 - C8	-95.3(3)	C4 - C5 - C6 - C1	1.3(5)
C7 - C1 - C6 - C5	-176.1(3)	C1 - C7 - C8 - N9	-175.5(2)
C2 - C1 - C6 - C5	-0.6(4)	O7 - C7 - C8 - N9	61.7(2)
C6 - C1 - C2 - C3	-0.5(4)	C7 - C8 - N9 - C10	-169.8(1)
C7 - C1 - C2 - C3	174.9(3)	C8 - N9 - C10 - C11	-65.6(1)
C1 - C2 - C3 - C4	0.7(4)	C8 - N9 - C10 - C12	175.7(2)
C1 - C2 - C3 - C14	-178.2(3)	C8 - N9 - C10 - C13	57.2(2)
C2 - C3 - C14 - O15	-167.3(3)	C3 - C14 - O15 - C16	-45.4(4)
C2 - C3 - C4 - C5	0.1(4)	C14 - O15 - C16 - O17	63.5(3)
C2 - C3 - C4 - O17	179.7(3)	C14 - O15 - C16 - C18	-58.1(4)
C4 - C3 - C14 - O15	13.9(4)	C14 - O15 - C16 - C19	177.0(3)
C14 - C3 - C4 - O17	-1.4(4)	O15 - C16 - O17 - C4	-48.1(3)
C14 - C3 - C4 - C5	179.0(3)	C18 - C16 - O17 - C4	76.0(3)
C3 - C4 - O17 - C16	18.8(4)	C19 - C16 - O17 - C4	-162.2(3)

Table A6: Hydrogen atom coordinates and isotropic displacement parameters, U_{iso} ($\text{\AA}^2 \times 10^3$), with e.s.d.'s in parentheses.

Atom	X/a	Y/b	Z/c	U_{iso}
H2	0.2071(5)	-0.0232(3)	0.8944(1)	50(6)
H5	-0.4874(5)	0.1293(4)	0.8422(1)	50(6)
H6	-0.3742(5)	0.1971(3)	0.9116(1)	50(6)
H7	-0.0670(5)	0.2382(3)	0.9641(1)	25(7)
H7A	0.2753(12)	0.2192(5)	0.9645(13)	54(11)
H8A	-0.2810(2)	0.0171(2)	0.9825(1)	52(5)
H8B	-0.0602(2)	-0.0814(2)	0.9827(1)	52(5)
H9A	0.0693(2)	0.0802(2)	1.0360(1)	36(8)
H11A	-0.4399(2)	-0.1574(2)	1.0867(1)	77(4)
H11B	-0.4462(2)	-0.1042(2)	1.0376(1)	77(4)
H11C	-0.4721(2)	0.0166(2)	1.0754(1)	77(4)
H12A	-0.1148(44)	-0.0625(16)	1.1344(1)	77(4)
H12B	-0.1484(37)	0.1051(17)	1.1169(4)	77(4)
H12C	0.0851(10)	0.0240(31)	1.1119(3)	77(4)
H13A	-0.0532(41)	-0.2742(13)	1.0845(5)	77(4)
H13B	0.1306(9)	-0.1905(5)	1.0565(10)	77(4)
H13C	-0.0856(35)	-0.2550(16)	1.0337(6)	77(4)
H14A	0.2954(5)	-0.1007(4)	0.8135(1)	52(5)
H14B	0.1445(5)	-0.2427(4)	0.8250(1)	52(5)
H18A	-0.2421(46)	-0.2991(14)	0.8186(2)	77(4)
H18B	-0.1677(32)	-0.3927(6)	0.7772(7)	77(4)
H18C	-0.4106(16)	-0.3242(18)	0.7798(8)	77(4)
H19A	-0.3894(8)	-0.1480(31)	0.7142(1)	77(4)
H19B	-0.1725(40)	-0.2423(16)	0.7032(2)	77(4)
H19C	-0.1620(38)	-0.0628(18)	0.7055(2)	77(4)

APPENDIX 2

CRYSTAL STRUCTURE DATA FOR 36

Table B1: Atomic coordinates and equivalent isotropic displacement parameters, $U_{(eq)}$ ($\text{\AA}^2 \times 10^3$), with e.s.d.'s in parentheses. $U_{(eq)}$ is defined as one third of the trace of the orthogonalised U_{ij} tensor.

Atom	X/a	Y/b	Z/c	$U_{(eq)}$
C1	0.3313(2)	0.6232(1)	0.8981(1)	41(1)
C2	0.4470(2)	0.6644(1)	0.8597(1)	44(1)
C3	0.5513(2)	0.7503(1)	0.8684(1)	44(1)
C4	0.5340(2)	0.7953(1)	0.9164(1)	43(1)
C5	0.4195(2)	0.7544(1)	0.9555(1)	47(1)
C6	0.3215(2)	0.6687(1)	0.9465(1)	46(1)
C7	0.2199(2)	0.5297(1)	0.8889(1)	42(1)
O7	0.2421(1)	0.4950(1)	0.8372(1)	50(1)
C8	-0.0023(2)	0.5422(1)	0.8994(1)	41(1)
N9	-0.1201(2)	0.4533(1)	0.8976(1)	40(1)
C10	-0.1661(2)	0.4027(1)	0.9480(1)	48(1)
C11	-0.3353(3)	0.4522(2)	0.9759(1)	91(1)
C12	-0.2103(4)	0.2975(2)	0.9378(1)	92(1)
C13	0.0155(3)	0.4064(2)	0.9834(1)	72(1)
C14	0.6813(3)	0.7948(1)	0.8273(1)	53(1)
O15	0.7215(2)	0.8931(1)	0.8396(1)	52(1)
C16	0.7820(2)	0.9083(1)	0.8917(1)	49(1)
O17	0.6238(2)	0.8818(1)	0.9269(1)	51(1)
C18	0.9636(3)	0.8513(2)	0.9067(1)	68(1)
C19	0.8067(4)	1.0153(1)	0.8980(1)	74(1)
C20	-0.2420(2)	0.4405(1)	0.8551(1)	40(1)
O20	-0.4085(1)	0.4037(1)	0.8576(1)	51(1)
N21	-0.1667(2)	0.4714(1)	0.8094(1)	57(1)
C22	-0.2758(2)	0.4710(1)	0.7607(1)	49(1)
C23	-0.2122(3)	0.3872(1)	0.7262(1)	68(1)
C24	-0.2554(2)	0.5656(1)	0.7323(1)	51(1)
C25	-0.4207(3)	0.6076(2)	0.7100(1)	76(1)
C26	-0.4044(5)	0.6929(2)	0.6825(1)	102(1)
C27	-0.2231(5)	0.7357(2)	0.6753(1)	98(1)
C28	-0.0595(4)	0.6952(2)	0.6977(1)	87(1)
C29	-0.0747(3)	0.6103(1)	0.7261(1)	67(1)

Table B2: Anisotropic displacement parameters ($\text{\AA}^2 \times 10^3$), with e.s.d.'s in parentheses. The anisotropic displacement factor exponent takes the form:

$$-2\pi^2[h^2a^2U_{11} + \dots + 2hka^*b^*U_{12}]$$

Atom	$U_{(11)}$	$U_{(22)}$	$U_{(33)}$	$U_{(23)}$	$U_{(12)}$	$U_{(13)}$
C1	344(1)	46(1)	42(1)	-1(1)	-4(1)	-1(1)
C2	44(1)	50(1)	38(1)	-7(1)	1(1)	-4(1)
C3	43(1)	50(1)	37(1)	-1(1)	2(1)	-4(1)
C4	42(1)	46(1)	40(1)	-3(1)	-2(1)	-5(1)
C5	47(1)	58(1)	35(1)	-5(1)	2(1)	-7(1)
C6	43(1)	56(1)	40(1)	0(1)	2(1)	-9(1)
C7	34(1)	46(1)	45(1)	-3(1)	-3(1)	-2(1)
O7	39(1)	58(1)	54(1)	-16(1)	1(1)	-1(1)
C8	35(1)	42(1)	46(1)	-1(1)	-2(1)	-1(1)
N9	38(1)	44(1)	39(1)	3(1)	-3(1)	-4(1)
C10	45(1)	57(1)	42(1)	10(1)	0(1)	-3(1)
C11	66(1)	153(2)	54(1)	18(1)	15(1)	28(1)
C12	137(2)	66(1)	72(1)	25(1)	-13(1)	-32(1)
C13	65(1)	93(1)	58(1)	29(1)	-16(1)	-6(1)
C14	60(1)	56(1)	42(1)	-2(1)	7(1)	-12(1)
O15	64(1)	53(1)	40(1)	5(1)	-3(1)	-11(1)
C16	55(1)	54(1)	40(1)	3(1)	0(1)	-12(1)
O17	58(1)	51(1)	44(1)	-6(1)	5(1)	-13(1)
C18	53(1)	96(1)	56(1)	7(1)	-4(1)	-3(1)
C19	100(2)	63(1)	59(1)	1(1)	2(1)	-29(1)
C20	33(1)	44(1)	43(1)	-1(1)	-1(1)	2(1)
O20	36(1)	63(1)	53(1)	2(1)	-3(1)	-9(1)
N21	33(1)	97(1)	42(1)	8(1)	-5(1)	-9(1)
C22	38(1)	71(1)	38(1)	2(1)	-3(1)	-3(1)
C23	79(1)	62(1)	62(1)	-3(1)	-5(1)	0(1)
C24	54(1)	59(1)	40(1)	-5(1)	-4(1)	5(1)
C25	69(1)	87(1)	72(1)	7(1)	-15(1)	12(1)
C26	124(2)	84(2)	96(2)	24(1)	-19(2)	33(1)
C27	147(3)	57(1)	89(2)	12(1)	2(2)	5(1)
C28	109(2)	71(1)	82(2)	-2(1)	10(1)	-24(1)
C29	62(1)	71(1)	67(1)	3(1)	0(1)	-9(1)

Table B3: Bond Lengths (Å) with e.s.d.'s in parentheses.

Bond	Length	Bond	Length
C1 - C2	1.379(2)	C14 - O15	1.425(2)
C1 - C6	1.394(2)	O15 - C16	1.412(2)
C1 - C7	1.517(2)	C16 - O17	1.445(2)
C2 - C3	1.401(2)	C16 - C18	1.507(3)
C3 - C4	1.384(2)	C16 - C19	1.502(3)
C3 - C14	1.503(2)	C20 - O20	1.236(2)
C4 - C5	1.387(2)	C20 - N21	1.345(2)
C4 - O17	1.371(2)	N21 - C22	1.450(2)
C5 - C6	1.378(2)	C22 - C23	1.521(2)
C7 - O7	1.418(2)	C22 - C24	1.506(2)
C7 - C8	1.533(2)	C24 - C25	1.382(3)
C8 - N9	1.468(2)	C24 - C29	1.377(3)
N9 - C10	1.500(2)	C25 - C26	1.380(4)
N9 - C20	1.378(2)	C26 - C27	1.373(5)
C10 - C11	1.513(3)	C27 - C28	1.365(4)
C10 - C12	1.512(3)	C28 - C29	1.388(3)
C10 - C13	1.526(3)		

Table B4: Bond Angles (degrees) with e.s.d.'s in parentheses.

Bonds	Angle	Bonds	Angle
C6 - C1 - C7	120.1(1)	C3 - C14 - O15	110.3(1)
C2 - C1 - C7	121.6(1)	C14 - O15 - C16	114.0(1)
C2 - C1 - C6	118.3(1)	O15 - C16 - C19	106.3(1)
C1 - C2 - C3	121.6(1)	O15 - C16 - C18	113.4(1)
C2 - C3 - C14	122.1(1)	O15 - C16 - O17	109.8(1)
C2 - C3 - C4	118.7(1)	C18 - C16 - C19	113.6(2)
C4 - C3 - C14	119.2(1)	O17 - C16 - C19	105.4(1)
C3 - C4 - O17	122.1(1)	O17 - C16 - C18	108.0(1)
C3 - C4 - C5	120.4(1)	C4 - O17 - C16	115.2(1)
C5 - C4 - O17	117.5(1)	N9 - C20 - N21	115.0(1)
C4 - C5 - C6	119.9(1)	N9 - C20 - O20	123.6(1)
C1 - C6 - C5	121.1(1)	O20 - C20 - N21	121.4(1)
C1 - C7 - C8	111.1(1)	C20 - N21 - C22	123.8(1)
C1 - C7 - O7	112.5(1)	N21 - C22 - C24	111.5(1)
O7 - C7 - C8	107.8(1)	N21 - C22 - C23	111.1(1)
C7 - C8 - N9	115.4(1)	C23 - C22 - C24	111.0(1)
C8 - N9 - C20	117.1(1)	C22 - C24 - C29	121.9(2)
C8 - N9 - C10	118.6(1)	C22 - C24 - C25	119.6(2)
C10 - N9 - C20	119.8(1)	C25 - C24 - C29	118.6(2)
N9 - C10 - C13	109.2(1)	C24 - C25 - C26	120.5(2)
N9 - C10 - C12	110.1(1)	C25 - C26 - C27	120.7(3)
N9 - C10 - C11	110.6(1)	C26 - C27 - C28	119.1(3)
C12 - C10 - C13	107.1(2)	C27 - C28 - C29	120.7(2)
C11 - C10 - C13	108.0(2)	C24 - C29 - C28	120.5(2)
C11 - C10 - C12	111.7(2)		

Table B5: Torsion Angles (degrees) with e.s.d.'s in parentheses.

Bonds	Angle	Bonds	Angle
C6 - C1 - C7 - O7	178.4(1)	C8 - N9 - C10 - C13	-39.6(2)
C2 - C1 - C7 - O7	-2.9(2)	C10 - N9 - C20 - O20	13.6(2)
C6 - C1 - C7 - C8	57.4(2)	C10 - N9 - C20 - N21	-166.4(1)
C2 - C1 - C7 - C8	-123.9(1)	C20 - N9 - C10 - C13	165.0(1)
C7 - C1 - C6 - C5	-179.2(1)	C20 - N9 - C10 - C12	47.7(2)
C2 - C1 - C6 - C5	2.1(2)	C20 - N9 - C10 - C11	-76.3(2)
C6 - C1 - C2 - C3	-0.7(2)	C3 - C14 - O15 - C16	47.9(2)
C7 - C1 - C2 - C3	-179.4(1)	C14 - O15 - C16 - O17	-63.5(2)
C1 - C2 - C3 - C4	-1.1(2)	C14 - O15 - C16 - C18	57.4(2)
C1 - C2 - C3 - C14	178.7(1)	C14 - O15 - C16 - C19	-177.1(1)
C2 - C3 - C14 - O15	162.8(1)	O15 - C16 - O17 - C4	46.2(2)
C2 - C3 - C4 - C5	1.6(2)	C18 - C16 - O17 - C4	-77.9(2)
C2 - C3 - C4 - O17	-176.8(1)	C19 - C16 - O17 - C4	160.4(1)
C4 - C3 - C14 - O15	-17.4(2)	N9 - C20 - N21 - C22	-175.5(1)
C14 - C3 - C4 - O17	3.4(2)	O20 - C20 - N21 - C22	4.5(2)
C14 - C3 - C4 - C5	-178.2(1)	C20 - N21 - C22 - C23	-102.5(2)
C3 - C4 - O17 - C16	-17.9(2)	C20 - N21 - C22 - C24	133.1(1)
C3 - C4 - C5 - C6	-0.3(2)	N21 - C22 - C24 - C25	-136.1(2)
C5 - C4 - O17 - C16	163.6(1)	N21 - C22 - C24 - C29	46.2(2)
O17 - C4 - C5 - C6	178.2(1)	C23 - C22 - C24 - C25	99.4(2)
C4 - C5 - C6 - C1	-1.6(2)	C23 - C22 - C24 - C29	-78.3(2)
C1 - C7 - C8 - N9	-173.1(1)	C22 - C24 - C29 - C28	177.1(2)
O7 - C7 - C8 - N9	63.3(2)	C22 - C24 - C25 - C26	-178.1(2)
C7 - C8 - N9 - C10	96.9(1)	C25 - C24 - C29 - C28	-0.6(3)
C7 - C8 - N9 - C20	-107.0(1)	C29 - C24 - C25 - C26	-0.3(3)
C8 - N9 - C20 - O20	-142.2(1)	C24 - C25 - C26 - C27	2.2(4)
C8 - N9 - C20 - N21	37.8(2)	C25 - C26 - C27 - C28	-3.0(4)
C8 - N9 - C10 - C11	79.2(2)	C26 - C27 - C28 - C29	2.0(4)
C8 - N9 - C10 - C12	-156.9(1)	C27 - C28 - C29 - C24	-0.2(4)

Table B6: Hydrogen atom coordinates and isotropic displacement parameters, U_{iso} ($\text{\AA}^2 \times 10^3$), with e.s.d.'s in parentheses.

Atom	X/a	Y/b	Z/c	U_{iso}
H2	0.4561(2)	0.6344(1)	0.8274(1)	71(2)
H5	0.4089(2)	0.7847(1)	0.9878(1)	71(2)
H6	0.2476(2)	0.6409(1)	0.9732(1)	71(2)
H7	0.2716(2)	0.4808(1)	0.9129(1)	71(2)
H7A	0.3456(15)	0.4644(13)	0.8348(2)	71(2)
H8A	-0.0185(2)	0.5714(1)	0.9335(1)	71(2)
H8B	-0.0554(2)	0.5870(1)	0.8739(1)	71(2)
H11A	-0.3411(15)	0.4298(9)	1.0114(2)	97(2)
H11B	-0.4577(4)	0.4374(9)	0.9586(4)	97(2)
H11C	-0.3144(12)	0.5207(2)	0.9756(5)	97(2)
H12A	-0.3357(12)	0.2918(2)	0.9203(6)	97(2)
H12B	-0.2153(24)	0.2633(3)	0.9703(1)	97(2)
H12C	-0.1081(14)	0.2705(3)	0.9162(5)	97(2)
H13A	-0.0134(8)	0.3740(10)	1.0156(3)	97(2)
H13B	0.0492(14)	0.4725(2)	0.9903(5)	97(2)
H13C	0.1248(7)	0.3751(10)	0.9664(3)	97(2)
H14A	0.8049(3)	0.7592(1)	0.8250(1)	71(2)
H14B	0.6160(3)	0.7910(1)	0.7936(1)	71(2)
H18A	1.0061(14)	0.8702(8)	0.9410(3)	97(2)
H18B	1.0677(8)	0.8638(9)	0.8821(4)	97(2)
H18C	0.9326(7)	0.7837(2)	0.9066(6)	97(2)
H19A	0.8450(24)	1.0295(2)	0.9333(2)	97(2)
H19B	0.6836(8)	1.0470(2)	0.8903(6)	97(2)
H19C	0.9072(18)	1.0380(2)	0.8745(5)	97(2)
H21	-0.0469(2)	0.4927(1)	0.8091(1)	71(2)
H22	-0.4163(2)	0.4621(1)	0.7690(1)	71(2)
H23A	-0.2816(17)	0.3904(6)	0.6936(2)	97(2)
H23B	-0.2427(20)	0.3274(1)	0.7433(3)	97(2)
H23C	-0.0721(5)	0.3909(6)	0.7200(5)	97(2)
H25	-0.5439(3)	0.5783(2)	0.7136(1)	71(2)
H26	-0.5174(5)	0.7216(2)	0.6687(1)	71(2)
H27	-0.2118(5)	0.7916(2)	0.6554(1)	71(2)
H28	0.0633(4)	0.7249(2)	0.6940(1)	71(2)
H29	0.0379(3)	0.5834(1)	0.7411(1)	71(2)

APPENDIX 3 (diskette) STRUCTURE FACTOR DATA FOR (+)-16 and 36

The attached diskette contains text files listing the observed and calculated structure factors with standard deviations for observed structure factors for both of the structures solved.

Compound	Filename
(+)-16	16sfac.txt
36	36sfac.txt